ISTANBUL TECHNICAL UNIVERSITY ★ GRADUATE SCHOOL OF SCIENCE ENGINEERING AND TECHNOLOGY

MOLECULAR AND PHYSIOLOGICAL INVESTIGATION OF LONGEVITY IN YEAST

Ph.D. THESIS

Mevlüt ARSLAN

Department of Molecular Biology-Genetics and Biotechnology

Molecular Biology-Genetics and Biotechnology Programme

DECEMBER 2017

ISTANBUL TECHNICAL UNIVERSITY ★ GRADUATE SCHOOL OF SCIENCE ENGINEERING AND TECHNOLOGY

MOLECULAR AND PHYSIOLOGICAL INVESTIGATION OF LONGEVITY IN YEAST

Ph.D. THESIS

Mevlüt ARSLAN
(521112106)

Department of Molecular Biology-Genetics and Biotechnology

Molecular Biology-Genetics and Biotechnology Programme

Thesis Advisor: Prof. Dr. Zeynep Petek ÇAKAR

DECEMBER 2017

İSTANBUL TEKNİK ÜNİVERSİTESİ ★ FEN BİLİMLERİ ENSTİTÜSÜ

MAYA HÜCRELERİNDE UZUN YAŞAMIN MOLEKÜLER VE FİZYOLOJİK YÖNDEN İNCELENMESİ

DOKTORA TEZİ

Mevlüt ARSLAN
(521112106)

Moleküler Biyoloji-Genetik ve Biyoteknoloji Anabilim Dalı

Moleküler Biyoloji-Genetik ve Biyoteknoloji Programı

Tez Danışmanı: Prof. Dr. Zeynep Petek ÇAKAR

ARALIK 2017

Mevlüt ARSLAN, a Ph.D. student of ITU Graduate School of Science Engineering and Technology student ID 521112106, successfully defended the thesis entitled "MOLECULAR AND PHYSIOLOGICAL INVESTIGATION OF LONGEVITY IN YEAST", which he prepared after fulfilling the requirements specified in the associated legislations, before the jury whose signatures are below.

Thesis Advisor :	**Prof. Dr. Zeynep Petek ÇAKAR** Istanbul Technical University	.....
Jury Members :	**Prof. Dr. Ayten YAZGAN KARATAŞ** Istanbul Technical University	.....
	Prof. Dr. Nevin GÜL KARAGÜLER Istanbul Technical University	.....
	Prof. Dr. Oğuz ÖZTÜRK Istanbul University	.....
	Prof. Dr. Kutlu ÜLGEN Boğaziçi University	.....

Date of Submission : 09 November 2017
Date of Defense : 26 December 2017

To my family,

FOREWORD

I would like to express my deep gratitude to Prof. Dr. Zeynep Petek ÇAKAR for giving me a chance and opportunity to work in her laboratory and conduct my PhD study. I am very thankful for her guidance, encouragement, understanding, and contribution to my Ph.D. study.

I place on record, my sincere gratitude to Dr. Burcu TURANLI-YILDIZ and Dr. Ceren ALKIM. I am thankful for their guidance, patience, kindness and for sharing their knowledge and experience in the laboratory.

I would like to thank all yeast laboratory members; Yusuf SÜRMELİ, Alican TOPALOĞLU, Ergi TERZİOĞLU, H.İbrahim KISAKESEN, Dr. Ülkü YILMAZ, Can HOLYAVKİN, Nazlı KOCAEFE, Dr. B. Gülçin BALABAN and Burcu HACISALİHOĞLU for sharing experience and helps. I would especially like to thank to Yusuf SÜRMELİ, Alican TOPALOĞLU and H.İbrahim KISAKESEN for endless help, kindness and friendship. I would also like to thank all yeast laboratory undergraduate researchers who have shared their time and helped me.

I would like to thank Rahmi İMAMOĞLU, Barbaros DÜZGÜN, H.İbrahim KISAKESEN and Ergi TERZİOĞLU for their friendship and good memories. I would like to thank Koray KIRIMTAY for kind friendship and help related with computer programs. I would also like to thank Dr. Yetkin ÖZTÜRK for his kindness and friendship.

I would like to thank ITU library, especially Prof. Dr. Mustafa İNAN library, to provide me a good environment for work and research. I would like to thank Scientific Research Projects of Istanbul Technical University for financial support. This thesis work was funded by Istanbul Technical University Ph.D. Thesis Support Project (Project no: 39557).

Most of all, I would like to express my gratitude to my family for their unconditional love and support. I would like to thank especially my wife Sümeyye Nur ARSLAN for her understanding and endless support, and daughter Asya ARSLAN for giving energy to work and conduct Ph.D. thesis.

December 2017

Mevlüt ARSLAN
(Vet. Med., Molecular Biologist and Geneticist)

TABLE OF CONTENTS

Page

ABBREVIATIONS

EMS	: Ethyl methane sulfonate
DNA	: Deoxyribo Nucleic Acid
RNA	: Ribonucleic Acid
RIN	**:** RNA Integrity Number
cDNA	: Complementary Deoxyribo Nucleic Acid
bp	: Base Pair
ds	: Double Strand
HPLC	: High Performance Liquid Chromatography
HSP	: Heat shock protein
MAT	: Mating type
OD	: Optical density
ROS	: Reactive oxygen species
YMM	: Yeast minimal medium
YPD	: Yeast extract - peptone - dextrose (Yeast complex medium)
NAD	: Nicotinamide Adenine Dinucleotide
ORF	: Open Reading Frame
PCR	: Polymerase Chain Reaction
rpm	: Revolution per minute
OD_{600}	: Optical Density at 600 nanometers
CLS	: Chronological lifespan
RLS	: Replicative lifespan
CFU	: Colony Forming Unit
AVG	: Average
CDW	: Cell Dry Weight
et al.	: and others
UV	: Ultraviolet
V	:Volt
etc.	: et cetera
h	: Hour
min	: Minute
sec	: Second
µg	: Microgram
ng	: Nanogram
µL	: Microliter
M	: Molar
mM	: Millimolar
µM	: Micromolar
µm	: Micrometer
mg	: Milligram
mL	: Milliliter
vs	:versus

LIST OF TABLES

Page

LIST OF FIGURES

Page

MOLECULAR AND PHYSIOLOGICAL INVESTIGATION OF LONGEVITY IN YEAST

SUMMARY

World population has changed in both developed and developing countries due to low birth and death ratio, resulting in relatively elder populations, which is a major challenge. Aging is a risk factor for several diseases such as Alzheimer, Parkinson, diabetes, cancer and cardiovascular diseases, due to declining cellular physiological functions with time. In recent years, researchers have been focusing on this issue due to the increasing socioeconomic concerns. The purpose is to understand the cellular aging process and to provide healthy lifespan. In aging research, the yeast *Saccharomyces cerevisiae*, the fruit fly *Drosophila melanogaster*, the worm *Caenorhabditis elegans*, rodents and primates have been used as model organisms.

The yeast *S. cerevisiae* is a unicellular eukaryotic microorganism and it has been used in industrial processes such as baking, wine and beer production since ancient times. It has also been commonly used as a eukaryotic model organism in genetic and molecular biological research since it does not need expensive and special media and cultivation conditions. The yeast *S. cerevisiae* is a commonly preferred model organism in aging studies because of the shortness of its life span, availability of its genome sequence data and extensive molecular tools and techniques, and its similarity to mammalian cells.

Aging studies can be performed by two ways in *S. cerevisiae*: by investigating the replicative life span (RLS) or the chronological lifespan (CLS). RLS has been developed because of the asymmetrical division of *S. cerevisiae* cells. In the method, after mitosis, the daughter cell is separated from the mother cell by using a micromanipulator, and the procedure is continued until the mother cell stops division. At the end of mitosis, the number of buds one mother cell produced are determined and the number of daughter cells is the RLS of *S. cerevisiae*. CLS is the length of time where non-dividing stationary phase yeast cells survive. In the method, cell viability at the beginning of the stationary phase of growth is determined by viable cell counting method on solid media. After that, viability of non-dividing cells at the stationary phase is monitored. Since (i) stationary phase cells produce energy from mitochondria, (ii) damage accumulates over time and (iii) cells exit from the cell cycle (G_0), CLS method is accepted as a convenient model to study aging of non-dividing cells (*e.g.,* neurons) in higher eukaryotic organisms.

Long-lived *S. cerevisiae, C. elegans* and *Drosophila* mutants have had a major role for understanding cellular aging mechanism. The studies share a similar approach, since the long-lived mutant strain is obtained first, and then it is investigated in detail to understand its molecular basis. These strategies show similarity to inverse metabolic engineering approach. In inverse metabolic engineering approach, first, the desired phenotype is obtained, and then, its genetic mechanism is identified. This approach is a very powerful strategy to obtain complex desired microbial phenotypes

with genetic complexity. So far, the approach has not been used to obtain chronologically long-lived yeast.

In the present study, inverse metabolic engineering approach was used to obtain chronologically long-lived *S. cerevisiae*. Furthermore, since previous aging research with model organisms has shown a close relationship between stress resistance and longevity, in the current study, CLS of previously obtained stress-resistant *S. cerevisiae* mutants was also investigated.

To isolate a chronologically long-lived yeast mutant by using inverse metabolic engineering, first, genetic diversity of the initial population for selection was increased by ethyl methane sulfonate (EMS)-mutagenesis. Successive batch cultivation of the initial mutant population was performed under gradually enhanced caloric restriction, since caloric restriction is known to extend lifespan. During successive batch cultivations, glucose concentration of the medium was decreased from 0.5% to 0.02%. In the last batch cultivation, since growth ratio of the mutant population decreased to 10%, the selection procedure was ended. After that, individual mutants were randomly picked from the last population. Semi-quantitative and quantitative CLS analyses were applied to these individual mutants. A single mutant (called SRM11) that has the highest chronological survival among the other mutants was chosen for further physiological and molecular analysis.

Quantitative CLS method based on viable cell counting on solid media is tedious for large studies where multiple strains and multiple conditions are tested, as a high number of plates and flasks is required for incubation. It is also labor-intensive. Therefore, in the present study, the semi-quantitative method was used for preliminary determination of CLS in mutants. A culture density adjustment step was introduced to the semi-quantitative method, for a more reliable evaluation of CLS of cultures at significantly different culture densities. Following the semi-quantitative CLS, quantitative CLS analysis was applied to the prominent mutants. The procedure was applied successfully and correctly determined the chronologically long-lived phenotypes in a wide range of strains and conditions.

Growth behavior of the mutant SRM11 was investigated by growth curve and biomass analysis. The purpose of these experiments was to determine whether any trade-off in growth physiology occurred or not. Analysis results showed that there was no trade-off in the growth fitness of the mutant SRM11 in both standard medium (2% YMM) and calorie-restricted medium (0.5% YMM). In this experiment, it was observed that 75% reduction of glucose concentration of the medium (from 2% to 0.5% glucose) did not affect growth ratio of the yeast strains when glucose was utilized.

High-Pressure Liquid Chromatography (HPLC) analysis was performed to investigate the metabolic profiles of the long-lived mutant SRM11 and the reference strain. For this purpose, glucose, ethanol, glycerol and acetate concentrations in culture samples were monitored by HPLC analysis. Even though there was no significant difference in glucose consumption between the reference strain and the mutant SRM11, there was a significant difference in the production of fermentative metabolites. The mutant SRM11 produced low amounts of ethanol, glycerol and acetate in standard glucose medium (2% YMM). These findings indicated a respirative shift in the metabolism of the mutant SRM11, showing that respirative metabolism is related to chronological longevity in *S. cerevisiae*. In 0.5% YMM, a limited ethanol and glycerol production was observed in the cultures of the reference

strain and the mutant SRM11, which indicates that at 0.5% glucose concentration, fermentation is limited.

Aging studies have shown a close relationship between stress resistance and longevity in model organisms. Therefore, stress resistance analysis of the long-lived mutant SRM11 was performed, using the semi-quantitative spot assay method. The results revealed that the mutant SRM11 highly resisted to copper stress. Also, SRM11 resisted to silver, phenylethanol, ethanol and boric acid stresses, indicating that these stress types may be related with chronological longevity.

Whole genome transcriptome of the long-lived mutant SRM11 was analyzed by using DNA microarray technology, to understand the molecular mechanisms of chronological longevity in yeast. DNA microarray analysis results revealed that 769 open reading frames (ORFs) were upregulated, 838 ORFs were downregulated by two-fold and higher in the long-lived SRM11 mutant, compared to the reference strain. For the interpretation of the gene expression change, Gene Ontology (GO) analysis was used. GO analysis of the upregulated genes indicated that oligosaccharide-carbohydrate metabolic biological process and response to oxidative stress were induced in SRM11. Furthermore, GO analysis of the downregulated genes revealed that ribosome subunits biogenesis, ribosome assembly and RNA processing were repressed in SRM11. These results suggest that repression of protein synthesis and activation of oligosaccharide-carbohydrate metabolic processes and response to oxidative stress are associated with the extension of chronological longevity in the yeast *S. cerevisiae*.

CLS of various stress-resistant *S. cerevisiae* mutants was also investigated by semi-quantitative and quantitative methods. Among the tested stress-resistant mutants, silver-resistant, ethanol-resistant, phenylethanol-resistant, oxidative stress-resistant mutants were determined as long-lived mutants. Resistance to oxidative stress has been shown to be related with chronological survival in yeast, however; resistance to silver, ethanol and phenylethanol stress has not been shown, yet. The present study, for the first time, showed that resistance to silver, ethanol and phenylethanol may be related with chronological longevity in the yeast *S. cerevisiae.*

In the current study, a comparative transcriptomic analysis of the long-lived stress resistant mutants (silver-resistant, phenylethanol-resistant and ethanol-resistant mutant and long-lived mutant SRM11) was also carried out to find a relationship between chronological longevity and stress resistance. The comparative transcriptomic analysis showed that 17 downregulated genes and 48 upregulated genes were overlapping in the long-lived and stress-resistant mutants. GO analysis of the overlapping upregulated genes showed that the upregulated genes were enriched in mostly oligosaccharide and carbohydrate metabolic process and generation of precursor metabolites and energy. GO analysis of the overlapping downregulated genes indicated that ribosomal subunits biogenesis and aminoacid transport biological process were repressed.

As a conclusion, the present study suggests that increased respirative metabolism, resistance to copper, silver, ethanol and phenylethanol stress, repression of protein synthesis and induction of oligosaccharide and carbohydrate metabolic processes are associated with chronological longevity in the yeast *S. cerevisiae.* Further detailed analyses at genomic and proteomic levels will help understand the complex molecular basis of the longevity in *S. cerevisiae.*

MAYA HÜCRELERİNDE UZUN YAŞAMIN MOLEKÜLER VE FİZYOLOJİK YÖNDEN İNCELENMESİ

ÖZET

Dünya popülasyonu, hem gelişmiş hem de gelişmekte olan ülkelerde, doğum ve ölüm oranlarındaki azalmadan dolayı, görece olarak yaşlanmaktadır. Bu durum büyük bir sorun oluşturmaktadır. Zamanla hücrelerin fizyolojik fonksiyonlarında gerçekleşen kayıplar nedeniyle yaşlanma; Alzheimer, Parkinson, diyabet, kanser ve kardiyovasküler hastalıklar gibi bazı ciddi hastalıklar için bir risk faktörüdür. Son yıllarda araştırmacılar, artan sosyoekonomik kaygılardan dolayı bu sorun üzerine odaklanmaktadırlar. Bu çalışmalardaki amaç, hücresel yaşlanma sürecinin anlaşılması ve sağlıklı bir yaşam sağlanmasıdır. Yaşlanma araştırmalarında *Saccharomyces cerevisiae* mayası, *Drosophila melanogaster* sineği, *Caenorhabditis elegans* kurdu, kemirgenler ve primatlar model organizma olarak kullanılmaktadır.

S. cerevisiae mayası tek hücreli ökaryotik bir mikroorganizmadır ve eski zamanlardan beri; ekmek, şarap ve bira yapımı gibi endüstriyel alanlarda kullanılmaktadır. *S. cerevisiae*, genetik ve moleküler biyolojik araştırmalarda pahalı ve özel besiyerlerine ve de kültür koşullarına gerek duymadığı için bir ökaryotik model organizma olarak yaygın şekilde kullanılmaktadır. *S. cerevisiae* mayası yaşlanma çalışmalarında; yaşam süresinin kısalığı, genom dizi verileri, memeli hücrelerine benzerliği ve mevcut olan kapsamlı moleküler araç ve tekniklerinden dolayı yaygın olarak tercih edilen bir model organizmadır.

Yaşlanma çalışmaları, *S. cerevisiae*'da kronolojik yaşam süresi ve replikatif yaşam süresinin incelenmesiyle iki yönden yürütülebilir. Replikatif yaşam süresi, *S. cerevisiae* hücrelerinin asimetrik bölünme geçirmesinden dolayı geliştirilmiştir. Bu yöntemde, yavru hücre mitoz bölünme sonrasında bir mikromanipülatör kullanılarak anne hücreden ayrılır ve bu işlem, anne hücre bölünmesini durduruncaya kadar sürdürülür. Mitozun sonunda bir anne hücrenin meydana getirdiği tomurcukların (bud) sayısı tespit edilir ve bu yavru hücrelerin (tomurcuk) sayısı, *S. cerevisiae*'nın replikatif yaşam süresidir. Kronolojik yaşam süresi ise, hücre üremesinin durağan evresindeki bölünmeyen hücrelerin hayatta kaldığı zamanın uzunluğudur. Bu yöntemde hücre canlılığı, üremenin durağan evresinin başlangıcında katı besiyerinde canlı hücre sayımı ile belirlenir. Bundan sonra, durağan evredeki bölünmesini durdurmuş (G_0) hücrelerin canlılığı izlenir. Kronolojik yaşam süresi yöntemi; (i) durağan evredeki maya hücrelerindeki hasarın zamanla artması, (ii) durağan evredeki hücrelerin hücre döngüsünden çıkmaları (G_0) ve (iii) bu hücrelerin enerjilerini mitokondriden sağlamaları nedeniyle, yüksek ökaryotik organizmaların bölünmeyen hücrelerinin (örn. nöronlar) yaşlanmasını çalışmak için de uygun bir model olarak kabul edilir.

Uzun yaşayan *S. cerevisiae*, *C. elegans* ve *Drosophila* mutantları hücresel yaşlanmanın mekanizmalarının anlaşılmasında büyük bir role sahiptir. Burada ilk olarak uzun ömürlü mutant suşlar elde edildiğinden ve sonrasında; bunun moleküler

temellerinin anlaşılması için detaylı incelemeler yapıldığından bu çalışmalar benzer yaklaşımlar sergilerler. Bu stratejiler, tersine metabolik mühendislik yaklaşımına da benzerlikler göstermektedir. Tersine metabolik mühendislik yaklaşımında ilk olarak istenilen fenotip elde edilir, sonra da bu fenotipin genetik mekanizmaları tespit edilir. Bu yaklaşım karmaşık bir genetiğe sahip, istenilen mikrobiyal fenotipleri elde etmek için çok güçlü bir yaklaşımdır. Bu yaklaşımdan, kronolojik olarak uzun ömürlü maya eldesi için henüz yararlanılmamıştır.

Bu çalışmada, tersine metabolik mühendislik yaklaşımı, kronolojik açıdan uzun ömürlü *S. cerevisiae* eldesi için kullanıldı. Ayrıca, model organizmalar kullanılarak yapılan literatürdeki yaşlanma çalışmaları, strese direnç ve uzun yaşam arasında yakın bir ilişki olduğunu gösterdiğinden, bu çalışmada; daha önce elde edilmiş olan strese dirençli *S. cerevisiae* mutantlarının kronolojik yaşam süreleri de ayrıca araştırıldı.

Tersine metabolik mühendislik yaklaşımıyla kronolojik olarak uzun ömürlü bir maya mutantı elde etmek için ilk olarak; etil metan sülfonat ile mutajenez yapılarak, başlangıç popülasyonunun genetik çeşitliliği artırıldı. Kalori kısıtlamasının yaşam süresini uzattığı bilindiği için, başlangıç mutant popülasyonunun ardışık olarak kesikli kültürleri, gittikçe düzeyi arttırılan kalori kısıtlamasıyla yapıldı. Bu ardışık kesikli kültürler süresince, besiyerinin glikoz konsantrasyonu, % 0.5'ten % 0.02'ye düşürüldü. Son kesikli kültürde, mutant popülasyonun büyüme oranları %10'a düştüğü için; seleksiyon işlemi sonlandırıldı. Bundan sonra mutant bireyler rastgele bir şekilde bu son popülasyondan seçildi. Yarı-kantitatif ve kantitatif kronolojik yaşam süresini tespit etme yöntemleri bu seçilen mutant bireylere uygulandı. Daha sonraki moleküler ve fizyolojik çalışmalar için, mutant bireyler içinde kronolojik olarak hayatta kalımı en yüksek olan mutant (SRM11 olarak adlandırılan) seçildi.

Katı besiyerinde canlı hücreleri sayma üzerine dayalı kantitatif kronolojik yaşam süresi tespit yöntemi; çok sayıda suşun ya da çok fazla koşulun test edildiği geniş ölçekli çalışmalar için, inkübasyon sırasında çok fazla sayıda pleyt ve kültür kabına gerek duyulması sebebiyle oldukça yorucu ve zahmetli bir yöntemdir. Bu nedenle bu çalışmada, mutant suşlarda kronolojik yaşam sürelerinin ön tespiti için yarı-kantitatif yöntem kullanıldı. Bu yönteme, yoğunlukları önemli derecede farklı olan kültürlerin kronolojik yaşam sürelerinin daha gerçekçi bir şekilde tespiti için kültür yoğunluklarını eşitleme adımı eklendi. Bu yarı-kantitatif yöntemin devamında, öne çıkan mutantların kronolojik yaşam sürelerinin analizi kantitatif yöntem ile de yapıldı. Bu süreç, başarılı bir şekilde uygulandı ve bir çok suş ve koşulda, kronolojik yönden uzun yaşayan fenotipler doğru bir şekilde belirlendi.

Mutant SRM11'in üreme özellikleri, biyokütle ve fizyolojik üreme analizleriyle araştırıldı. Bu deneylerdeki amaç, üreme fizyolojisi yönünden bir kayıp (trade-off) meydana gelip gelmediğinin tespitini yapmaktı. Analiz sonuçları, mutant SRM11'in hem kalorisi kısıtlanan besiyerinde (% 0.5 glikoz) hem de standart besiyerinde (% 2 glikoz) üreme özelliği yönünden bir kaybının olmadığını gösterdi. Bu çalışmada, besiyeri glikoz konsantrasyonunun %75 oranında düşürülmesi (%2'den %0.5'e) maya suşlarında, besiyerinde glikoz kullanılıyor olduğu zamanki büyüme oranlarını etkilemedi.

Yüksek basınçlı likit kromatografi (HPLC) analizi, uzun ömürlü mutant SRM11 ve referans suşun metabolik profillerini incelemek için kullanıldı. Bu amaçla kültür örneklerinin glikoz, etanol, gliserol ve asetat konsantrasyonları, HPLC analizleri ile izlendi. Referans suş ve mutant SRM11 arasında glikoz tüketimi açısından önemli

bir fark gözlenmemesine rağmen, fermentatif metabolitlerin üretiminde önemli bir fark gözlendi. Mutant SRM11 standart glikozlu besiyerinde (% 2) düşük miktarda etanol, gliserol ve asetat üretti. Bu bulgu, mutant SRM11'in metabolizmasında solunuma yönelişini ve de solunuma dayalı metabolizmanın, kronolojik yönden uzun yaşamla ilişikili olduğunu göstermektedir. % 0.5 glikoz besiyerinde, referans suş ve mutant SRM11' in kültürlerinde az miktarda etanol ve gliserol üretimi gözlendi. Bu durum; %0.5 glikoz konsantrasyonunda fermentasyonun sınırlı olduğunu göstermektedir.

Model organizmalardaki yaşlanma çalışmaları, stres direnci ile uzun yaşam arasında yakın bir ilişki olduğunu göstermektedir. Bu nedenle, uzun ömürlü mutant SRM11'de, strese direnç analizi, yarı-kantitatif damlatma yöntemi (spot assay) kullanılarak uygulandı. Sonuçlar mutant SRM11'in bakır stresine yüksek düzeyde dirençli olduğunu gösterdi. SRM11, ayrıca gümüş, feniletanol, etanol ve borik asit streslerine de direnç gösterdi. Bu sonuçlar, bu stres türlerinin kronolojik yönden uzun yaşamla ilişkili olabileceğini göstermektedir.

Mayada kronolojik yönden uzun yaşamın moleküler mekanizmalarını anlamak için DNA mikrodizi teknolojisi kullanılarak, uzun ömürlü mutant SRM11'in tüm genom transkriptomu analiz edildi. DNA mikrodizi analiz sonuçları, referans suşla karşılaştırıldığında, uzun yaşayan mutant SRM11'de iki-kat ve üstü 769 açık okuma bölgesi (ORF)'nin ifadesinin arttığını ve 838 açık okuma bölgesinin ifadesinin de azaldığını gösterdi. Gen ifadelerindeki bu değişimi yorumlamak için, Gen Ontoloji (GO) analizi kullanıldı. İfadesi artmış olan genlerin GO analizi, oligosakkarit-karbonhidrat metabolik biyolojik prosesleri ve oksidatif strese yanıt işlevlerinin SRM11'de aktive edildiğini gösterdi. Ayrıca, SRM11'de ifadesi azalan genlerin GO analizi, ribozomal altünite biyogenezi ve ribozomun bileşenlerinin bir araya gelmesi (assembly) ve RNA işleme süreçlerinin baskılandığını gösterdi. Bu sonuçlar, oligosakkarit-karbonhidrat metabolik prosesi ve oksidatif strese yanıt işlevinin artması ve protein sentezinin baskılanmasının, *S. cerevisiae* mayasında kronolojik yönden uzun yaşamın artırılması ile ilişkili olabileceğini önermektedir.

Çeşitli streslere dirençli *S. cerevisiae* mutantlarının kronolojik yönden yaşam süreleri de yarı-kantitatif ve kantitatif yöntemlerle araştırıldı. Test edilen strese dirençli mutantlar arasında, gümüşe-dirençli, etanole-dirençli, feniletanole-dirençli, oksidatif strese-dirençli mutantlar, uzun ömürlü mutantlar olarak tespit edildi. Oksidatif stres direncinin mayada kronolojik olarak hayatta kalma ile ilişkili olduğu gösterilmişti, fakat; gümüş, etanol, feniletanol streslerine dirence dair bir veri, literatürde mevcut değildi. Bu çalışma, *S. cerevisiae* mayasında gümüş, etanol ve feniletanole direncin, kronolojik yönden uzun yaşamla ilişkili olabileceğini ilk defa gösterdi.

Bu çalışmada ayrıca, stres direnci ve kronolojik yönden uzun yaşam arasındaki ilişkiyi belirlemek amacıyla, uzun ömürlü ve strese dirençli mutantların (gümüşe-dirençli, feniletanole-dirençli, etanole-dirençli mutantlar ve uzun ömürlü mutant SRM11) karşılaştırmalı transkriptomik analizleri yapıldı. Karşılaştırmalı transkriptomik analizler, uzun ömürlü ve strese dirençli mutantlarda ortak olarak 17 tane ifadesi azalan ve 48 tane ifadesi artan genin bulunduğunu gösterdi. İfadesi ortak olarak artmış genlerin GO analizi, bunların oligosakkarit-karbonhidrat metabolik prosesleri, enerji ve öncül metabolitlerin oluşumu ile ilgili biyolojik işlevlerde gruplandıklarını gösterdi. İfadesi ortak olarak azalmış genlerin GO analizi ise, ribozomal altbirimlerin oluşumu ve aminoasit taşınımı gibi biyolojik işlevlerin baskılandığını gösterdi.

Sonuç olarak bu çalışma; artan solunum metabolizmasının, bakır, gümüş, etanol ve feniletanol streslerine direncin, protein sentezinin baskılanmasının, oligosakkarit ve karbonhidrat metabolik proseslerinin aktive edilmesinin, *S. cerevisiae* mayasında kronolojik yönden uzun yaşamla ilişkili olabileceğini göstermektedir. Genomik ve proteomik düzeyde yapılacak detaylı analizler, *S. cerevisiae*'de uzun yaşamın karmaşık moleküler temellerinin anlaşılmasına yardımcı olacaktır.

1. INTRODUCTION

1.1 *Saccharomyces cerevisiae*

The yeast *Saccharomyces cerevisiae* is a facultative anaerobic, unicellular eukaryotic microorganism, and also known as baker's yeast or budding yeast. *S. cerevisiae* is systematically found in the fungi kingdom; its taxonomic classification is shown in Table 1.1.

Table 1.1 : Scientific taxonomy of *S. cerevisiae* (Solomon et al., 1999).

Kingdom	Fungi
Phylum	Ascomycota
Class	Hemiascomycetales
Order	Saccharomycetales
Family	Saccharomycetaceae
Genus	Saccharomyces
Species	*Saccharomyces cerevisiae*

S. cerevisiae cells can have a volume of 70-120 μm^3, and their shape is mainly oval-ellipsoidal with 5-10 μm diameters (Figure 1.1); however, the size is highly variable according to the environmental status (e.g. stress factors or availability of nutrients) and the age of the organism.

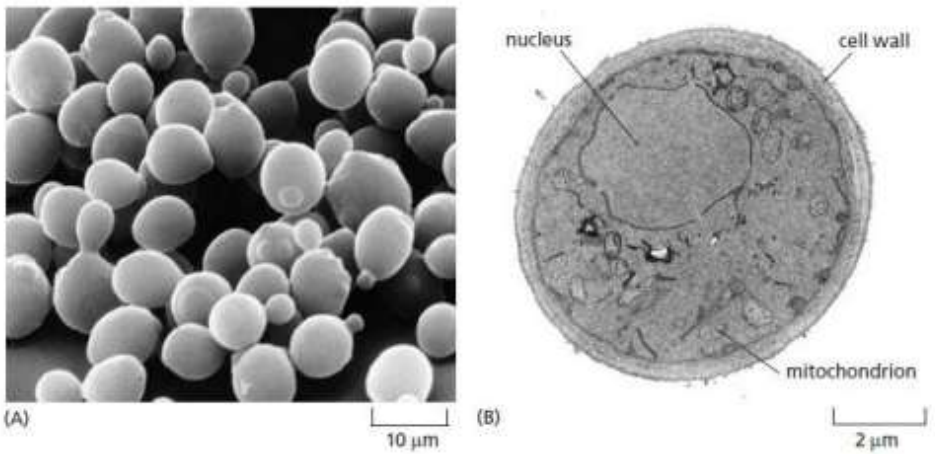

Figure 1.1 : Microscopic view of *S. cerevisiae.* (A) A scanning electron micrograph (SEM) image of the cluster of *S. cerevisiae* cells. (B) A transmission electron micrograph (TEM) image of the yeast *S. cerevisiae* (Alberts et al., 2008).

The cell wall of *S. cerevisiae* consists of mainly glucose, N-acetylglucosamine and mannose residues (Sherman, 2002). The cell wall has the function of stabilization of internal osmotic condition. Internal osmolarity of *S. cerevisiae* and the other fungi species is usually higher than outside of the cell. The cell wall controls the excessive water influx toward intracellular space, preventing cell lysis (Klis et al., 2006; Kollar et al., 1997).

The yeast *S. cerevisiae* can exist in both haploid (n) and diploid (2n, two homologous or heterologous copies of each chromosome) state. Reproduction of *S. cerevisiae* can be either vegetative or sexually. The both forms, 2n and n, can divide through mitosis. In mitosis, mother cell emerges as a small bud from the surface of the mother cell, which is defined as budding. This reproduction type is vegetative growth (Figure 1.2). After the mitotic cycle, a bud scar is formed on the cell wall. The number of buds formed by one mother cell is about 20-30 during its lifetime. The age of a cell can be determined by the number of bud scars formed on the cell wall (Lodish et al., 1995; Solomon et al., 1999).

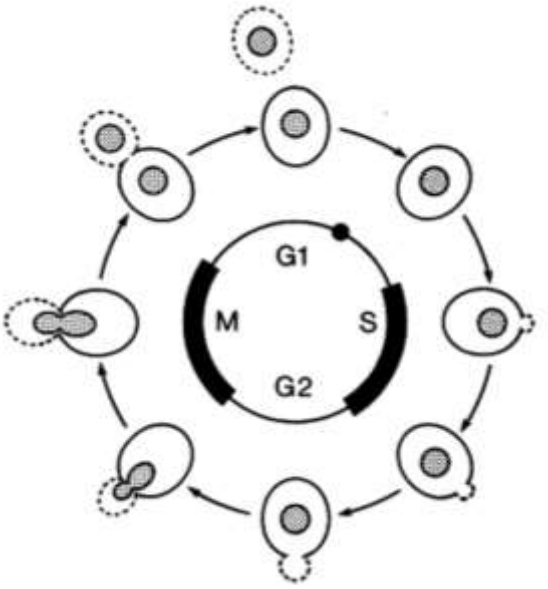

Figure 1.2 : Mitotic cell cycle of *S. cerevisiae* (Herskowitz, 1988).

Haploid *S. cerevisiae* can be either 'a' or 'α' mating type based on the allele at 'MAT' locus (MATa and MATα). Each mating type responds to the pheromones, a-factor or α-factor, of the opposite mating type. Different mating type cells detect each other and fuse when present in the same medium. The fusing of two different mating type cells results in the formation of a single diploid (2n) cell. Diploid cells

might undergo meiosis under nitrogen starvation conditions and form an ascus structure involving four ascospores, two of each mating type. This reproduction of *S. cerevisiae* cell is the sexual type (Figure 1.3) (Alberts et al., 2002; Herskowitz, 1988; Madigan and Martinko, 2006).

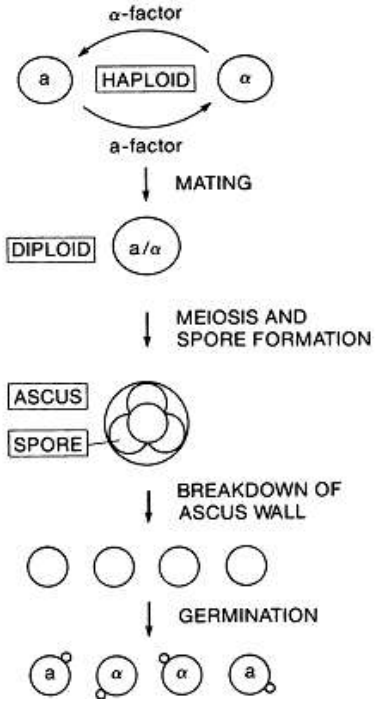

Figure 1.3 : Miotic cell cycle of *S. cerevisiae* (Herskowitz, 1988).

S. cerevisiae has sixteen chromosomes with a 12068 kilobases (kb) genome size. The yeast chromosome III was the first sequenced chromosome in 1992 (Oliver et al., 1992). After four years, all the yeast chromosomes were completely sequenced and made public (Goffeau et al., 1996). The whole genome of *S. cerevisiae* defines nearly 6000 open reading frames (ORFs) encoding protein or protein products (Goffeau et al., 1996). More than 90% of these genes have been deleted to find their potential functions (Cherry et al., 1998).

1.2 Industrial Importance of *S. cerevisiae*

S. cerevisiae is the most popular microorganism for both traditional and modern industrial production processes (Piskur et al., 2006). It is mainly used in baking, beer and wine production since thousand years and it is one of the earliest domesticated microorganism in history.

In baking, *S. cerevisiae* produces carbon dioxide (CO_2) as a result of the fermentation of fermentable sugars. This leads to a dough rise with a finer texture and gives flavour to the bread (El-Fiky et al., 2012; Shima and Takagi, 2009). In alcoholic beverages, beer and wine, *S. cerevisiae* is used to convert sugar into ethanol in the presence of fermentable sugars and other essential nutrients (Walker and Stewart, 2016). In addition to this usage of *S cerevisiae* in the food industry, it is directly used as a nutritional supplement for human diet, especially for low-meat and vegetarian diets since it is a rich source of vitamin B (Ratledge, 2001).

In the energy industry, *S. cerevisiae* has been used for bioethanol production from biomass resources such as lignocellulosic biomass, molasses, sweet sorghum cane extract, starch based substrate and other wastes (Sun and Cheng, 2002). Bioethanol production is a worldwide interested issue since natural energy resources such as petroleum and coal have been consumed at high rates, have negative effects on the environment and the fact that they might eventually run out (Siqueira et al., 2008). Bioethanol production also serves for pharmacology, cosmetics, medicine, food sectors as well as for transportation and fuel cell systems (Babu et al., 2011; Nigam and Singh, 2011; Zhao and Bai, 2009).

In the health industry, *S. cerevisiae* has also been used for the production of vaccine and some specific heterologous proteins. Production of Hepatitis B vaccine has been achieved by the expression of the surface antigens of Hepatitis B in *S.cerevisiae* (Emini et al., 1986; Moller et al., 2017).

1.3 *S. cerevisiae* as A Model Organism

S. cerevisiae is one of the most used unicellular eukaryotic model organism in molecular biology and genetics research. It does not need the use of expensive and special media for cultivation, and it has a fast growth rate (generation time is 90 min. under optimum conditions) in solid or liquid media, which make this organism easy to cultivate. In addition to this advantage, molecular methods such as gene deletion, disruption and replacement can be easily performed on it (Sherman, 1991). In fact, it is the first eukaryotic organism to have a transformed DNA (Hinnen et al., 1978). Besides, its whole genome has been sequenced (Goffeau et al., 1996), and a large amount of data and information are available (*e.g*. The Saccharomyces Genome Database; SGD). Furthermore, it has similarity (as homolog and ortholog) to

mammalian cells. Its genome has 30.8% homology with the mammalian genome (p-value: $1x10^{-10}$) (Botstein et al., 1997). A range of genes which play important roles in human genome has also close homology with yeast genome (Table 1.2).

Table 1.2 : Sequence similarity of some of the yeast genes and its human homolog (Botstein et al., 1997).

Yeast Gene	Human homolog	% Similarity of Sequence	p-value
ACT1	Cytoskeletal gamma actin	94	$1.4x10^{-243}$
RHO1	GTP-binding, Ras-like (bovine *RHO*)	81	$3.1x10^{-92}$
CDC28	Cell cycle control (*CDC2*)	78	$5.0x10^{-130}$
SOD1	Superoxide dismutase (*SOD-1*)	69	$8.9x10^{-56}$
MSH2	Mutator gene (*MSH2*, colon cancer)	65	$3.8x10^{-255}$
GEF1	Voltage-gated chloride ion channel	58	$3.4x10^{-95}$
YCF1	Cystic fibrosis conductance regulator (*CFTR*)	57	$2.4x10^{-157}$

Owing to all these advantages, *S. cerevisiae* has taken a pivotal role as a model organism in human disease research (Karathia et al., 2011). Discovery of the fundamental genetic and cellular processes such as cell cycle regulation (Hartwell, 2002), intracellular transport (Nakano, 2004) and regulation of protein folding (Lindquist et al., 2009) has been achieved by the studies performed in *S. cerevisiae*.

1.4 Aging

Population aging is a common and regularly growing issue of today's world. (Harford, 2009; Sanderson and Scherbov, 2007; Zweifel et al., 1999). According to United Nations (UN)'s aging report, there were 48% more elderly people (60 years or over) in 2015 than that of in 2000 worldwide. The number of elderly people is predicted to be tripled from 2000 until 2050 (Figure 1.4). In contrast to the elderly population, it is predicted that the number of children (under age 10 and age between 10 and 24) will not change significantly until 2050. Besides, the population of adults who are 25-59 years old is growing faster than that of children. These data clearly show that elderly population is growing dramatically due to the declining death and birth ratio in the world.

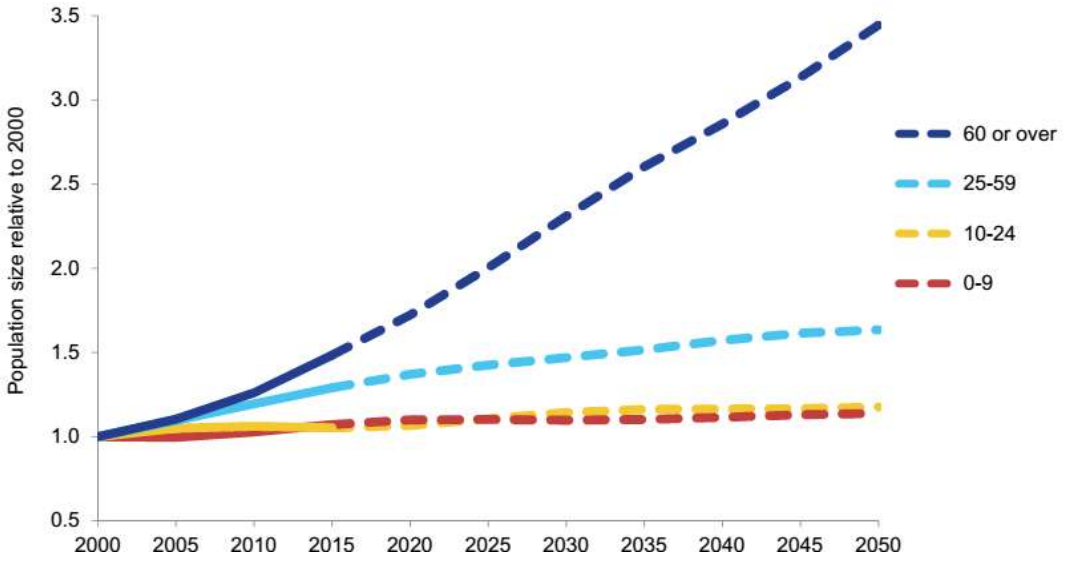

Figure 1.4 : Changes in global population of broad age group in 2015 relative to 2000, and estimated global population of these ages until 2050 (Url-1).

According to UN's report (Url-1), China has the highest number of elderly people for both 60-80 years old and 80 years old or over. It can be said that nearly one in four persons is elderly (60 years old or over) in China. The only five countries: China, India, the United States, Japan and the Russian Federation accounted for half of the world's elderly population (aged 60 years or over). In 2015, China, the United States, India, Japan and Germany had 48 percent of the world's population aged 80 years or over (Figure 1.5).

Turkey ranked as the 20th in the list of the highest elderly population (60 years old and over) in the world. According to Turkey Statistics Institution (TSI) data (Url-2), aged population of 65 years old and over was 3.3% in 1950, it increased to 4.3% in 1990 and reached 7.7% in 2013. TII estimates that Turkey's aged population will rise up to 10.2% and 20.8% until 2023 and 2050, respectively.

Aging is an inevitable, highly complex and multifactorial biological phenomenon for both multicellular and unicellular eukaryotic organisms (Goldberg et al., 2009; Guarente et al., 2008; Nigam et al., 2012). Disorders arising from repair and detoxification mechanisms with aging lead to the build-up of damage on DNA and proteins in the cell. Thus, it results in several age-related and neurodegenerative disorders including Alzheimer's disease, Parkinson's disease, Huntington's disease and Amyotrophic lateral sclerosis, cancer and cardiovascular diseases (Niccoli and Partridge, 2012; Nicholls, 2002). Due to age-related diseases, aging indirectly results

in loss of well-qualified labor, and an increase in health care costs. Thus, it has both economical and social importance.

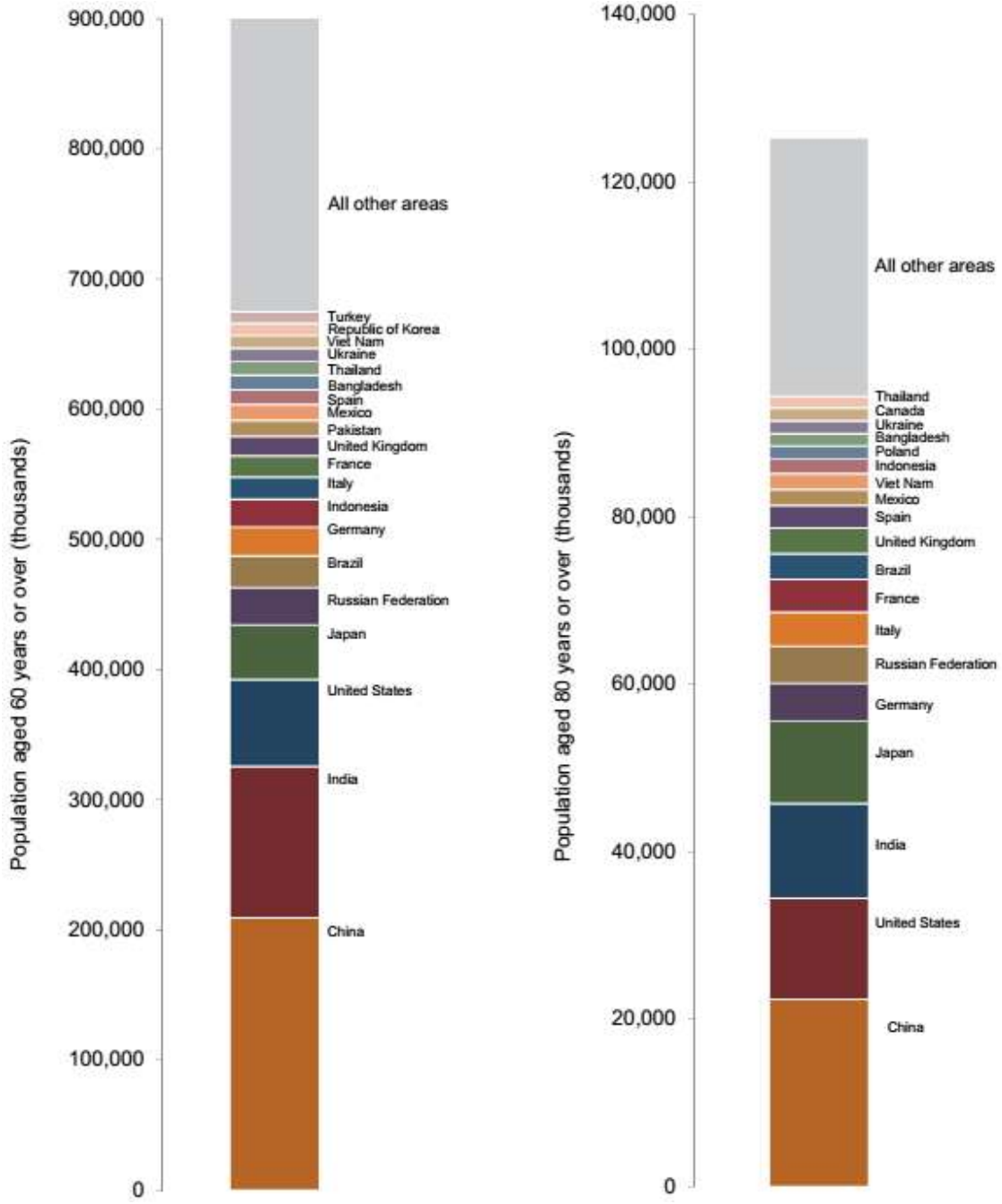

Figure 1.5 : The histogram of population aged 60 years or over (left) and 80 years or over (right) in various countries in 2015 (Url-1).

1.5 *S. cerevisiae* as a Model of Aging

Given that population aging is a fact and a socioeconomic concern, aging studies have become important. If these studies provide genetic and cellular mechanisms of

aging, healthy aging can be achieved, the incidence of age-related diseases can be reduced, and eventually loss of well-qualified labor can be decreased and, costs of health care of elderly can be reduced (Longo et al., 2012). In recent years, a variety of studies have been carried out to achieve these goals. In these studies, *S. cerevisiae*, *Drosophila melanogaster*, *Caenorhabditis elegans* and *Mus musculus* have been extensively used as model organisms (Harrison et al., 2009; Honjoh and Nishida, 2011; Lin et al., 2014). Among these model organisms, *S. cerevisiae* is commonly preferred in aging studies because of the shortness of its life span (5-10 days), availability of its complete genome sequence data and extensive molecular tools and techniques (Goffeau, 2000; Sherman, 1991). Aging studies in *S.cerevisiae* can be performed in two ways; replicative and chronological aging/lifespan (Longo et al., 2012).

1.5.1 Replicative lifespan

Replicative lifespan (RLS) is the number of daughter cells (budding) formed by one mother cell. RLS is developed because of the asymmetrical division of *S. cerevisiae*. The replicative aging is the result of the mitotic division of yeast cells. For RLS determination, the daughter cell is separated after mitosis from the mother cell by using a micromanipulator, and the process is continued until the mother cell stops division. At the end of limited mitosis, the number of buds that one mother cell produced is determined and expressed as RLS (Mortimer and Johnston, 1959) (Figure 1.6). Laboratory yeast strains generally produce about 25 daughter cells, which require 2-3 weeks (Steffen et al., 2009). During the cell division in yeast, extrachromosomal ribosomal DNA circles (ERCs) segregate asymmetrically to the mother cells, which is the major reason for the replicative senescence in the yeast (Sinclair and Guarente, 1997). *SIR2* gene is one of the most popular aging genes in yeast. It encodes a sirtuin family on NAD-dependent protein deacetylases and extends RLS of yeast preventing the formation of ERCs (Kaeberlein et al., 1999).

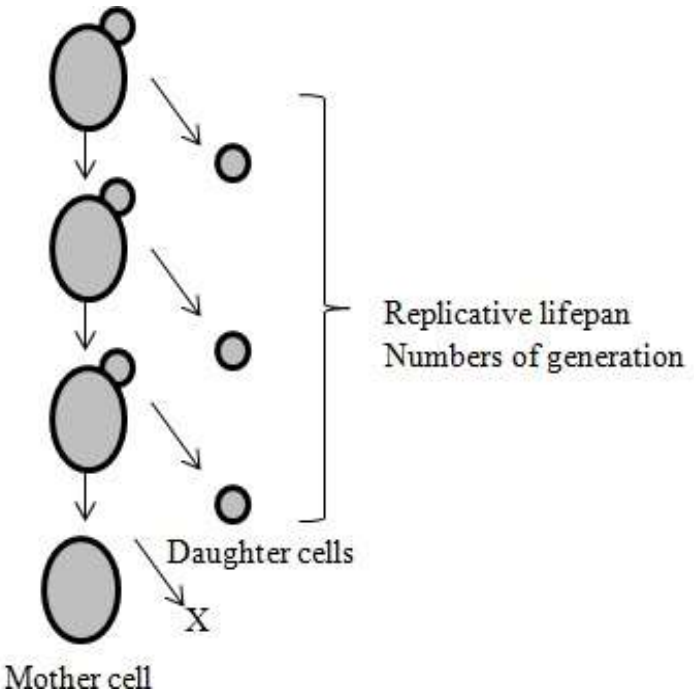

Figure 1.6 : Replicative lifespan of *S. cerevisiae*.

1.5.2 Chronological lifespan

Chronological lifespan (CLS) is the length of the time in which non-dividing (G_0) stationary phase yeast cells survive. The ability of the stationary phase yeast cells to survive is an essential feature for both aging research and industrial applications.

In batch, aerobic cultures, *S. cerevisiae* uses glucose in the medium in a respirofermentative way: ethanol is produced until glucose depletion. When glucose in the medium is depleted, the cell growth stops and the cells switch to the mitochondrial respiration mode. In this step, after the switch to respiration, two-carbon metabolites such as ethanol and glycerol are utilized, and cells restart growing at a reduced rate. This second growth phase is called post-diauxic growth. After post-diauxic growth, cells enter the stationary phase, cell division stops, and the cell density remains constant (Figure 1.7) (Busti et al., 2010). At the beginning of the stationary phase (generally the third day of cultivation), the viable cell number in the culture is determined by the viable cell counting method and the viability is tracked and the survival time of the non-dividing (G_0) stationary phase yeast cells (CLS) is determined (Figure 1.8).

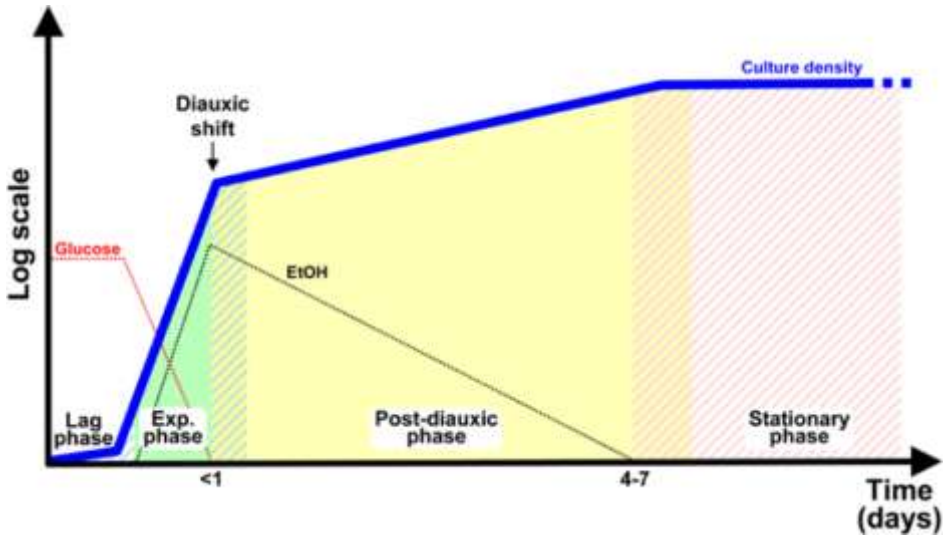

Figure 1.7 : Growth phases of *S.cerevisiae* in batch, aerobic cultivation with glucose as the carbon source (Busti et al., 2010).

CLS of the yeast cells resembles the aging of non-dividing cells (G_0) or postmitotic tissue of the higher eukaryotic organisms. Therefore, it is an important model to study aging of higher eukaryotes (Bishop and Guarente, 2007; Fabrizio and Longo, 2007; Harris et al., 2003; Longo et al., 1996; MacLean et al., 2001; Maclean et al., 2003). According to Longo et al. (1996), CLS resembles the aging of higher eukaryotic organisms since (i) stationary phase cells produce energy from mitochondria, (ii) damage accumulates over time and (iii) cells exit from the cell cycle (G_0).

The fundamental cellular aging processes including Tor/S6K and Ras/Adenylate cyclase (AC)/PKA have been elicited using CLS method in the yeast *S. cerevisiae*. The Tor/S6K pathway is mainly activated by amino acids and other nutrients (Fabrizio et al., 2001), whereas the Ras/adenylate cyclase (AC)/PKA pathway is principally activated by glucose, but also affected by other nutrients (Fabrizio et al., 2003; Longo, 1999). Tor1 is highly conserved phosphatidylinositol kinase kinase family serine/threonine kinase enzyme (Schmelzle and Hall, 2000). Also, Tor1 is a specific receptor of rapamycin which is an immunosuppressive and antiproliferative drug. Pharmacological or genetic inhibition of TOR/S6K pathway results in an extension of life span in the yeast (Powers et al., 2006). In line of the yeast CLS discovery, Tor1 signaling inhibition led to an extension of mice lifespan and healthspan (Harrison et al., 2009).

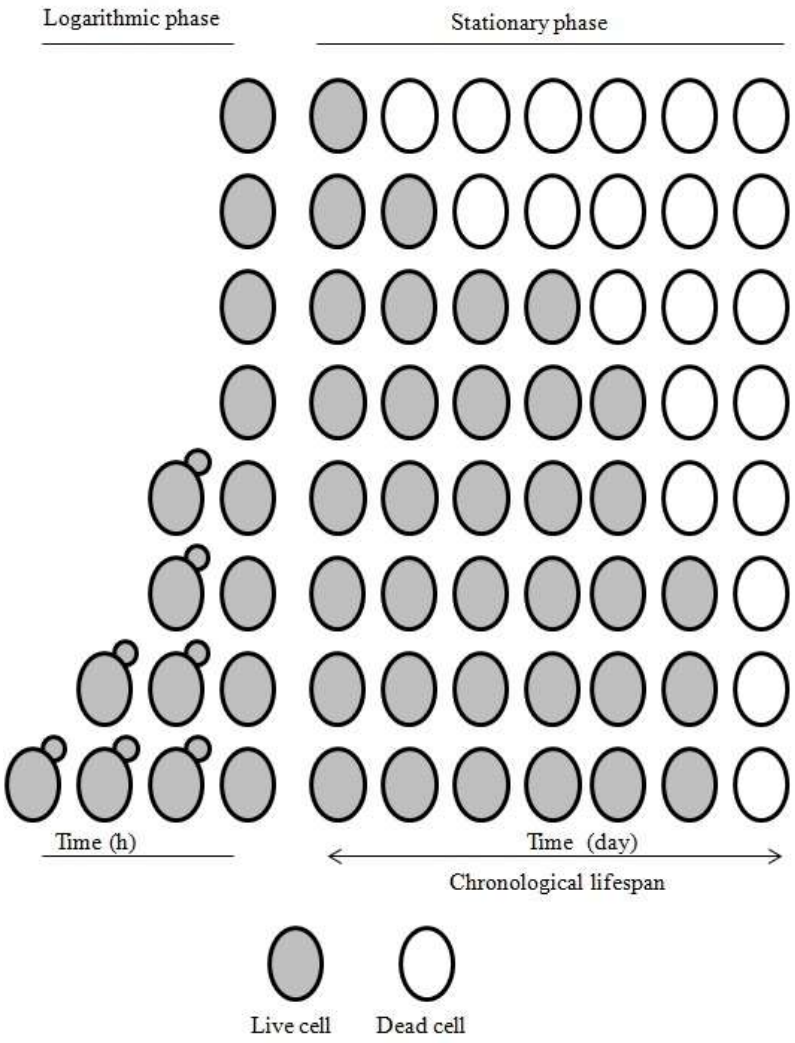

Figure 1.8 : A schematic view of CLS of *S. cerevisiae.*

1.6 Metabolic engineering approaches

1.6.1 Rational metabolic engineering

Metabolic engineering was defined by Bailey in 1991 as "the improvement of cellular activities by manipulation of enzymatic, transport, and regulatory functions of the cell with the use of recombinant DNA technology" (Bailey, 1991). In this approach, a deep knowledge of the genetic, biochemical and functional mechanisms of the desired phenotype is required to achieve the desired goals or the desired phenotypes. This is the major limitation of rational metabolic engineering approach for many studies. The other limitation is the complexity of cellular metabolic responses since the cell activates an alternative metabolic pathway as a response to the inhibition of an existing pathway. Another limitation of this approach is the difficulty of cloning in industrial strains due to their genetic complexity such as

polyploidy, or issues related to the use of genetically modified organisms (GMO) in the food industry (Bailey, 1991; Bailey et al., 1996; Çakar et al., 2012). Due to these limitations, an alternative strategy called inverse metabolic engineering has been introduced (Bailey et al., 1996).

1.6.2 Inverse metabolic engineering

Inverse metabolic engineering strategy has been developed as an alternative strategy to overcome limitations of rational metabolic engineering strategy. In the inverse metabolic engineering approach; first, the desired phenotype is obtained, second, the genetic mechanisms and the cellular pathways of the obtained phenotype are identified, and then, the phenotype is endowed to another organism relevant for industrial production (Bailey et al., 1996) (Figure 1.9).

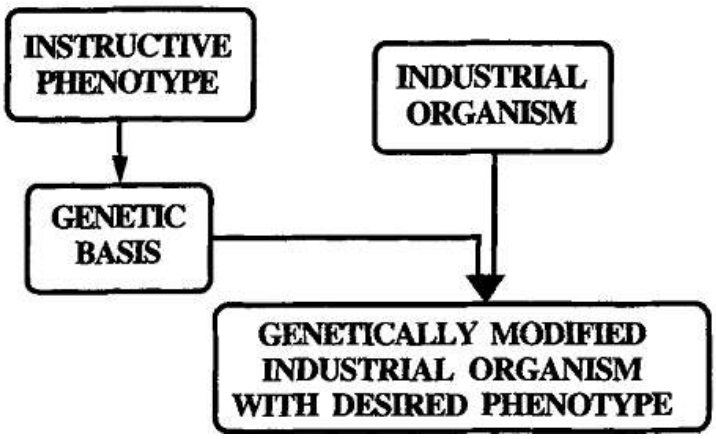

Figure 1.9 : Basics of the inverse metabolic engineering (Bailey et al., 1996).

Evolutionary engineering is an inverse metabolic engineering approach. It consists of repeating cycles of variation and selection of the phenotype of interest (Figure 1.10). In evolutionary engineering, a chemical and/or physical random mutagenesis followed by a systematic selection process is used to obtain desired phenotypes (Çakar, 2009). Chemical mutagenesis (e.g. ethyl methane sulfonate) followed by a selection which involves a systematic application of the stress factors, have been successfully used to obtain stress-resistant yeast strains in various studies (Alkım et al., 2013; Çakar et al., 2009; Çakar et al., 2005; Küçükgöze et al., 2013; Sen et al., 2011). The major advantage of evolutionary engineering is to provide genetically complex desirable phenotypes without the need for extensive genetic or biochemical information.

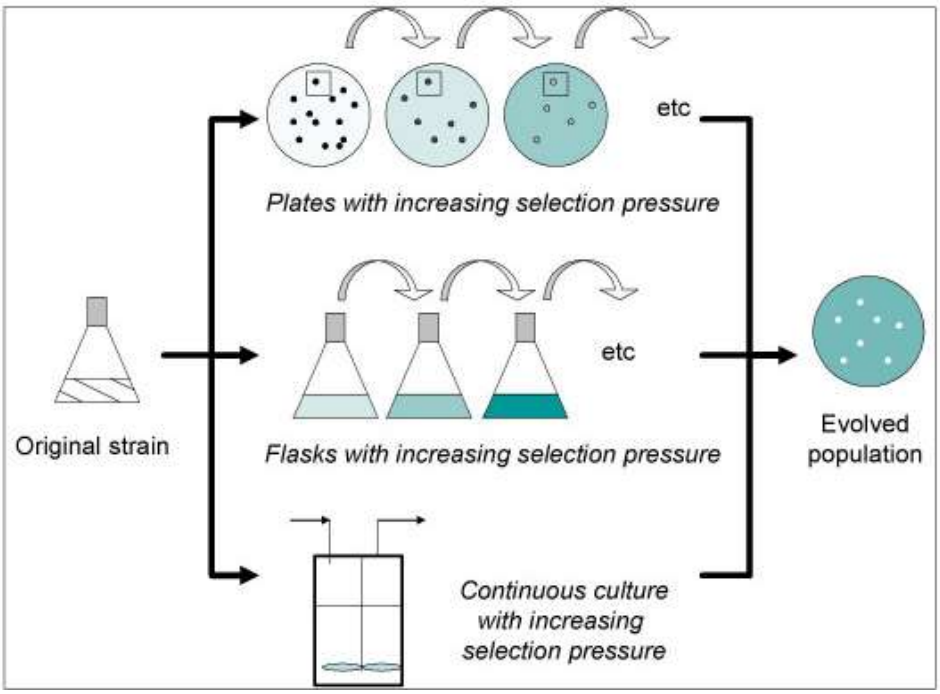

Figure 1.10 : A schematic view of evolutionary engineering (Hahn-Hagerdal et al., 2005).

1.7 Aim of the study

The aim of this thesis study was, first, to obtain a chronologically long-lived *S. cerevisiae* strain using evolutionary engineering strategy and to investigate the underlying genetic and cellular mechanisms of that phenotype. The second aim of the study was to investigate CLS of stress-resistant *S. cerevisiae* strains which had been previously obtained using inverse metabolic engineering strategy, as longevity is associated with stress resistance (Cypser and Johnson, 1999; Martin et al., 1996; Murakami and Johnson, 1998).

2. MATERIALS AND METHODS

2.1 Materials

2.1.1 Yeast strains

S. cerevisiae strain CEN.PK 113-7D (van Dijken et al., 2000) (*MATa, MAL2-8^c, SUC2*) was used as the reference strain (called as 905) which was kindly provided by Dr. Laurent Benbadis from the University of Toulouse, France.

The chronologically long-lived mutant SRM11 was obtained in this study, using evolutionary engineering, an inverse metabolic engineering approach (Section 2.2.1.2).

The stress-resistant *S.cerevisiae* mutants used in this study are shown in Table 2.1. All of these mutants have been previously obtained, by using evolutionary engineering based on ethyl methane sulfonate (EMS) mutagenesis and batch selection under relevant stress conditions.

Table 2.1 : The stress-resistant *S. cerevisiae* mutant strains used in this study.

Name	Description of the strain	Reference
M9	Nickel-resistant *S.cerevisiae*	(Küçükgöze et al., 2013)
CI25E	Cobalt-resistant *S.cerevisiae*	(Alkım et al., 2013)
B2 and B8	Ethanol-resistant *S.cerevisiae*	(Turanli-Yildiz et al., 2017)
T8	NaCl-resistant *S.cerevisiae*	(Sezgin, 2010)
F1	Freeze-thaw resistant *S.cerevisiae*	(Yılmaz Ü, 2013)
C9	2-phenylethanol-resistant *S.cerevisiae*	(Holyavkin, 2013)
H7	Hydrogen peroxide-resistant *S.cerevisiae*	(Yılmaz, 2009)
FD11	Propolis-resistant *S.cerevisiae*	(Demir, 2016)
F3	SO_2-resistant *S.cerevisiae*	(Korkmaz, 2011)
2E	Silver-resistant *S.cerevisiae*	(unpublished-E.Terzioğlu)
M8FE	Iron-resistant *S.cerevisiae*	(Balaban, 2016)

2.1.2 Yeast culture media

In this study, 2% (w/v) glucose –Yeast Minimal Medium (YMM), Yeast extract-peptone-dextrose (YPD) medium, and Calorie-restricted (CR) medium were used for cultivation or selection experiments. The ingredients of 2% YMM and YPD are shown Table 2.2 and Table 2.3, respectively. To prepare CR medium, only the glucose concentration of YMM was restricted.

Table 2.2 : Composition of yeast minimal medium (2% YMM).

Ingredient	Amount
Yeast nitrogen base without amino acids	6.7 g
Glucose	20 g
Agar (for solid media)	20 g
Distilled water (dH_2O)	up to 1 L

Table 2.3 : Composition of yeast extract peptone dextrose medium (YPD).

Ingredient	Amount
Yeast extract	10 g
Glucose	20 g
Peptone	20 g
Agar (for solid media)	20 g
dH_2O	up to 1 L

2.1.3 Cultivation and conservation conditions

Cultivation of yeast strains was carried out at 30°C and 150 rpm in 2% YMM, CR-YMM or YPD medium (nutrient-rich medium). Stock cultures of yeast strains were stored in 30% (v/v) glycerol in 1.5 ml microcentrifuge tubes in a -80°C deep freezer. The frozen stock cultures were inoculated in 10 ml of YPD medium in 50 ml culture tubes and incubated overnight at 30ºC and 150 rpm in a rotary shaker. Precultures of yeast strains, unless otherwise stated, were prepared from the overnight cultures grown in YPD medium. Overnight grown cultures in YPD were washed twice with 2% YMM and inoculated into fresh 2% YMM to an initial OD_{600} of 0.1 and incubated overnight (≈16 h) at 30ºC and 150 rpm.

2.1.4 Chemicals, kits/enzymes, equipments and software

The list of kits and enzymes used in this study is shown in Table 2.4.

Table 2.4 : Kits and enzymes used in this study.

Kits and Enzymes	Company	Country
RNeasy Mini Kit	Qiagen	Germany
Agilent RNA 6000 Nano Kit	Agilent	USA
RNA Spike-In Kit One-color	Agilent	USA
Absolutely RNA Nanoprep Kit	Agilent	USA
Gene expression Hybridization Kit	Agilent	USA
Gene Expression Wash Buffers	Agilent	USA
Hybridization Chamber gasket slides (8 microarrays/slide)	Agilent	USA
Low Input Quick Amp Labeling Kit	Agilent	USA
RNA 6000 Nano LabChip Kit	Agilent	USA
Lyticase	Sigma	USA
DNase	Qiagen	Germany

The list of equipment used in this study is shown in Table 2.5.

Table 2.5 : List of equipment used in this study.

Equipment	Company	Country
Laminar Flow Hood	Biolab Faster BH-EN 2003	Italy
Autoclave	Zealway GR110DF	USA
Autoclave	Tuttnauer Systec Autoclave 2540ml - 2870ELVC	Switzerland
Autoclave	Tomy SX 700E	China
Benchtop Centrifuge	Beckman Coulter Allegra 25R	USA
Microfuge	Eppendorf Centrifuge 5424	Germany
Ultracentrifuge	Beckman Coulter, Avanti J-30I	Germany
Deep Freezer (-80ºC)	Sanyo (-80°C) Ultra Low MDT- U40865	Japan
Microwave oven	Beko	Turkey
Refrigerator (+4ºC, -20ºC)	Arçelik 3011 NY	Turkey
Electrophoresis system	BioRad	USA
Gel illustration system	Biolab	Turkey
Ultrapure Water System	USF-Elga UHQ	USA
Glass slides for microarray analysis	Agilent	USA
Hybridization Chamber	Agilent	USA
Hybridization oven rotator for Agilent Microarray Hybridization Chambers	Agilent	USA
Hybridization oven	Agilent	USA
Agilent Bioanalyzer 2100	Agilent	USA
Agilent Microarray Scanner	Agilent	USA

Table 2.5 (continued): List of equipment used in this study.

Equipment	Company	Country
Nanodrop	Thermo Fisher Scientific 2000	USA
High Pressure Liquid Chromatography	Shimadzu	Japan
Aminex©HPX-87H column	BioRad	USA
Thermal Cycler	Bio-Rad My cyclerTM	USA
Thermal Cycler	TC-412 Techne	USA
Thermomixers	Eppendorf, Thermomixer Comfort	Germany
Spectrophotometer	Shimadzu UV-1700	Japan
Microplate Reader	Biorad Model 3550 UV	USA
Orbital Shaker Incubators	Certomat S II Sartorius	
Incubator	Nüve EN400 - EN500	Turkey
Balance	Precisa BJ 610 C - 620 SCS	Switzerland
pH-meter	Mettler Toledo MP220	Germany
Light Microscope	Olympus CH30	USA
Magnetic Stirrer	Labworld	Germany
Water Bath	Julabo SW22	Germany
Micropipettes	Eppendorf	Germany
Vortex mixer for chip	MS2-S8/MS2-S9, IKA	China
Vortex mixer	Heidolph REAX top	Germany

Software and websites used in this study are shown in Table 2.6.

Table 2.6 : The software and websites used in this study.

Software and websites	
Saccharomyces genome database (SGD)	http://www.yeastgenome.org/
YEASTRACT	http://www.yeastract.com
FunCat	http://mips.helmholtz-muenchen.de/funcatDB/
SGD, GO Slim Mapper	http://www.yeastgenome.org/cgi-bin/GO/goSlimMapper.pl
GeneSpring	GeneSpring 12.6 version, Agilent Tech.
Primer-3-Plus	http://www.bioinformatics.nl/cgi-bin/primer3plus/primer3plus.cgi
2100 Expert software	Agilent Tech.

2.2 Methods

2.2.1 Inverse metabolic engineering approach to obtain chronologically long-lived *S.cerevisiae*

Evolutionary engineering strategy was applied as an inverse metabolic engineering approach. Chemical mutagenesis (EMS) was applied to the reference strain (905) to increase the genetic diversity of the starting population before selection. EMS mutagenesis of the reference strain was applied such that 10% of the initial culture survived the mutagenesis procedure (Lawrence, 1991). That chemically mutagenized culture (called 906) with increased genetic diversity was used in the batch selection experiments of evolutionary engineering, as described previously (Çakar et al., 2009; Küçükgöze et al., 2013; Turanli-Yildiz et al., 2017). In this study, gradually increasing levels of caloric restriction (starvation stress) was used as the selection strategy to obtain chronologically long-lived *S. cerevisiae.*

2.2.1.1 Glucose screening experiment

In this experiment, the growth of *S. cerevisiae* in 2% YMM (control) and various CR media (0.50%, 0.45%, 0.40%, 0.35%, 0.30%, 0.25%, 0.12%, 0.08%, 0.05% and 0.02% [glucose (w/v)]) was investigated by spectrophotometric analyses at 600 nm wavelength. Overnight cultures of 905 and 906 in 2% YMM were inoculated into 10 ml fresh 2% YMM or 10 ml defined CR media (described above) in 50 ml-test tube to an initial OD_{600} of 0.2, and incubated at 30ºC and 150 rpm. Cell growth of 905 and 906 in CR media and in 2% YMM was determined by spectrophotometer at the 24th h of incubation. Then, the growth ratio of 905 and 906 was calculated. The growth ratio was determined by dividing OD_{600} of the calorie-restricted culture to that of the control (standard glucose) culture (2.1).

$$Growth\ ratio = \frac{OD_{600}\ value\ of\ the\ calorie\text{-}restricted\ group}{OD_{600}\ value\ of\ the\ control\ group} \tag{2.1}$$

2.2.1.2 Selection strategy under increasing caloric restriction conditions

The selection strategy involved successive batch cultivation of the EMS-mutagenized culture (906) in gradually increasing caloric restriction conditions. For this aim, the glucose concentration of the medium was gradually decreased between each

successive passage, which varied between 0.5% and 0.02% (w/v) glucose. Briefly, overnight grown EMS-mutagenized culture (906) in 2% YMM was inoculated both in 10 ml 0.5% YMM (initial CR medium) and 10 ml 2% YMM (Control) in 50 ml culture tubes to an initial OD_{600} of 0.2, and incubated at 30ºC and 150 rpm for 24 h. After the incubation, OD_{600} values of the cultures were determined by a spectrophotometer, and their growth ratio was determined using equation (2.1). The culture that grew in 0.5% YMM was named as the first population. The first population was centrifuged at 10.000xg for 3 min, and washed twice with sterile distilled water and then inoculated into 10 ml 0.48% YMM and 10 ml 2% YMM (in two separate culture tubes) to an initial OD_{600} of 0.2 to obtain the second population. For each successive passage, an aliquot of 1 ml culture was washed twice with sterile distilled water and stored in 30% (v/v) glycerol at -80°C. Following this procedure, the glucose concentration of the medium was decreased from 0.5% up to 0.02% until the last (53^{rd}) population.

2.2.1.3 Obtaining individual mutants

The last population (53^{rd}) was diluted 10-fold in sterile distilled water (from 10^{-1} to 10^{-6}). 100 µl from both 10^{-4} to 10^{-5} dilutions were spread on 2% YMM agar plates. The spread plates were incubated at 30ºC for 72 h. After incubation, single colonies were obtained, and 12 individual mutants (from single colonies) were randomly picked up from the 10^{-4}-diluted (appropriate dilution) on YMM plate. The individual mutants were inoculated in 10 ml YPD in 50 ml culture tubes and incubated overnight (≈16 h). Next day, 1 ml of overnight cultures were centrifuged and washed twice with sterile distilled water and stored at -80ºC in 30% (v/v) glycerol.

2.2.1.4 Semi-quantitative CLS analysis of individual mutants

Growth phase analysis in different calorie containing medium

CLS of mutant individuals was investigated by semi-quantitative CLS method (spot assay). CLS experiment begins at the beginning of the stationary phase of growth (Fabrizio and Longo, 2003). Therefore, first, growth phase analysis was performed in 2% YMM and CR media (0.25% and 0.5% glucose) to find out when the yeast cells enter the non-dividing stationary phase. For this purpose, overnight preculture of the reference strain was incubated in 20 ml 2% YMM, 0.5% YMM and 0.25% YMM in 100 ml flasks to an initial OD_{600} of 0.1. Incubation was performed at 30°C and 150

rpm. In defined time intervals, optical density (OD_{600}) of the cultures was measured by spectrophotometer upon appropriate dilutions. The experiment was performed in triplicate.

Semi-quantitative CLS assay

Quantitative CLS method based on viable cell counting on serially diluted plates can be labor-intensive and challenging for testing a high number of strains due to the requirement of a range of flasks for incubation. Therefore, CLS of mutant individuals was preliminarily determined by the semi-quantitative method. Semi-quantitative CLS assay was carried out by improving the previously described method (Smith et al., 2007a). In the present study, an initial cell density adjustment step was introduced to the method. Briefly, overnight precultures of the mutant individuals and the reference strain were transferred into 20 ml fresh CR medium (0.5% YMM or 0.25% YMM) in 100 ml flasks to an initial OD_{600} of 0.1 and cultivated at 30°C and 150 rpm. OD_{600} of the cultures were measured on the first day (stationary phase of growth) of incubation. The first day was considered as 'day 0' of the CLS experiment. Samples were withdrawn from cultures and their OD_{600} values (at stationary phase) were determined and adjusted to 6 ($\approx 1.2x10^8$cells/ml). Ten-fold serial dilutions (from 10^{-1} to 10^{-4}) of these cultures were obtained in sterile distilled water. Next, five µl each of the cultures at $OD_{600} = 6$ (10^0) and their dilutions (from 10^{-1} to 10^{-4}) were spotted onto YPD plates. The plates were then incubated at 30ºC for 72 h and photographed. During the CLS experiment, the same procedure (sampling, adjustment of OD_{600} to 6 according to OD_{600} of the first day, serial dilutions and spotting onto YPD plates) was repeated every second day. At the end of the experiment, images belonging to different time points were cut and joined to a single image to evaluate CLS of the strains (Arslan et al., in press)(Figure 2.1).

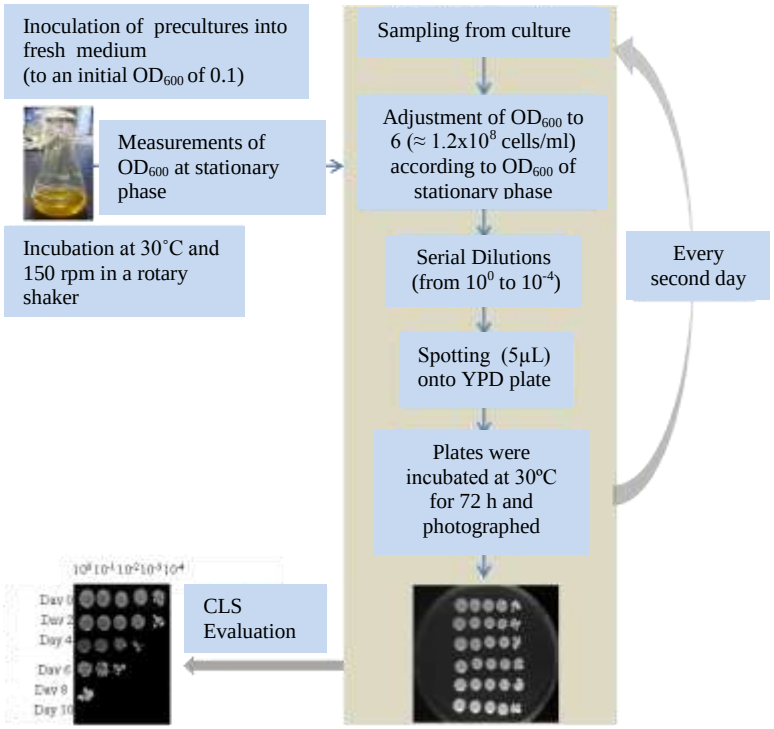

Figure 2.1 : The semi-quantitative CLS method. Yeast cells were inoculated into shake flasks and incubated at 30ºC and 150 rpm. At the stationary phase of growth, their OD_{600} values were determined and adjusted to 6. The samples were diluted and spotted onto YPD plates. After three days of incubation, plates were photographed. This procedure was repeated every second day (Modified from Arslan et al., in press).

2.2.1.5 Quantitative CLS assay of the selected mutant SRM11 in 0.5% YMM

To verify the semi-quantitative CLS results and to determine quantitatively CLS of the prominent mutants, traditional CLS method was performed in CR media (0.25% or 0.5% YMM), as described previously (Fabrizio and Longo, 2003; Longo et al., 2012). Briefly, overnight precultures of the mutant individuals and the reference strain were inoculated into 20 ml CR medium (0.25% YMM or 0.5% YMM) in 100 ml flasks (culture volume to flask volume ratio 1:5) to an initial OD_{600} of 0.1 and were incubated until the stationary phase of growth (the first day). At this time point, the initial viability of the culture was determined by viable cell counting (Colony forming unit-CFU). For this aim, 100 µl samples were withdrawn from cultures, and diluted by 10-fold in sterile distilled water, and then spread onto YPD plates. The plates were incubated at 30°C for 72 h. The initial viability was considered as 100% viability and ‘day 0’ of the CLS experiment. Every second day; viability of the cultures was determined and the viability of the cultures was monitored (Figure 2.2). The experiment was performed in triplicate.

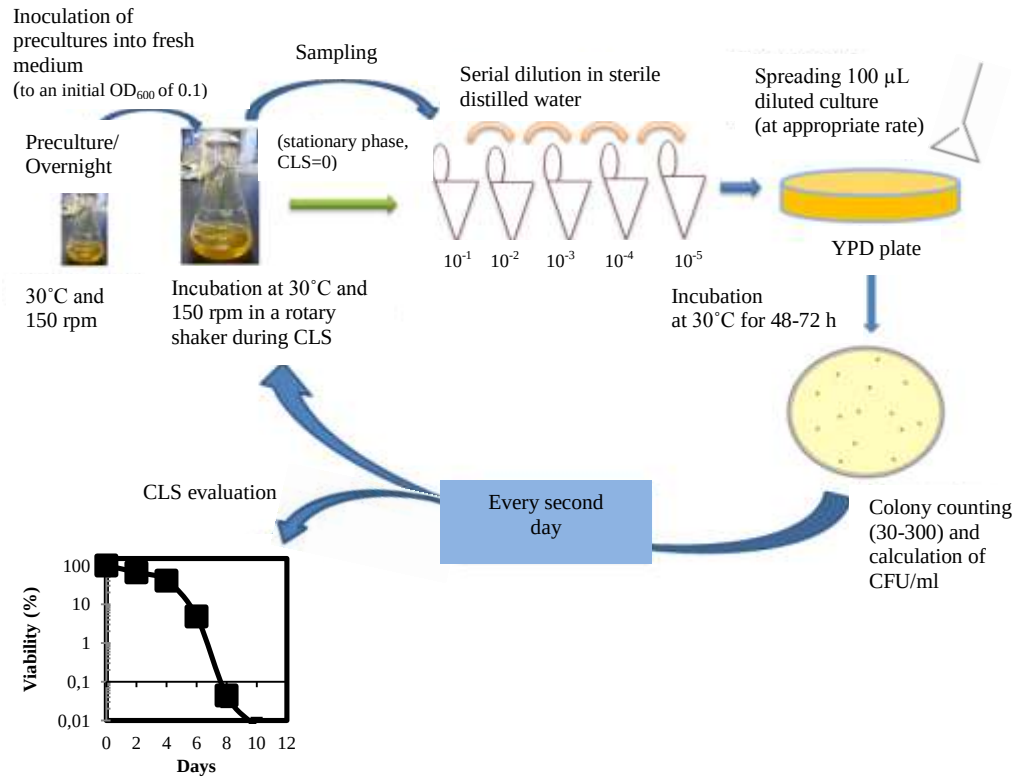

Figure 2.2 : A schematic description of the quantitative CLS method (Modified from Arslan et al., in press).

2.2.1.6 Quantitative CLS analysis of the selected mutant SRM11 in 2% YMM

Traditional CLS method was performed in 2% YMM (expired culture/medium), as described previously (Fabrizio and Longo, 2003; Longo et al., 2012). Briefly, overnight precultures were transferred into 100 ml fresh YMM in 500 ml flasks (culture volume: flask volume ratio 1:5) to an initial OD_{600} of 0.1 and were incubated until the third day of cultivation. The third day of incubation (stationary phase of growth) was considered to be 'day 0' of the CLS experiment, and the initial viability of the culture was determined by viable cell counting (Colony forming unit-CFU). For this purpose, 100 µl samples were withdrawn from the cultures and diluted by 10-fold in sterile distilled water, spread onto YPD plates and then incubated at 30°C for 72 h. The initial viability was considered as 100% viability and every second day; the viability of the cultures was tracked by the CFU method (Figure 2.2). The experiment was performed in triplicate.

2.2.1.7 CLS analysis of the selected mutant SRM11 in ammonium sulfate

For the analysis of CLS in ammonium sulfate, overnight grown cultures in 2% YMM were transferred in 100 ml fresh 2% YMM in 500 ml flasks to an initial OD_{600} of 0.1 and incubated at 30ºC and 150 rpm for 72 h (until the stationary phase of growth).

Then, OD_{600} values of the expired cultures were measured and adjusted to 6 unit of OD_{600} per ml. Then, 10 ml cultures were washed three times with either sterile distilled water or 0.5M NH_4SO_4 solution at 5.400xg and 4ºC for 10 min (Beckman Centrifuge). Cells were resuspended in either 10 ml sterile distilled water or 10 ml 0.5M NH_4SO_4 in 50 ml culture tubes. The tubes were placed in the rotary shaker in inclined position to keep the cells in suspension, and incubated at 30ºC and 150 rpm. Every second day, cultures were washed (as described above) with sterile distilled water or 0.5M NH_4SO_4 solution to prevent adaptive re-growth phenomenon (Fabrizio et al., 2004). Viability in the cultures was monitored semi-quantitative spot assay method. Briefly, cultures were diluted 10-fold (from 10^{-1} to 10^{-4}) in sterile distilled water and spotted onto YPD agar plate. The plates were incubated at 30ºC for three days, and then photographed.

2.2.1.8 Genetic stability test

To investigate whether the mutant SRM11 was genetically stable or not, the mutant SRM11 was passaged ten times in control (nonselective) medium (2% YMM). For this purpose, overnight preculture in 2% YMM was transferred in 10 ml fresh 2% YMM in 50 ml culture tube to an initial OD_{600} of 0.2. Then, the culture was incubated at 30ºC and 150 rpm for 24 h, and the first passage was obtained. The procedure was repeated until the 10^{th} passage. All passages were aliquoted and stored in 30% (v/v) glycerol at -80ºC. CLS of 1^{st}, 5^{th} and 10^{th} passages was determined in CR medium (0.5% YMM) by semi-quantitative CLS method, as described in Section 2.2.1.4.

2.2.1.9 Mating type switching/diploidization control by PCR

Mating type switching/diploidization was checked by PCR analysis in the mutant SRM11 (Huxley et al., 1990). Briefly, stock cultures were streaked onto YPD agar plate and incubated at 30ºC for 2 days. After incubation process, single colonies were picked and suspended in 20 µl 0.02M NaOH solution then heated at 99ºC for 10 min. After that, the tubes were placed on ice to cool down. The solution was used as the DNA template for PCR analysis. Three primers which are specific to MAT locus were used together in the PCR reaction (Table 2.7). PCR ingredients of each reaction and the PCR protocol are shown in Table 2.8 and Table 2.9, respectively.

Table 2.7 : PCR primers for mating type determination (Huxley et al., 1990).

Primer no	Primer name	5' ➔ 3'
1	**MAT locus**	AGTCACATCAAGATCGTTTATGG
2	**MATa**	ACTCCACTTCAAGTAAGAGTTTG
3	**MATα**	GCACGGAATATGGGACTACTTCG

Table 2.8 : Ingredients of the PCR mix.

Ingredient	Amount
i-taq	0.4 µl
10 xBuffer	2 µl
DNA solution	1 µl
Glycerol (30%)(v/v)	5 µl
Primer 1 (2.5 mM)	1 µl
Primer 2 (2.5 mM)	1 µl
Primer 3 (2.5 mM)	1 µl
dNTP	2 µl
dWater	11.6 µl
Total	25 µl

Table 2.9 : The PCR protocol.

PCR Step	Condition	Cycle
Initial denaturation	95°C 3 min	1
Denaturation	95°C 30 sec	
Annealing	56°C 30sec	29
Extension	72°C 45 sec	
Final extension	72°C 5 min	1

The PCR products were separated in 1.5% (w/v) agarose gels in 1xTBE buffer (0.8g Tris Base, 5.5g Boric Acid, 2 ml 0.5M EDTA in 1000 ml dH_2O). PCR products (5 µl) were stained by Syber Gold (1 µl of 10x dilution) and mixed with the loading dye and loaded in the wells of the 1.5% (w/v) agarose gel. After that, the PCR products were run in 1xTBE buffer for 60 min at 100 V, using electrophoresis. The gel was then visualized by a transilluminator under UV light.

2.2.2 Physiological analyses of the long-lived mutant SRM11

2.2.2.1 Growth curve analysis

To determine the growth behavior of the mutant SRM11, a growth physiology experiment was performed. For this purpose, OD_{600} values of the overnight cultures in YPD was determined, and the cells were washed twice with sterile distilled water and then inoculated into 20 ml fresh 2% YMM (in 100 ml flasks) to an initial OD_{600} of 0.2. The cultures were incubated overnight (≈16 h) at 30ºC and 150 rpm. For

growth in CR medium, pre-cultivation of cells was performed in 0.5% YMM. Finally, precultures of 905 and the mutant SRM11 were inoculated into fresh 200 ml (0.5% YMM or 2% YMM) in 1l flasks to an initial OD_{600} of 0.2. Cultures were incubated at 30ºC and 150 rpm. Samples were withdrawn from the cultures at specific time intervals during incubation, and OD_{600} of the cultures were determined spectrophotometrically. The experiment was performed in triplicate to calculate average values and standard deviations.

Naturel logarithm of the OD_{600} values ($LnOD_{600}$) were calculated. Specific growth rates (μ) were calculated according to the Ln OD_{600} values by using equation (2.2).

$$\mu = \frac{\Delta \ln OD600}{\Delta t} \tag{2.2}$$

Generation times of 905 and mutant SMR11 were calculated using equation (2.3).

$$\text{Generation time (h)} = \frac{Ln2}{\mu} \tag{2.3}$$

2.2.2.2 Cell dry weight analysis

Cell dry weight (CDW) analysis was performed to determine biomass production of the mutant SRM11 and the reference strain. For this purpose, firstly the 2 ml microcentrifuge tubes were dried in an oven at 80ºC for 48 h. Then, the tubes were left in a desiccator for 3 h and were weighed to determine their initial weight. During the growth experiment, at specific time intervals, 2 ml samples were taken from cultures into the preweighed tubes and they were centrifuged at 14.000 g for 5 min. The supernatant was carefully removed and the tubes containing cell pellets were left in an oven at 80ºC for 48 h. Next, the tubes were left in the desiccator for 3 h. Finally, the tubes were weighed and the initial weight was subtracted from the final. The difference gave the biomass. The experiment was conducted in triplicate.

2.2.2.3 Metabolite analysis by High Pressure Liquid Chromatography (HPLC)

Metabolite analysis in the mutant SRM11 was carried out by HPLC. During the growth experiments, 1 ml samples were withdrawn from the cultures at specific time intervals and centrifuged at 14.000xg for 5 min. After centrifugation, supernatants were transferred to other microcentrifuge tubes (1.5 ml). The samples were stored at -20ºC until HPLC analysis. The experiments were carried out in triplicate.

For the HPLC process, HPLC samples were filtered by using 0.22 µm sterile filters (TPP, Switzerland). Aminex© HPX-87H column (Bio-Rad) was used to detect the metabolites in the cultures. The column uses both size exclusion and ligand exchange mechanisms, having a polystyrene divinylbenzene matrix. 5 mM sulfuric acid was used as the mobile phase in the process. HPLC measurements were performed at 60ºC and at a flow rate of 0.6 ml/min and 20 µl sample injection volume. Each sample was run for 25 min. According to known standards (Table 2.10), the unknown metabolite concentrations in the culture samples were obtained. The standards were prepared as shown in Table 2.11, using solution A and B (Table 2.12).

Table 2.10 : Concentrations and retention time of metabolites in HPLC standards. Retention times are given in ± 0.2 min range

Metabolite(g/l)	Glucose	Ethanol	Glycerol	Acetate
Standard 1	20	15	1	2
Standard 2	15	11.25	0.75	1.5
Standard 3	10	7.5	0.5	1
Standard 4	5	3.75	0.25	0.5
Standard 5	2.5	1.875	0.125	0.25
Standard 6	1.125	0.937	0.0625	0.125
Standard 7	0.2	0.15	0.01	0.02
Retention Time (min)	8.43	19.95	12.5	13.81

Table 2.11 : Standard solutions of HPLC standards (Std: Standard solution).

Standard solution	Mixing Volumes	Eluent Volume	Final Volume
Standard 1	1 ml Solution A 3 ml Solution B	2 ml Eluent	6 ml
Standard 2	0.75 ml Std1	0.25 ml Eluent	1 ml
Standard 3	0.50 ml Std1	0.50 ml Eluent	1 ml
Standard 4	0.25 ml Std1	0.75 ml Eluent	1 ml
Standard 5	0.125 ml Std1	0.875 ml Eluent	1 ml
Standard 6	0.063 ml Std1	0.937 ml Eluent	1 ml
Standard 7	0.010 ml std1	0.990 ml Eluent	1 ml

Table 2.12 : Contents of Solution A and B.

Solution A	
Glucose	120 g
Add to dH_2O up to Final volume 1000 ml	
Solution B	
Ethanol	30 g
Glycerol	2 g
Acetate	4 g
Add to dH_2O up to Final volume 1000 ml	

2.2.2.4 Stress resistance estimation

Stress resistance estimation in the mutant SRM11 was carried out by semi-quantitative spot assay method. For this aim, overnight grown cultures in 2% YMM were transferred into 10 ml fresh YMM in 50 ml culture tubes to an initial OD_{600} of 0.2. The cultures were incubated at 30ºC and 150 rpm. When OD_{600} values of the cultures reached 2 (corresponding to mid-exponential phase), 4 OD_{600} unit cell per ml was harvested by centrifugation (at 10.000xg for 3 min.), and then, 10-fold serial dilutions (from 10^{-1} to 10^{-4}) were performed in sterile distilled water. Five µl of both adjusted cultures and their dilutions (from 10^{-1} to 10^{-4}) were spotted onto 2% YMM plate (control) and 2% YMM plate containing stress: 0.5 and 0.75 mM $CuSO_4$, 0.5 mM $CuCl_2$, 10 µM $AgNO_3$, 2.5 mg/mL 2-phenylethanol, 12% (v/v) ethanol, 1 mM H_2O_2, 0.4 mM $NiCl_2$, 10 mM $ZnCl_2$, 10 mM $AlCl_3$, 5% NaCl, 20 ng/mL Rapamycin and 80 mM H_3BO_3. The plates were incubated at 30ºC for 72 h. After incubation, the plates were photographed.

For the heat shock stress, five µl of both adjusted cultures and their 10-fold dilutions (described above), were spotted onto 2% YMM plates, and the plates were left in an oven at 55ºC for 50 min. After the heat shock application, plates were taken from the oven, placed at 30ºC and incubated at 30ºC for 72 h, and then photographed.

2.2.3 Transcriptomic profiling of the long-lived mutant SRM11

To gain insight into the chronological longevity of the mutant SRM11 at the molecular level, whole genome transcriptomic analysis was carried out. Whole genome transcriptome of the mutant SRM11 and the reference strain were analyzed using Agilent DNA Microarray System. DNA microarray analysis consisted of several steps: total RNA extraction, quality analysis of the extracted total RNA samples, cDNA synthesis and labeling cRNA, hybridization on microarray chips and data analysis.

2.2.3.1 Total RNA extraction

Total RNA extraction was carried out using RNeasy Mini Kit (Qiagen). Briefly, precultures of the mutant SRM11 and the reference strain were grown in 10 ml 2% YMM in 50 ml culture tubes at 30ºC and 150 rpm for about 16 h. Overnight cultures were inoculated in 20 ml fresh YMM to an initial OD_{600} of 0.1 and incubated at 30°C

and 150 rpm. When their OD_{600} values reached 1 (≈ $2x10^7$cells/ml), which corresponds to the mid-exponential phase of growth, total RNA isolation was carried out according to manufacturer's procedure (RNeasy Mini Kit, Qiagen). The RNA extraction kit buffers and their contents are shown in Table 2.13. Briefly, ≈ $2x10^7$cells per ml were harvested by centrifugation at 10.000xg for 3 min at room temperature. Supernatants were removed, and pellets were washed twice with sterile distilled water. Enzymatic lysis procedure was performed to disrupt cell wall of yeast cells. For this purpose, cells were transferred into 1.5 ml freshly prepared Y1 solution (before use 0.1% β-mercaptoethanol and lyticase (50 U final concentration) were added). Cells were incubated at 30°C for 30 min with gentle shaking. Spheroplasts were centrifuged at 300xg for 5 min, and then supernatants were removed. 350 µl Buffer RLT containing 1% β-mercaptoethanol was added and vigorously vortexed to lyse spheroplasts. After lysis, 350 µl 70% (v/v) ethanol was added to the lysate and mixed by pipetting. Mixtures were transferred to RNeasy spin columns placed in 2 ml collection tube and centrifuged at 8.000xg for 15 sec. Then, 700 µl Buffer RW1 was added to spin columns and centrifuged at 8.000xg for 15 sec. After the step, 500 µl Buffer RPE was added to spin columns and centrifuged at 8.000xg for 15 sec. Again, 500 µl Buffer RPE was added to spin columns and centrifuged at 8.000xg for 2 min to the re-wash spin column. Then, the optional step was performed. To do that, spin columns were placed in new 2 ml collection tubes and centrifuged at full speed (16.000xg) for 1 min. Finally, spin columns were placed in a new 1.5 ml RNase-free microfuge tube. To elute RNAs from spin columns, 40 µl RNase-free water was added onto spin columns and centrifuged at 8.000xg for 1 min and the RNA was eluted. The purified total RNAs were stored at -80°C until use.

Table 2.13 : Qiagen RNA Extraction Kit buffers and their contents.

Buffer	**Content (amount)**
RLT Buffer	10 µl β-mercaptoethanol per 1 ml RLT buffer was added.
Y1 Buffer	1 M sorbitol and 0.1 M EDTA is prepared and adjusted to pH 7.4. Just before use, 0.1% β-mercaptoethanol and lyticase were added.
RPE Buffer	Before use, four volumes of ethanol were added to RPE buffer.
RW1	Not indicated.

2.2.3.2 Quality analysis of the purified total RNA

Purified total RNA concentrations were determined by using a UV-Vis spectrophotometer (NanoDrop 2000, Thermo Scientific). RNA concentrations of >150 ng/µl were required for quality analysis. RNA integrity numbers (RIN) of RNA samples were determined using Agilent 2100 Bioanalyzer instrument and the RNA 6000 Nano Assay Kit (Cat: 5067-1511, Agilent, USA). Following the manufacturer's instructions, electropherograms of RNA samples were analyzed, and RIN values were determined. Samples with RIN values of > 9 were selected for DNA microarray analysis.

2.2.3.3 cDNA synthesis and labeling cRNA

RNA samples with sufficient quality were diluted to 133 ng/µl using RNase-free water. 1.5 µl of this diluted RNA (total 200 ng) was taken and used for DNA microarray analysis. As an internal control, Spike RNA (Agilent One-color RNA Spike-in Kit) was used, for this aim, Spike RNA was diluted 1:20, 1:25, 1:10 (totally 1:5000) for 200 ng total RNA. Two µl from the last dilution was added to RNA samples. Then, T7 primer mix (Table 2.14) was prepared and 1.8 µl of this mix was added in each tube that contained 3.5 µl of total RNA and diluted RNA spike-in controls. The tubes (Primer and the templates) were then incubated at 65ºC for 10 min for the denaturation of RNA, and then cooled down to 4ºC for 5 min. 4.7 µl cDNA master mix (Table 2.15) was added to each tube. After that, tubes were incubated at 40ºC for 2 h, and then at 70ºC for 15 min, and lastly kept at 4ºC.

Table 2.14 : T7 primer mix composition.

Component	Volume (µl) per reaction
T7 Primer	0.8
Nuclease-free Water	1

Table 2.15 : cDNA Master mix composition.

Component	Volume (µl) per reaction
5× First Strand Buffer	2
0.1 M Dithiothreitol (DTT)	1
10 mM dNTP Mix	0.5
Affinity Script RNase Block Mix	1.2

After cDNA synthesis process, cRNA labeling process was performed. To do that, Transcription Master Mix was prepared just before use (Table 2.16). The T7 RNA Polymerase Blend enzyme was added to the mix just before use. Six µl of the Transcription Master Mix was added to each sample tube. After that, the tubes were incubated at 40ºC for 2 h for labeling (Cy3) and synthesis of cRNA.

Table 2.16 : Composition of the Transcription Master Mix.

Component	**Volume (µl) per reaction**
Nuclease-free water	0.75
5× Transcription Buffer	3.2
0.1 M DTT	0.6
NTP Mix	1
T7 RNA Polymerase Blend	0.21
Cyanine 3-CTP	0.24
Total volume	6

Cy3-labeled cRNA was purified by Absolutely RNA Nanoprep Kit according to manufacturer's instructions. Purifed Cy3-labeled cRNA concentration and Cyanine dye concentration was determined by spectrophotometric measurements. After that, specific activities of the samples were determined.

2.2.3.4 Hybridization

For hybridization of Cy3-labeled cRNA to the microarrays, firstly, purified Cy3-labeled cRNA was diluted to 100 ng per µl using RNase-DNase-free water. Then, the Cy3-labeled cRNA was fragmented. To do that, fragmentation mix was prepared as shown in Table 2.17, incubated at 60°C for exactly 30 min to fragment the Cy3-labeled cRNA, and then immediately cooled on ice for one minute. After fragmentation process, 25 µl of 2×Hi-RPM Hybridization Buffer was added into each tube to stop the fragmentation reaction. Thus, 50 µl hybridization mix was obtained (Table 2.18). 40 µl of hybridization mix was loaded on the microarray slides (Yeast Gene Expression Array V2) and the slides were chambered. The slide chambers were placed into the hybridization oven, and hybridized at 65°C and 10 rpm for 17 h.

Table 2.17 : Fragmentation mix.

Component	Volume (µl) per sample
Cy3-labeled cRNA (diluted 100 ng/ µl)	6
Nuclease-free water	13
10x Gene expression blocking reagent	5
25x Fragmentation buffer	1

Table 2.18 : Hybridization mix.

Component	Volume (µl) per sample
25x Fragmentation mix	25
2×Hi-RPM Hybridization Buffer	25

2.2.3.5 Data analysis

After hybridization, the microarray slides were washed according to the manufacturer's instructions. The slides were then scanned by Agilent C Scanners.

Obtained signals were analyzed by Agilent Genespring GX software (Version 12.6). First, Quantile Normalization was performed on the signals. Next, probes were filtered by a flag with condition of 'at least 100% of the value in any one out of two conditions have acceptable value'. Obtained probes were then filtered by error using CV (coefficient of variation) filter with a cut-off value of 50%. After that, statistical significance was determined by using Moderated t-test with Bonferroni FEWR (Family Wise Error Rate) correction. Probes with a corrected-p value <0.05 were accepted as differentially expressed. The probe sets were filtered base on fold-change values lower than 2-fold. Thus, 2-fold and higher up- or downregulated genes were determined.

For the interpretation of microarray data, biological process analysis of the upregulated and downregulated genes was carried out by the SGD Slim Mapper based on Gene Ontology (GO) annotations for yeast genes (http://www.yeastgenome.org). Functional categorization of the upregulated and downregulated genes was also performed to interprete microarray results, using *FunCa*t database. In addition to these, Yeastract database was used to determine the transcription factors that regulate the induced genes in the mutant SRM11 (Abdulrehman et al., 2011).

2.2.4 CLS analysis of stress-resistant *S. cerevisiae* mutants

CLS of stress-resistant *S.cerevisiae* mutants that had been previously obtained by evolutionary engineering were preliminarily determined by the semi-quantitative method. CLS of the prominent mutant strains was also investigated by quantitative methods.

2.2.4.1 Semi-quantitative CLS determination of the stress-resistant yeast mutants

Quantitative CLS analysis of multiple strains can be labor-intensive due to a large space requirement in shaking incubators and the need for a high number of plates to be spread. Therefore, chronological survival of the several stress-resistant *S. cerevisiae* mutants was preliminarily determined in this study by semi-quantitative yeast spot assay. To do that, a previously described method was followed with some improvements (Smith et al., 2007a). In the present study, a cell density adjustment step was added to the method for a reliable CLS comparison of different strains at different culture densities. Briefly, overnight precultures in 2% YMM were transferred into 20 ml fresh 2% YMM (culture volume: flask volume ratio 1:5) in 100 ml flasks to an initial OD_{600} of 0.1 and cultivated at 30°C and 150 rpm. OD_{600} values of the cultures were determined on the third day (stationary phase of growth) of incubation. The third day was considered as 'day 0' of the CLS experiment. The rest of the procedure was carried out as described in Section 2.2.1.4 (Figure 2.1).

2.2.4.2 Quantitative CLS assay of stress-resistant yeast mutants in expired medium

CLS of the prominent mutants in semi-quantitative spot assay was also carried out quantitatively. The experiment was performed as described in Section 2.2.1.6.

2.2.4.3 Quantitative CLS assay of stress-resistant yeast mutants in water

To determine CLS in water, a previously described method (Fabrizio & Longo, 2003, Wei et al., 2008) was used. Briefly, precultures grown in 2% YMM were transferred into 100 ml YMM in 500 ml flasks to an initial OD_{600} of 0.1, and incubated at 30°C and 150 rpm for three days, when the cells reached the stationary phase of growth. Next, the cultures were centrifuged at 5.400xg and 20ºC for 10 min, supernatants were discarded and the pellets were resuspended in distilled water. The pellets were

then washed 3 times with sterile distilled water at 5.400xg and 20ºC for 10 min. After the washing step, cell pellets were resuspended in 50 ml sterile distilled water in 250 ml flasks or 10 ml sterile distilled water in 50 ml culture tubes. The cultivation in water was performed at 30°C and 150 rpm in a rotary shaker. Culture tubes were incubated in inclined position to keep cells in suspension. The initial viability at the beginning of the incubation in water was determined by viable cell counting method and accepted as the initial survival (100%). During the incubation in water, every two days, the viability was determined. Cells in water were washed twice every four days (as described above) to get rid of the cellular debris released by death cells and to prevent adaptive re-growth phenomenon.

2.2.5 Comparative transcriptomic analysis of long-lived and stress-resistant *S. cerevisiae* mutants

Transcriptomic data of the long-lived and stress-resistant *S.cerevisiae* mutants were compared with those of the reference strain to determine the common genes of longevity and stress resistance. Transcriptomic data of the stress-resistant mutant strains (C9, B8 and 2E) had been previously obtained by following the procedure described in Section 2.2.3. Transcriptomic data of the long-lived and stress-resistant yeast mutants were compared with those of the reference strain, using Agilent GeneSpring GX software. Primary data analysis was done using Agilent Genespring GX software, as described in Section 2.2.3.5.

3. RESULTS

3.1 Inverse metabolic engineering approach to obtain chronologically long-lived *S. cerevisiae*

3.1.1 Determination of the growth ratio in calorie-restricted media

Growth ratios of the reference strain (905) and EMS-mutagenized (906) cultures under calorie-restricted medium were investigated by spectrophotometric measurements. 905 and 906 were cultivated in control (2% glucose) or defined CR-media and their cell growth was determined by spectrophotometric measurements at the 24th hour of incubation. The data are given in Table 3.1.

Table 3.1 : Growth analysis of 905 and 906 in control and calorie-restricted YMM at the 24th hour of incubation.

YMM	**905**		**906**	
Glucose (%)	**AVE OD_{600}**	**STD OD_{600}**	**AVE OD_{600}**	**STD OD_{600}**
(Control) 2.00	5.40	0.18	5.38	0.21
0.50	3.89	0.20	3.74	0.06
0.45	4.08	0.03	3.40	0.10
0.40	3.37	0.08	3.37	0.04
0.35	4.02	0.10	3.13	0.07
0.30	3.29	0.13	2.75	0.08
0.25	3.19	0.07	2.93	0.15
0.12	2.37	0.10	2.49	0.22
0.08	1.78	0.05	1.75	0.36
0.05	1.20	0.22	1.24	0.11
0.02	0.74	0.17	0.63	0.04

AVE and STD indicate arithmetic mean and standard deviation values of three independent results, respectively.

According to the obtained OD_{600} results, growth ratios of 905 and 906 were calculated by using equation (1.2). The growth ratio results are shown in Figure 3.1.

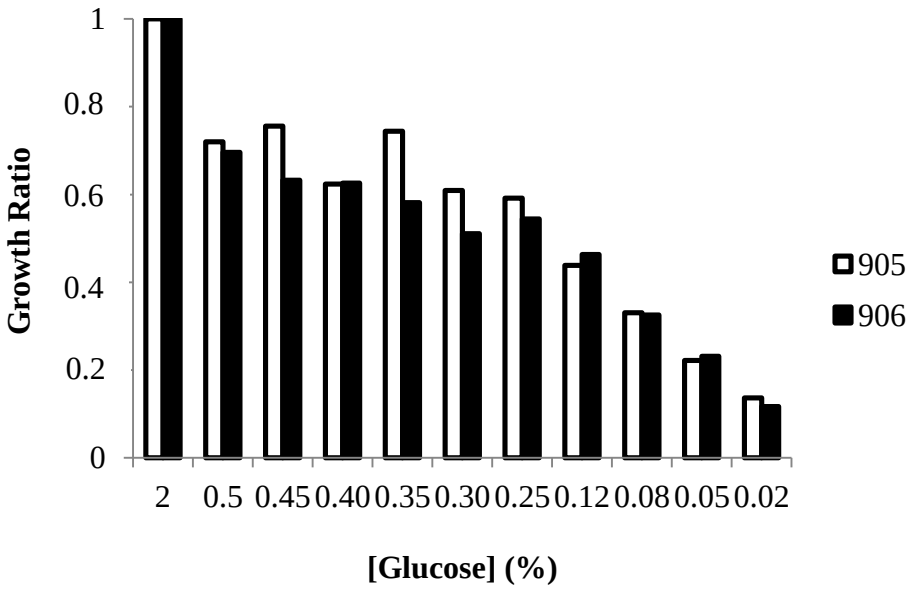

Figure 3.1 : Growth ratios of 905 and 906 in control (2% YMM) and defined CR media at the 24th hour of incubation.

Growth ratio of 905 varied between 0.14 to 0.76. For 905, the maximum growth ratio was obtained with %0.45 YMM, while the minimum growth ratio was obtained with 0.02% YMM (Figure 3.1). Growth ratio of 906 at the 24th h of incubation varied between 0.70 to 0.12. The maximum growth ratio for 906 at the 24th h was observed at 0.50% YMM while the minimum growth ratio was obtained with 0.02% YMM. The growth ratio of 905 fluctuated between 0.50% YMM and 0.35% CR-YMM. However, the growth ratio gradually decreased at glucose percentages lower than 0.35%. Growth ratio of 906 slightly decreased between 0.50% YMM and 0.25% YMM, whereas it rapidly decreased between 0.12% YMM and 0.02% YMM at the 24th h of incubation.

3.1.2 Selection strategy under increasing levels of caloric restriction

According to the results of the growth experiment, 0.5% YMM slightly inhibited growth. Also, 0.5% glucose medium is generally used for caloric restriction in yeast aging studies (Lin et al., 2000; Lin et al., 2002). Thus, 0.5% YMM was chosen as the initial caloric restriction condition for the selection process. Populations of 906 were obtained in 10 ml CR-YMM in 50 ml culture tubes at 30°C and 150 rpm for 24 h and their growth were monitored by measuring OD_{600} in a spectrophotometer. For each successive population, glucose concentration of the medium was decreased by 0.02%, unless indicated in a different way. During the selection process, the OD_{600}

values of each population and their corresponding control culture were determined. OD_{600} values of each population in CR and control medium are shown in Table 3.2 and Table 3.3, respectively.

Table 3.2 : OD_{600} of each population of 906 in defined CR-YMM at 24th h of incubation.

Generations	[Glucose(%)]	OD_{600}	OD_{600}	OD_{600}	AVE.	STD.
1	0.50	3.54	3.57	3.55	3.55	0.02
2	0.48	4.06	4.17	4.15	4.13	0.06
3	0.46	4.73	4.56	4.65	4.65	0.09
4	0.44	4.18	4.33	4.21	4.24	0.08
5	0.42	3.86	3.87	3.95	3.89	0.05
6	0.40	3.63	3.87	3.73	3.74	0.12
7	0.38	3.75	3.67	3.78	3.73	0.06
8	0.36	4.21	4.16	4.21	4.19	0.03
9	0.34	4.23	4.08	4.89	4.40	0.43
10	0.32	3.90	3.88	3.92	3.90	0.02
11	0.30	3.88	4.15	4.00	4.01	0.14
12	0.28	3.46	3.50	3.44	3.47	0.03
13	0.26	3.47	3.70	3.47	3.55	0.13
14	0.24	3.75	3.78	3.84	3.79	0.05
15	0.22	3.26	3.29	3.27	3.27	0.02
16	0.20	3.31	3.41	3.33	3.35	0.05
17	0.18	3.12	3.16	3.16	3.15	0.02
18	0.16	2.96	3.37	3.00	3.11	0.23
19	0.14	2.35	2.42	2.50	2.42	0.08
20	0.12	2.09	2.37	2.08	2.18	0.16
21	0.10	1.75	1.77	1.88	1.80	0.07
22	0.10	2.11	1.78	2.06	1.98	0.18
23	0.10	1.95	2.12	2.01	2.03	0.09
24	0.10	2.04	2.04	1.61	1.90	0.25
25	0.10	2.24	2.22	1.86	2.11	0.21
26	0.08	1.60	1.56	1.44	1.53	0.08
27	0.08	1.54	1.92	1.62	1.69	0.20
28	0.08	1.81	2.04	2.30	2.05	0.25
29	0.08	1.97	1.73	1.63	1.78	0.17
30	0.08	1.63	1.70	1.47	1.60	0.12
31	0.08	1.46	1.57	1.66	1.56	0.10
32	0.06	1.14	1.19	1.21	1.18	0.04
33	0.06	1.18	1.26	1.31	1.25	0.07
34	0.06	1.20	1.28	1.25	1.24	0.04
35	0.06	1.24	1.21	1.24	1.23	0.02
36	0.06	1.21	1.17	1.24	1.21	0.04
37	0.04	0.75	0.70	0.76	0.74	0.03
38	0.04	0.72	0.75	0.79	0.75	0.04
39	0.04	0.69	0.78	0.79	0.75	0.06
40	0.04	0.92	0.95	0.95	0.94	0.01

Table 3.2 (Continued) : OD_{600} of each population of 906 in defined CR-YMM at 24^{th} h of incubation.

Generations	[Glucose(%)]	OD_{600}	OD_{600}	OD_{600}	AVE.	STD.
41	0.04	0.86	0.87	0.89	0.87	0.02
42	0.04	0.95	1.01	1.03	1.00	0.04
43	0.04	0.73	0.73	0.70	0.72	0.02
44	0.02	0.66	0.60	0.63	0.63	0.03
45	0.02	0.50	0.45	0.42	0.46	0.04
46	0.02	0.60	0.58	0.57	0.58	0.02
47	0.02	0.60	0.67	0.63	0.63	0.04
48	0.02	0.57	0.65	0.55	0.59	0.05
49	0.02	0.72	0.77	0.60	0.70	0.09
50	0.02	0.64	0.58	0.61	0.61	0.03
51	0.02	0.61	0.57	0.57	0.58	0.02
52	0.02	0.55	0.55	0.60	0.57	0.03
53	0.02	0.55	0.53	0.55	0.54	0.01

AVE and STD indicate arithmetic mean values and standard deviation values of three independent measurements, respectively.

Table 3.3 : OD_{600} of each population of 906 in control medium (2% YMM) at 24^{th} h of incubation.

Generations	OD_{600}	OD_{600}	OD_{600}	AVE.	STD.
1	4.83	4.91	5.00	4.91	0.09
2	5.19	5.17	5.42	5.26	0.14
3	5.31	5.45	5.28	5.35	0.09
4	5.55	5.59	5.46	5.53	0.07
5	5.03	5.06	5.17	5.09	0.07
6	5.05	5.15	5.35	5.18	0.15
7	5.30	5.26	5.30	5.29	0.02
8	5.89	5.11	5.32	5.44	0.40
9	5.70	5.42	5.74	5.62	0.17
10	5.11	5.13	5.26	5.17	0.08
11	5.02	5.01	5.12	5.05	0.06
12	5.12	5.20	5.16	5.16	0.04
13	5.42	5.43	5.35	5.40	0.04
14	5.20	5.25	5.28	5.24	0.04
15	5.44	5.41	5.44	5.43	0.02
16	5.64	5.51	5.55	5.57	0.07
17	5.29	5.35	5.34	5.33	0.03
18	5.74	5.66	5.61	5.67	0.07
19	5.36	5.61	5.53	5.50	0.13
20	5.52	5.29	5.25	5.35	0.15
21	5.47	5.46	5.48	5.47	0.01
22	5.52	5.46	5.56	5.51	0.05
23	5.75	5.53	5.53	5.60	0.13
24	4.97	4.98	4.99	4.98	0.01
25	5.86	5.78	5.67	5.77	0.10
26	5.18	5.67	5.47	5.44	0.25

Table 3.3 (Continued): OD_{600} of each population of 906 in control medium (2% YMM) at 24th h of incubation.

Generations	OD_{600}	OD_{600}	OD_{600}	AVE.	STD.
27	5.60	5.56	5.77	5.64	0.11
28	5.47	5.49	5.62	5.53	0.08
29	6.03	5.73	5.86	5.87	0.15
30	5.56	5.57	5.50	5.54	0.04
31	5.20	5.33	5.31	5.28	0.07
32	5.27	5.49	5.49	5.42	0.13
33	603	6.12	5.75	5.97	0.19
34	5.17	5.18	5.07	5.14	0.06
35	5.53	5.71	5.66	5.63	0.09
36	5.18	5.34	5.32	5.28	0.09
37	5.01	5.19	5.10	5.10	0.09
38	5.04	4.86	5.13	5.01	0.14
39	5.22	5.18	4.93	5.11	0.16
40	5.50	5.49	5.28	5.42	0.12
41	5.69	5.67	5.52	5.63	0.09
42	5.44	5.48	5.42	5.45	0.03
43	4.74	4.83	4.84	4.80	0.06
44	5.44	5.52	5.52	5.49	0.05
45	5.21	5.18	5.15	5.18	0.03
46	5.79	5.76	5.77	5.77	0.02
47	5.82	5.75	5.73	5.77	0.05
48	5.74	5.90	5.86	5.83	0.08
49	5.55	5.63	5.52	5.57	0.06
50	6.61	5.75	5.82	6.06	0.48
51	5.46	5.53	5.50	5.50	0.04
52	5.41	5.47	5.57	5.48	0.08
53	5.79	5.75	5.55	5.70	0.13

AVE and STD indicate arithmetic mean and standard deviation values of three independent measurements, respectively.

Calculated growth ratios for each population of 906 are shown in Figure 3.2. Growth ratios of the populations of 906 fluctuated until 14th population. After 14th population, they gradually decreased. Glucose concentration of the medium was progressively decreased until the 21st population (0.1% glucose) of 906, where the growth ratio decreased to 0.33. Thus, the glucose concentration of the medium was kept at 0.1% for the next four passages (populations) to allow sufficient time for the adaptation of cells to starvation stress. The same adaptive approach was applied for 0.08%, 0.06%, 0.04% and 0.02% glucose concentrations during selection.

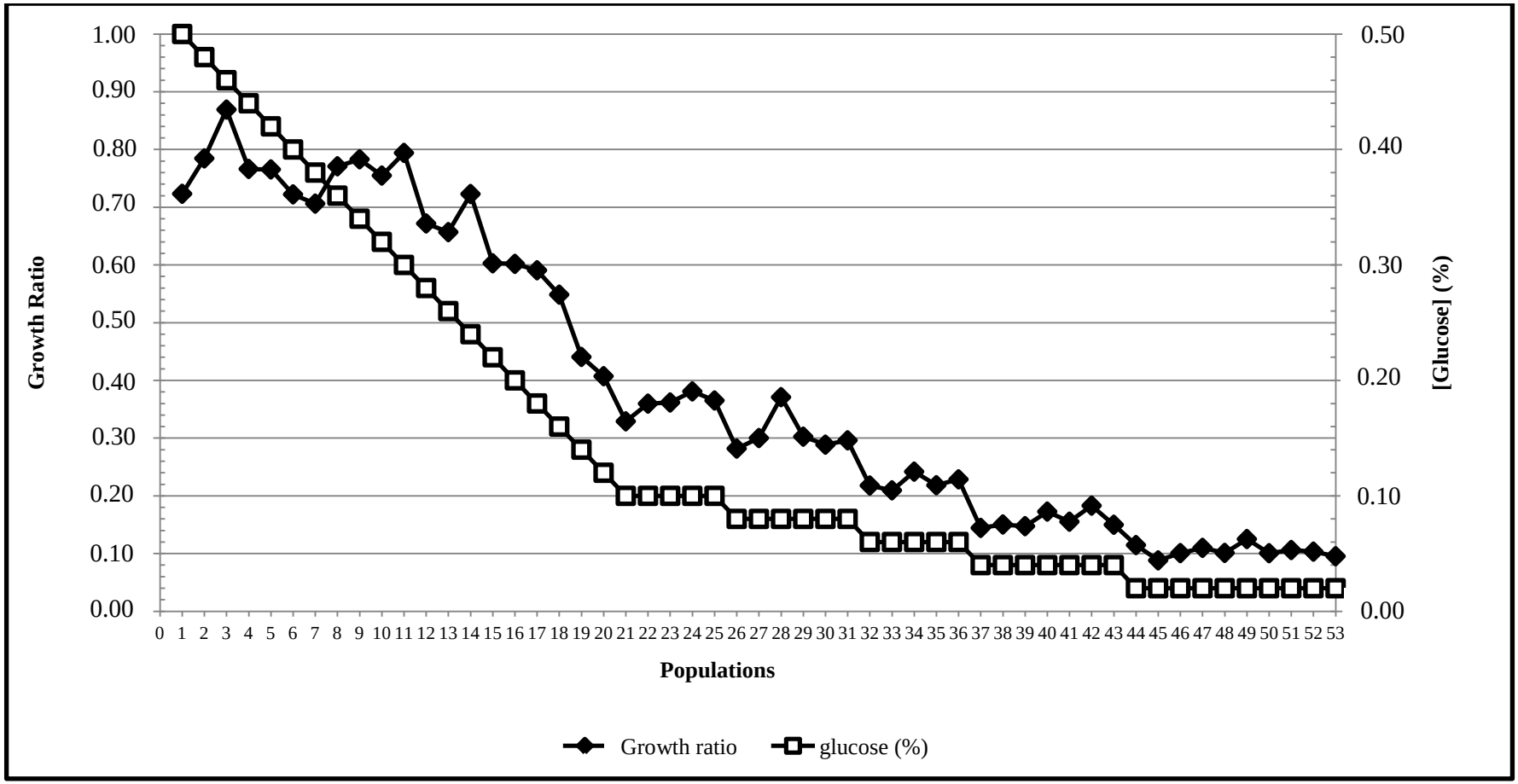

Figure 3.2 : Growth ratios of populations of 906 in different CR-YMM during 53 passages of selection.

3.1.3 Isolation of individual mutants from the final population

In the final (53^{rd}) population, the growth ratio decreased to 10%. Thus, the selection process was stopped at this stage and the last population (culture) was diluted 10-fold in sterile distilled water and 10^{-4} to 10^{-5} dilutions were spread on 2% YMM plate. Single colonies belonging to each individual mutant were obtained at 10^{-4} dilution, and twelve individual mutants (named as SRM1-SRM12) were randomly selected from the 10^{-4} diluted plate (Figure 3.3).

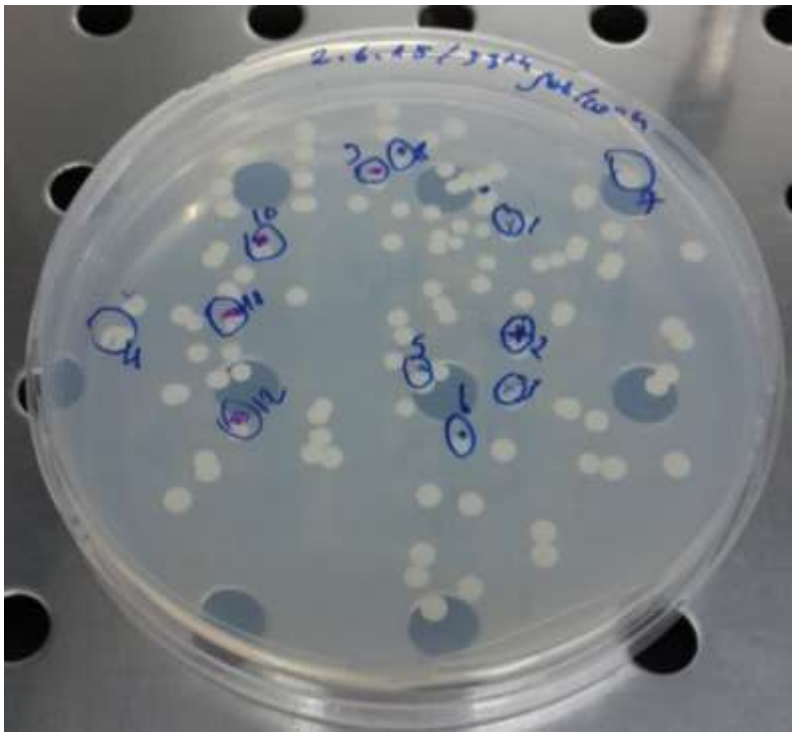

Figure 3.3 : Selected individuals from the last population (53^{rd}) of 906. Selected individuals were named SRM1 to SRM12.

3.1.4 Semi-quantitative CLS analysis of individual mutants

3.1.4.1 Growth behavior in YMM and CR-YMM

CLS of the selected individual mutants (SRM1 to SRM12) was investigated by semi-quantitative method (spot assay) in 0.5% YMM and 0.25% YMM.

CLS experiment begins at the beginning of the stationary phase of the growth (Fabrizio and Longo, 2003). Thus, growth behavior of the reference strain was determined in both standard 2% YMM and CR media (0.5% YMM and 0.25% YMM). According to the results (Figure 3.4), the culture density **(**OD_{600}) of 905

incubated in 0.50% and 0.25% YMM did not change after the first day of incubation. During the first day of incubation, 905 showed almost similar growth in both 0.5 and 2% glucose. The OD_{600} value 905 incubated in 2% glucose increased until the third day of incubation and remained constant after the third day.

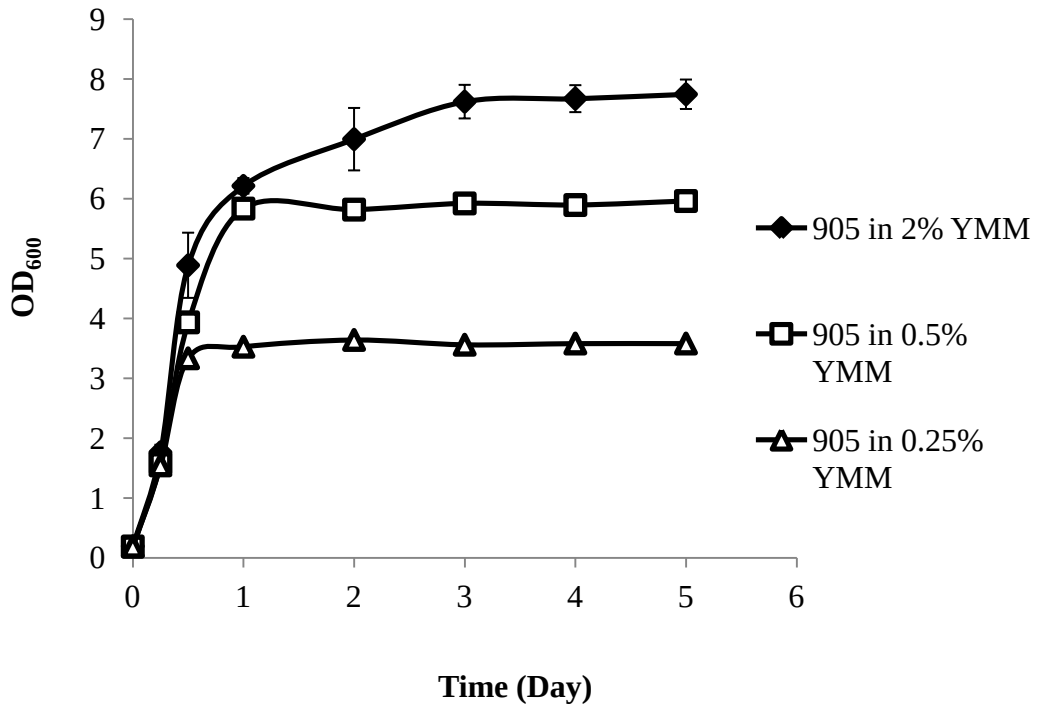

Figure 3.4 : Growth behavior of 905 in YMM and CR-YMMs.

According to the obtained results, it can be concluded that yeast cells growing in both 0.25% YMM and 0.5% YMM enter the non-dividing stationary phase at the first day of incubation. However, cells growing in 2% YMM enter the stationary phase at the third day of incubation. Thus, the initiation time of the CLS experiment (Day 0) in 0.25% and 0.5% YMM was considered as the first day of cultivation, while in 2% YMM it was considered as the third day of cultivation.

3.1.4.2 Semi-quantitative CLS analysis of the individual mutants in 0.5% YMM

To investigate CLS of the selected individual mutants in CR-medium (0.5% YMM), semi-quantitative spot assay was preliminarily performed. The individual mutants were incubated in 0.5% YMM, and OD_{600} values of the cultures were measured at the first day of cultivation (stationary phase of growth) in 0.5% YMM. OD_{600} values of the cultures are shown in Table 3.4.

Table 3.4 : OD_{600} values of 905, the last population of selection (LP906) and individual mutants (SRM1-SRM12) in 0.5% YMM at the first day of cultivation.

Strains	OD_{600}	OD_{600}	OD_{600}	AVE.	STD.
905	5.90	6.10	6.02	6.01	0.10
LP906	5.98	5.92	6.11	6.00	0.10
SRM1	6.04	6.09	5.93	6.02	0.08
SRM2	6.11	5.89	6.03	6.01	0.11
SRM3	5.94	5.97	6.08	6.00	0.07
SRM4	6.09	6.11	5.86	6.02	0.14
SRM5	5.91	5.89	6.08	5.96	0.10
SRM6	5.92	6.06	6.11	6.03	0.10
SRM7	5.92	6.03	6.14	6.03	0.11
SRM8	6.08	6.12	5.89	6.03	0.12
SRM9	6.12	5.98	6.04	6.05	0.07
SRM10	6.14	6.03	5.89	6.02	0.13
SRM11	5.90	5.98	6.13	6.00	0.12
SRM12	5.93	5.99	6.12	6.01	0.10

AVE and STD indicate arithmetic mean and standard deviation values of three independent measurement, respectively.

OD_{600} of culture samples were adjusted to 6, and then 10-fold dilutions were spotted onto YPD plate, and every second day, the viability of the cultures were tracked. According to the semi-quantitative results (Figure 3.5), CLS of the selected individual mutants was different from each other. SRM9 and SRM10 had lower viability than the reference strain (in 0.5% YMM). However, the viability of the mutants; SRM4, SRM6, SRM8, SRM11 and SRM12 was higher than that of reference strain (905). Among the selected individual mutants, the highest viability was observed in SRM11, where its viability was almost 100-fold higher than that of the reference strain.

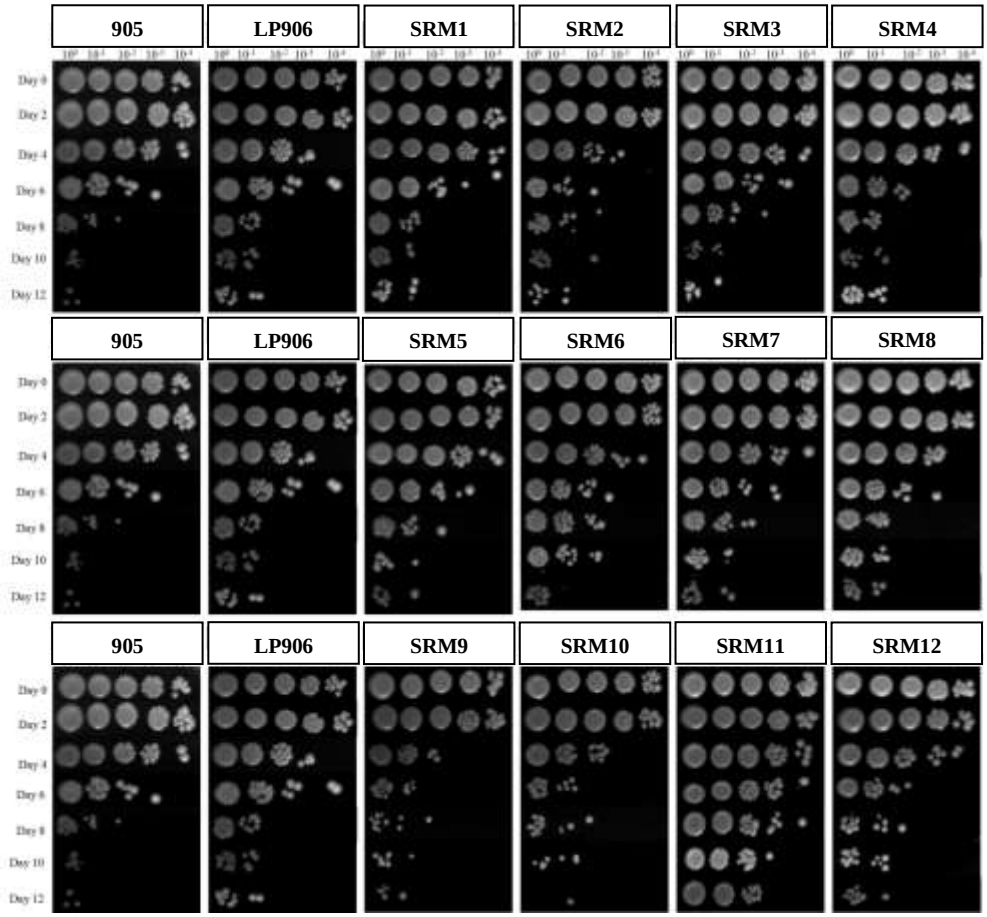

Figure 3.5 : CLS of selected individual mutants (SRM1-12), the last population (LP906) and the reference strain (905) in 0.5% YMM, as determined by the semi-quantitative spot assay.

After the first semi-quantitative analysis of CLS, the best mutant individual, SRM11, was selected for further detailed analysis. Duplicate semi-quantitative CLS analysis was performed with both the mutant SRM11 and the reference strain to verify the preliminary semi-quantitative CLS results. The mutant SRM11 and the reference strain were incubated in 0.5% YMM, and OD_{600} of the cultures were measured at the first day of incubation. OD_{600} values of the cultures are shown in Table 3.5.

Table 3.5 : OD_{600} values of 905 and SRM11 in 0.5% YMM at the first day of cultivation.

Strains	OD_{600}	OD_{600}	OD_{600}	AVE.	STD.
905-1	5.80	5.95	6.10	5.95	0.15
905-2	5.95	5.90	6.21	6.02	0.17
SRM11-1	6.11	6.01	5.90	6.01	0.11
SRM11-2	6.15	5.90	6.12	6.06	0.14

AVE and STD indicate arithmetic mean values and standard deviation values of three independent measurements, respectively.

Viability in the cultures was tracked by spot assay, as described previously. According to the duplicate semi-quantitative CLS results in 0.5% YMM (Figure 3.6), the mutant SRM11 had also better survival than the reference strain. A slight variation was observed between independent duplicate cultures. During the chronological aging in 0.5% YMM, the viability of SRM11 was at least 10-fold higher than that of the reference strain.

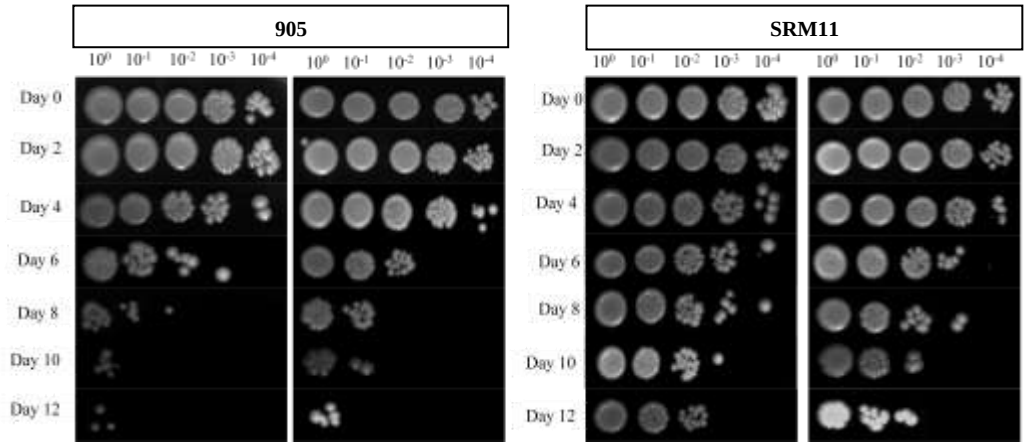

Figure 3.6 : Duplicate semi-quantitative CLS results of 905 and the mutant SRM11 in 0.5% YMM.

3.1.4.3 Semi-quantitative CLS analysis of the individual mutants in 0.25% YMM

Similar to the semi-quantitative CLS analysis in 0.5% YMM, CLS of the mutant SRM11 was also analyzed in 0.25% YMM. To do that, precultures of the mutant SRM11 and the reference strain (905) were inoculated in 0.25% YMM and incubated until the first day of incubation. At that time point of incubation (stationary phase), OD_{600} values of the cultures were determined. The data are shown in Table 3.6. It is important to note that the culture densities (OD_{600}) in 0.25% YMM were about 2-fold lower than those in 0.5% YMM (Table 3.4).

Table 3.6 : OD_{600} values of 905 and SRM11 in 0.25% YMM at the first day of cultivation.

Strains	OD_{600}	OD_{600}	OD_{600}	AVE.	STD.
905-1	2.89	3.07	3.01	2.99	0.09
905-2	3.11	3.02	3.16	3.10	0.07
SRM11-1	3.11	3.02	2.99	3.04	0.06
SRM11-2	2.89	3.05	3.16	3.03	0.14

The viability of the cultures was tracked by semi-quantitative spot assay during 12 days. According to the duplicate spot assay results (Figure 3.7), the mutant SRM11 had significantly higher viability than the reference strain in 0.25% YMM. The viability of SRM11 was at least 10-fold higher than that of the reference strain at the fourth and sixth days of the chronological aging experiment. The viability of the mutant SRM11 was approximately 100-fold higher than that of 905 at the 10^{th} and 12^{th} days of chronological aging. During chronological aging, the viability of the mutant SRM11 was approximately 100-fold higher than that of 905. In the experiment, a slight variation in viability was observed among the duplicate cultures of 905 on day 2 and 4 of the CLS experiment.

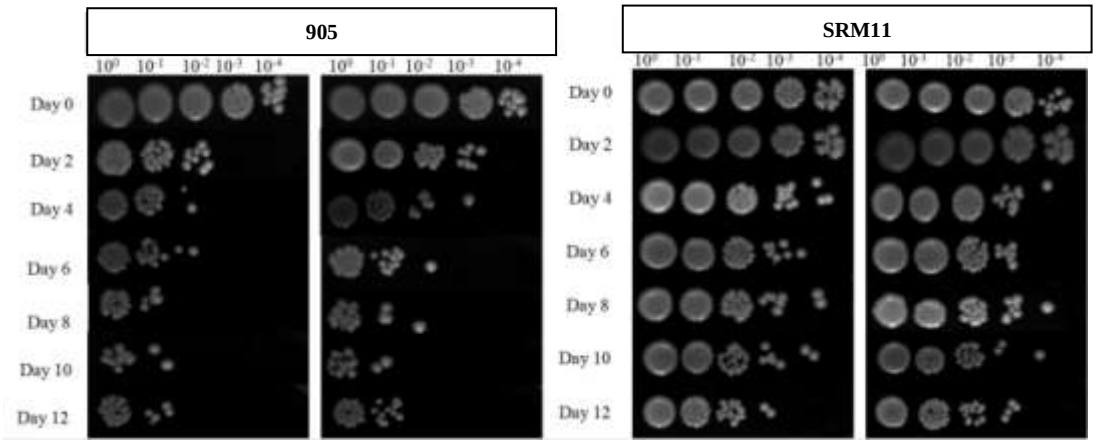

Figure 3.7 : Duplicate semi-quantitative CLS results of the mutant SRM11 and the reference strain (905) in 0.25% YMM.

3.1.5 Quantitative CLS analysis of selected mutant individuals

To verify semi-quantitative CLS results and quantitatively determine CLS of the mutant SRM11, the conventional quantitative CLS method was applied using CR-medium (0.5% YMM) and standard medium (2% YMM).

In 0.5% YMM, by the day 4 of the CLS experiment, no significant differences were observed between the viabilities of SRM11 and the reference strain. The difference in viabilities of the cultures was observed first on day 6 of the CLS experiment, when SRM11 had about 10-fold higher viability than the reference strain. Even though the viability of SRM11 culture sharply decreased until day 6, the culture was still viable on day 10 of the CLS experiment, unlike the reference strain 905 (Figure 3.8).

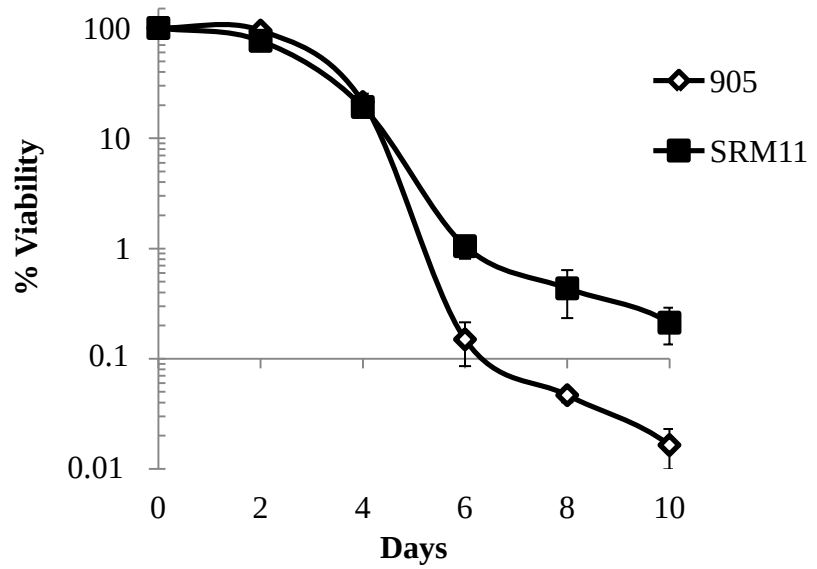

Figure 3.8 : Quantitative CLS results of the mutant SRM11 and 905 in 0.5% YMM.

In 0.25% YMM, the viability of the cultures significantly decreased on day 2 of the CLS experiment (Figure 3.9). The difference in the viabilities between SRM11 and 905 was observed on day 4 of the CLS experiment, when the viability of the reference strain decreased to about 0.1%. The viability of SRM11 almost stopped to decrease after day 6, and did not fall under 1%.

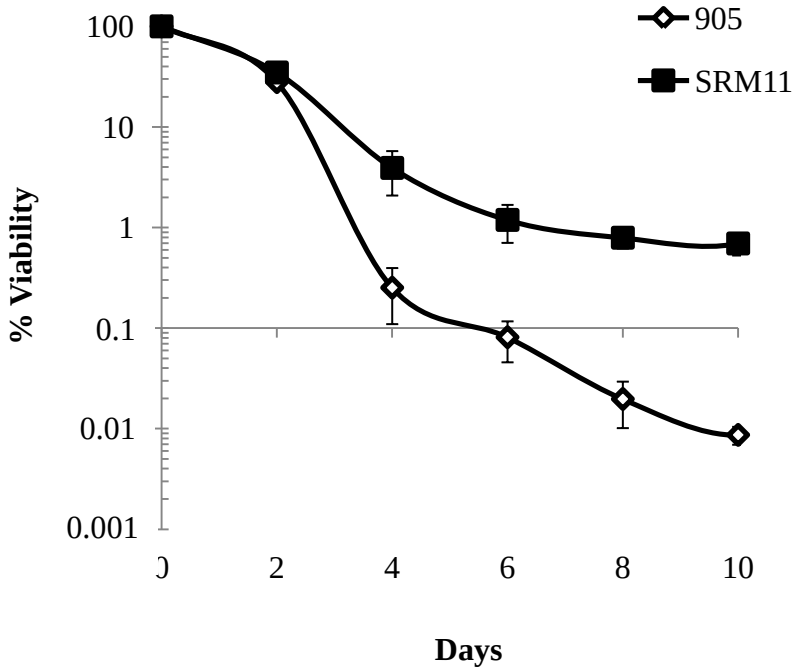

Figure 3.9 : Quantitative CLS results of the mutant SRM11 and 905 in 0.25% YMM.

CLS of the mutant SRM11 was also higher than that of the reference strain in standard glucose medium (2% YMM) (Figure 3.10). Percent viability 905 decreased below 0.1 on day 8 of the CLS experiment, whereas the % viability of SRM11 was about 5. CLS of the reference strain was about 8 days in 2% YMM, whereas the CLS of SRM11 was found to be approximately 12. Thus, quantitative CLS analysis results showed that the mutant SRM11 had 50% extended chronological lifespan in standard glucose medium (2% YMM), compared to 905.

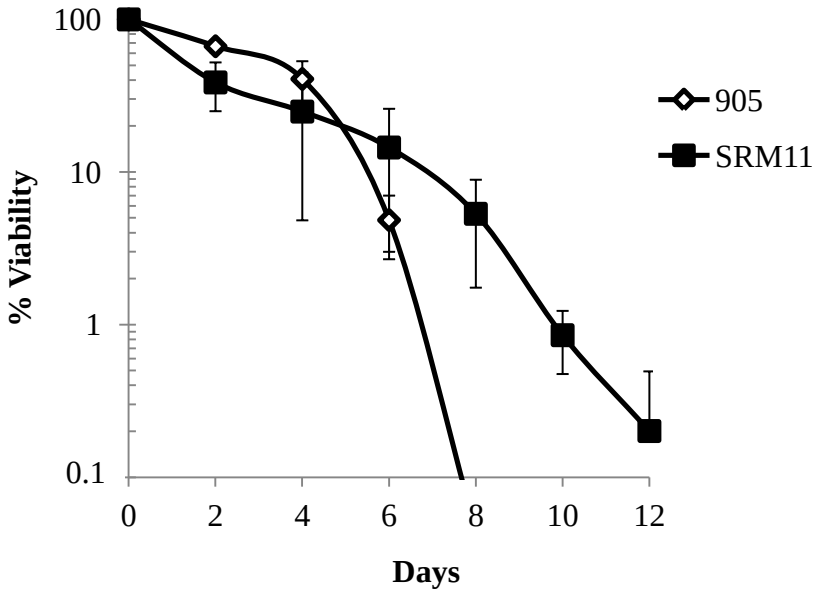

Figure 3.10: Quantitative CLS results of the mutant SRM11 and 905 in 2% YMM.

Caloric restriction generally extends chronological lifespan in yeast (Smith et al., 2007a). However, in the present study, it was observed that caloric restriction did not extend CLS of the reference strain 905, a member of the CEN.PK strain family: the CLS of 905 in CR-media was about 6 days, but in standard glucose medium, it was about 8 days.

3.1.6 CLS of the mutant SRM11 in ammonium sulfate

During the selection process, carbon to nitrogen (C:N) ratio of the culture medium significantly changed due to caloric restriction. Ammonium has a lifespan-shortening effect in the yeast *S. cerevisiae* (Santos et al., 2012). Thus, CLS of the mutant SRM11 was also determined in ammonium sulfate. Stationary phase cultures were transferred into sterile distilled water (control) or ammonium sulfate solution (0.5 M) and culture viabilities were monitored by semi-quantitative spot assay. Interestingly, SRM11 had a longer lifespan than the reference strain in the presence of ammonium

(Figure 3.11). It can be concluded that the mutant SRM11 might have gained resistance to ammonium, which prevented its lifespan-shortening effect.

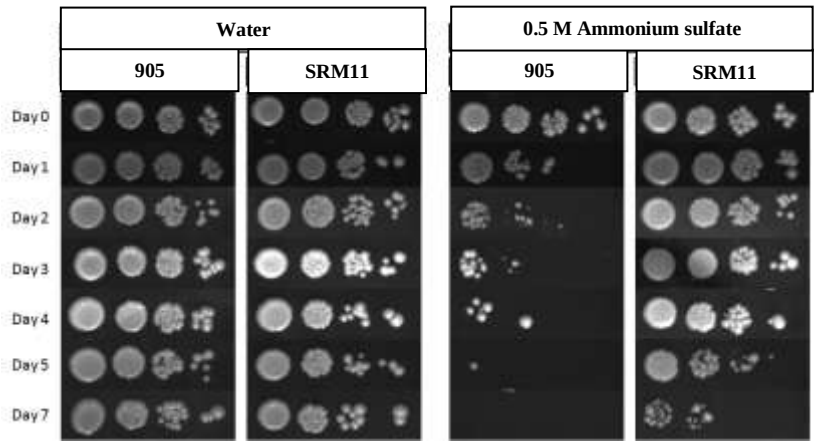

Figure 3.11 : Viability of the mutant SRM11 and 905 in ammonium sulfate, determined by spot assay. Dilutions from left (10^{-1}) to right (10^{-4}). Sterile distilled water was used as the control condition in the experiment.

3.1.7 Genetic stability test

Semi-quantitative and quantitative CLS analyses showed prolonged lifespan of the mutant SRM11. Genetic stability analysis was performed to determine whether the mutant SRM11 was genetically stable or not. For this purpose, the mutant SRM11 was cultured in standard (nonselective) medium (2% YMM) during 10 successive passages. CLS of the 1st, 5th and 10th passages were investigated in 0.5% YMM by the semi-quantitative CLS method. According to the semi-quantitative CLS results (Figure 3.12), passages of the mutant SRM11 showed almost similar lifespan pattern in 0.5% YMM. Therefore, it can be concluded that the mutant SRM11 was a genetically stable strain.

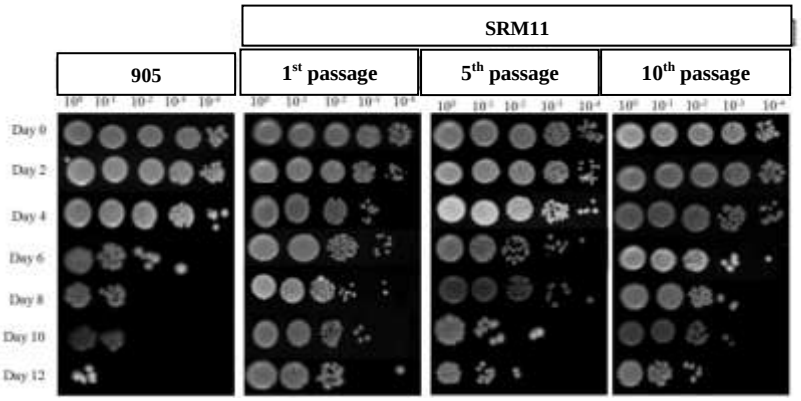

Figure 3.12 : Genetic stability test of SRM11(1st, 5th and 10th passages) in 0.5% YMM by spot assay.

3.1.8 Mating type switching/self-diploidization test by PCR

Mating type switching or self-diploidization was observed in mutant yeast strains selected in the presence of ethanol stress (Turanli-Yildiz et al., 2017). To test for this in the SRM11 mutant, PCR analysis was performed in mating type regions by specifically designed primers. It was expected to obtain a 544 bp DNA fragment for MATa (primers MAT locus and HMRa) and a 404 bp DNA fragment for MATα (primers MAT locus and HMRα). For a diploid strain, both bands were expected. According to electrophoresis results (Figure 3.13), no self-diploidization/mating type switching was observed in the mutant SRM11. The results verified that the mutant SRM11 is a MATa type haploid yeast strain.

Figure 3.13 : Agarose gel electrophoresis results of the PCR products obtained in the diploidy test. L: marker (GeneRuler™ 100bp Plus, Fermentas), 1: haploid (a) reference stain, 2: haploid (α) reference stain, 3: diploid reference strain (2n, a/ α), 4: the mutant SRM11 strain, 5: negative control.

3.2 Physiological analyses of the mutant SRM11

3.2.1 Growth analysis

To determine the growth behavior of the mutant SRM11, growth analysis was performed in both standard medium (2% YMM) and calorie-restricted medium (0.5% YMM), along with 905. Cell growth was monitored by measuring optical

densities (OD_{600}) of the cultures. The OD_{600} values of 905 and the mutant SRM11 grown in 2% YMM are shown in Table 3.7 and Table 3.8, respectively.

Table 3.7 : OD_{600} values of 905 grown in 2% YMM during 72 h of incubation. Ave and Std indicate arithmetic average and standard deviations of three biological repeats.

Time (h)	OD_{600}	OD_{600}	OD_{600}	Ave. (OD_{600})	Std. (OD_{600})
0	0.22	0.21	0.22	0.21	0.00
3	0.52	0.53	0.53	0.53	0.00
6	1.62	1.80	1.87	1.76	0.13
7.5	2.60	2.67	2.71	2.66	0.06
9	4.55	4.37	4.47	4.46	0.09
12	5.41	5.03	5.49	5.31	0.25
15	5.84	5.80	6.01	5.88	0.11
18	5.81	5.91	5.76	5.83	0.08
21	6.13	6.02	6.05	6.07	0.06
24	5.63	5.72	6.27	5.87	0.35
30	6.08	6.06	6.27	6.14	0.12
40	6.49	6.33	6.51	6.44	0.10
46	6.47	6.37	6.25	6.36	0.11
50	6.41	6.14	6.35	6.30	0.14
54	6.45	6.48	6.72	6.55	0.15
63	6.41	6.32	6.90	6.54	0.31
67	6.55	6.73	7.35	6.88	0.42
72	6.74	6.56	7.62	6.97	0.57

Table 3.8 : OD_{600} values of SRM11 grown in 2% YMM during 72 h of incubation. Ave and Std indicate arithmetic average and standard deviations of three biological repeats.

Time (h)	OD_{600}	OD_{600}	OD_{600}	Ave. (OD_{600})	Std. (OD_{600})
0	0.21	0.22	0.21	0.21	0.00
3	0.56	0.54	0.54	0.54	0.01
6	1.67	1.78	1.77	1.74	0.06
7.5	2.79	2.78	2.66	2.74	0.07
9	4.48	4.64	4.56	4.56	0.08
12	5.42	5.57	5.45	5.48	0.08
15	5.82	6.06	6.01	5.96	0.13
18	5.90	6.17	6.05	6.04	0.14
21	6.35	6.10	6.31	6.25	0.13
24	6.41	6.28	6.20	6.30	0.11
30	6.52	6.01	6.43	6.32	0.27
40	6.47	6.27	6.45	6.40	0.11
46	6.31	6.16	6.34	6.27	0.10

Table 3.8 (continued) : OD_{600} values of SRM11 grown in 2% YMM during 72 h of incubation. Ave and Std indicate arithmetic average and standard deviations of three biological repeats.

Time (h)	OD_{600}	OD_{600}	OD_{600}	Ave. (OD_{600})	Std. (OD_{600})
50	6.45	6.42	6.46	6.44	0.02
54	6.21	6.71	6.60	6.51	0.26
63	6.58	6.61	6.54	6.58	0.04
67	6.48	6.65	6.88	6.67	0.20
72	6.70	6.85	6.70	6.75	0.09

$LnOD_{600}$ values were calculated using the optical density values of the cultures. Calculated $lnOD_{600}$ results are shown in Figure 3.14. The lag phase was not observed and the exponential phase continued until about the 12^{th} h of incubation. Cell growth almost stopped about the 15^{th} h (Figure 3.14). After 48^{th}, slight post-diauxic growth was detected for both cultures (Table 3.8 and Table 3.9). The maximum specific growth rate (μ_{max}) for both 905 and SRM11 was 0.34 h^{-1} and the generation time was determined as 2.02 h for both strains. As a result, there was no difference between the growth behaviors of 905 and the mutant SRM11.

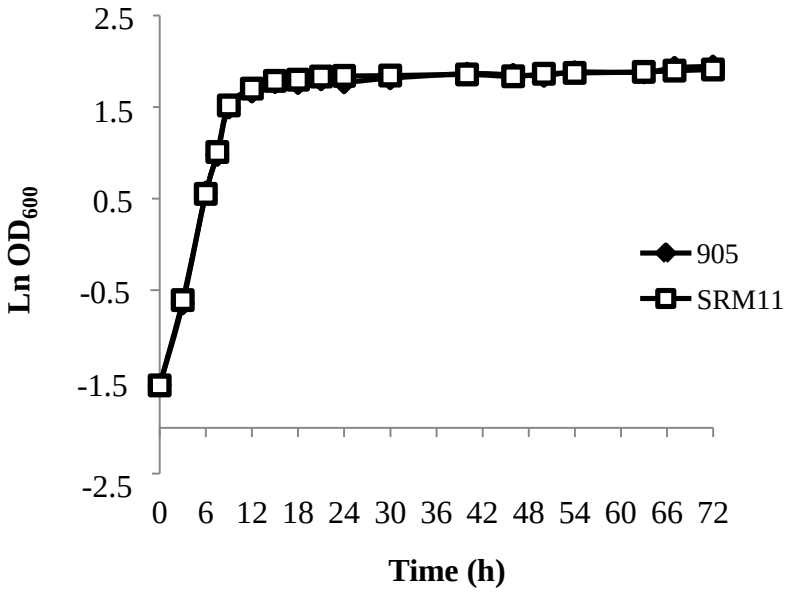

Figure 3.14 : Ln OD_{600} values of 905 and SRM11 in 2% YMM.

Growth analysis of 905 and the mutant SRM11 were also performed under caloric restriction condition (0.5% YMM). The optical density values of 905 and the mutant SRM11 grown in 0.5% YMM are shown in Table 3.9 and Table 3.10, respectively.

Table 3.9 : OD_{600} values of 905 grown in 0.5% YMM during 72 h of incubation.

Time (h)	OD_{600}	OD_{600}	OD_{600}	Ave. (OD_{600})	Std. (OD_{600})
0	0.24	0.24	0.24	0.24	0.00
3	0.61	0.66	0.62	0.63	0.03
6	2.13	2.09	2.13	2.12	0.02
7.5	3.29	3.25	3.08	3.21	0.11
9	3.43	3.66	3.51	3.53	0.12
12	4.12	4.05	4.11	4.09	0.04
15	4.89	5.00	4.93	4.94	0.06
18	5.60	5.69	5.81	5.70	0.11
21	6.14	6.35	6.41	6.30	0.14
24	6.24	6.35	6.15	6.25	0.10
27	6.37	6.48	6.32	6.39	0.08
30	6.11	6.28	6.72	6.37	0.31
35	6.33	6.30	6.23	6.29	0.05
50	6.35	6.30	6.23	6.29	0.06
58	5.89	6.15	6.15	6.06	0.15
72	5.95	6.31	6.01	6.09	0.19

Ave and Std indicate arithmetic average and standard deviations of three biological repeats.

Table 3.10 : OD_{600} values of SRM11 grown in 0.5% YMM during 72 h of incubation.

Time (h)	OD_{600}	OD_{600}	OD_{600}	Ave. (OD_{600})	Std. (OD_{600})
0	0.24	0.25	0.26	0.25	0.01
3	0.64	0.63	0.63	0.63	0.01
6	2.21	2.19	2.24	2.21	0.03
7.5	3.34	3.28	3.30	3.31	0.03
9	3.68	3.59	3.51	3.59	0.09
12	4.27	4.20	3.99	4.15	0.15
15	5.54	4.92	4.83	5.10	0.39
18	5.88	5.74	5.91	5.84	0.09
21	6.44	6.46	6.34	6.41	0.06
24	6.32	6.19	6.50	6.34	0.16
27	6.27	6.60	5.99	6.29	0.31
30	6.27	6.40	6.21	6.29	0.10
50	6.24	6.26	6.37	6.29	0.07
58	6.35	6.17	5.75	6.09	0.31
72	6.19	6.35	6.40	6.31	0.11

Ave and Std indicate arithmetic average and standard deviations of three biological repeats.

$LnOD_{600}$ values were calculated using the optical density values of the cultures. Calculated $LnOD_{600}$ results are plotted in Figure 3.15.

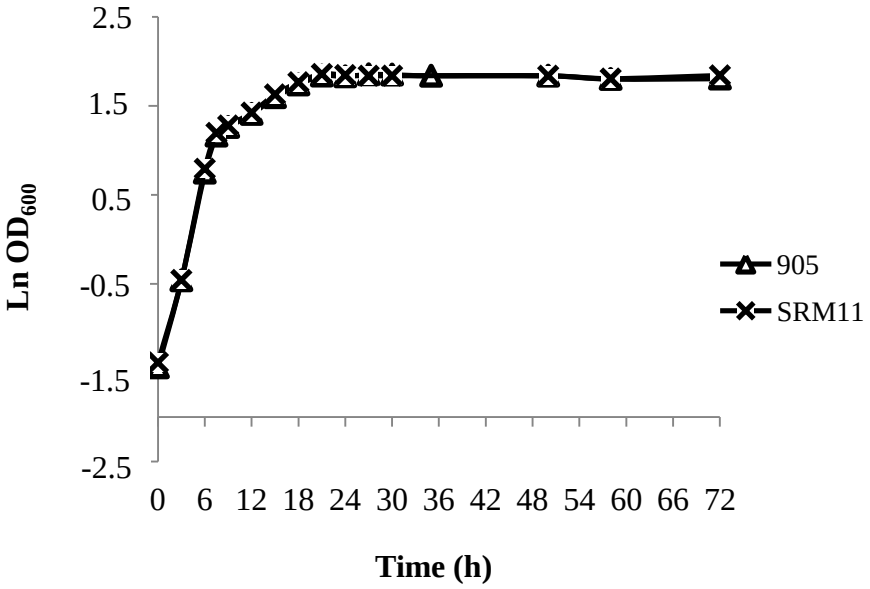

Figure 3.15 : $LnOD_{600}$ versus time of 905 and SRM11 in calorie-restricted medium (0.5% YMM).

The lag phase was not observed in SRM11 and 905 in calorie-restricted medium (Figure 3.15). Interestingly, two different exponential phases were observed in both 905 and the mutant SRM11. The first exponential phase was observed from the beginning until the 7.5th h of cultivation, and the second was observed from the 7.5th h to the 21st h of cultivation. As expected, the maximum specific growth rate (μ_{max}) during the first exponential phase was higher than during the second one. μ_{max} was calculated as 0.35 h^{-1} for the first exponential, and 0.05 h^{-1} for the second exponential growth phase. The generation time was calculated as 1.96 h and 12.63 h for the first and second exponential phases of growth, respectively. After the 21st h of cultivation, no growth was observed in any of the cultures. According to the results, there was no difference in the growth behavior of 905 and the mutant SRM11 in calorie-restricted medium (0.5% YMM).

3.2.2 Cell dry weight (CDW) analysis

To determine the biomass production of the mutant SRM11 and 905, CDW analysis was carried out. For this purpose, at specific time points during the growth experiment, samples were taken from the cultures into dried and preweighed tubes, the tubes were centrifuged and the supernatant were then removed. The tubes containing cell pellets were then left open in an oven to obtain dry cell pellets. Next, the tubes were weighed and the initial weight was subtracted from the final weight. Thus, the CDW per ml of culture was determined. According to CDW results (Figure

3.16), there was no significant difference in the biomass production of these two strains in standard medium (2% YMM) and calorie-restricted medium (0.5% YMM). It should be noted that the CDW in the reference strain culture significantly increased at post-diauxic phase (between 30 h and 72 h, $p<0.05$) compared to the mutant SRM11, in 2% YMM. This was also observed in the OD_{600} data (Table 3.7). This result might indicate metabolic differences between the strains.

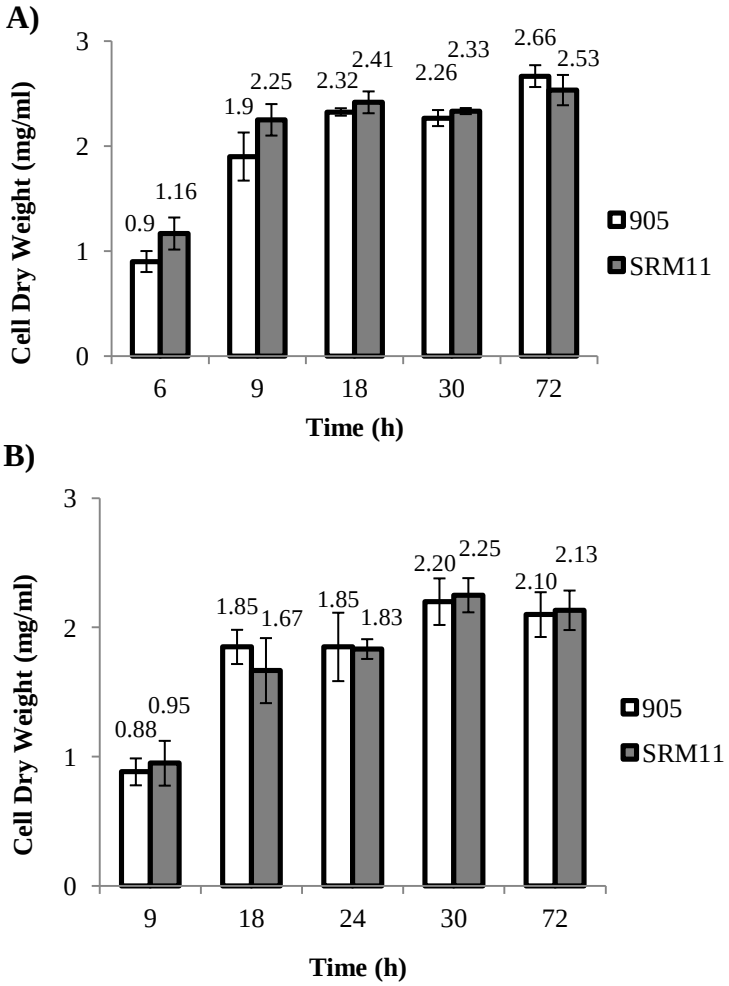

Figure 3.16 : Biomass production (cell dry weight (mg/ml)) of 905 and the mutant SRM11 in (A) 2% YMM and (B) 0.5% YMM.

3.2.3 Metabolite analysis by HPLC

HPLC analysis was carried out to gain insight into the metabolic profiles of the mutant SRM11 and the reference strain (905). Using known standards, standard curves for glucose and ethanol (Figure 3.17), glycerol and acetate (Figure 3.18) were obtained.

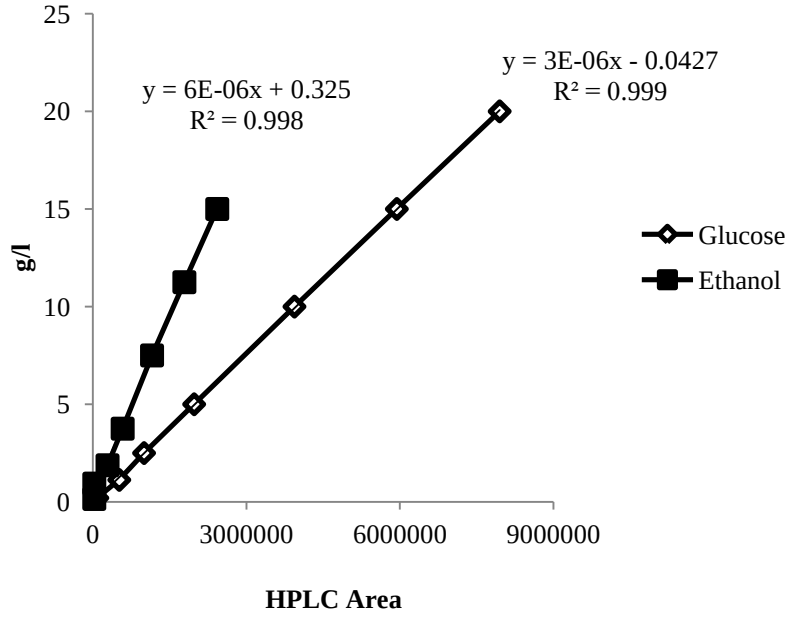

Figure 3.17 : Standard HPLC curves for glucose and ethanol.

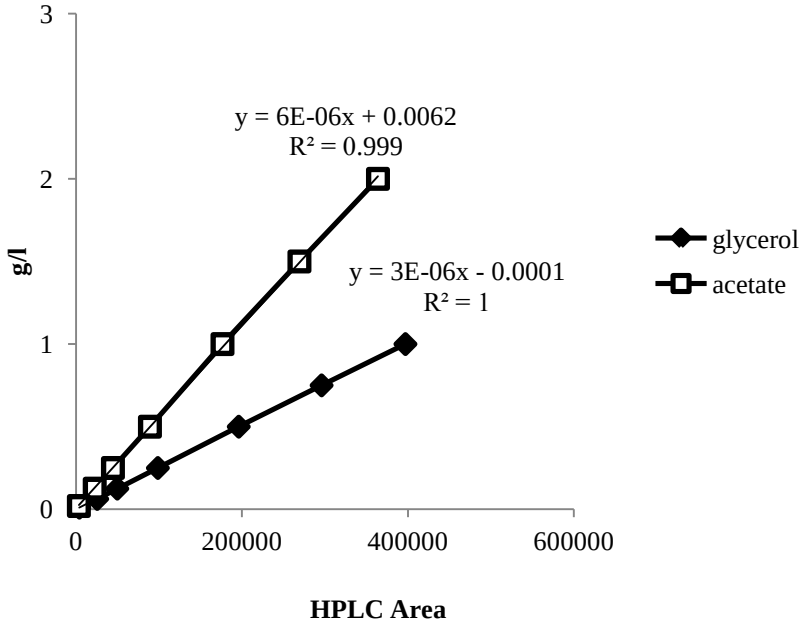

Figure 3.18 : Standard HPLC curves for glycerol and acetate.

According to the standard curves, unknown amounts of each metabolite in culture samples were quantified. Calculated data for both 905 and the mutant SRM11 are indicated in Tables 3.11 and 3.12, respectively, and also plotted in Figures 3.19-3.22.

Table 3.11: Metabolite levels of 905 grown in 2% YMM during 72 h of incubation.

	Glucose (g/l)		Ethanol (g/l)		Glycerol (g/l)		Acetate (g/l)	
Time (h)	**AVE.**	**STD.**	**AVE.**	**STD.**	**AVE.**	**STD.**	**AVE.**	**STD.**
0	19.99	0.80	0.00	0.00	0.00	0.00	1.08	0.04
3	17.98	0.60	0.58	0.11	0.02	0.00	1.24	0.15
6	15.85	0.34	1.20	0.06	0.06	0.00	1.16	0.01
9	12.21	0.93	3.39	0.11	0.18	0.01	1.37	0.02
12	9.18	1.08	7.97	0.63	0.61	0.05	2.45	0.19
15	0.40	0.09	8.17	0.33	0.69	0.01	2.46	0.17
27	0.00	0.00	8.28	0.07	0.76	0.01	2.60	0.05
46	0.00	0.00	8.00	0.27	0.77	0.05	2.45	0.10
50	0.00	0.00	6.62	0.20	0.64	0.02	2.02	0.06
54	0.00	0.00	5.74	0.23	0.55	0.01	1.73	0.01
58	0.00	0.00	5.46	0.41	0.54	0.04	1.74	0.12
72	0.00	0.00	3.72	0.77	0.49	0.01	1.33	0.14

AVE and STD indicate arithmetic mean and standard deviation values of three independent results, respectively.

Table 3.12 : Metabolite levels of SRM11 grown in 2% YMM during 72 h of incubation.

	Glucose (g/l)		Ethanol (g/l)		Glycerol (g/l)		Acetate (g/l)	
Time (h)	**AVE.**	**STD.**	**AVE.**	**STD.**	**AVE.**	**STD.**	**AVE.**	**STD.**
0	19.99	0.80	0.00	0.00	0.00	0.00	1.08	0.04
3	17.41	0.25	0.51	0.02	0.02	0.00	1.12	0.06
6	15.40	0.08	1.08	0.02	0.06	0.00	1.13	0.05
9	10.71	0.67	2.86	0.39	0.15	0.01	1.20	0.09
12	6.70	0.17	6.59	0.36	0.50	0.01	1.97	0.13
15	0.23	0.08	7.14	0.10	0.58	0.05	1.94	0.03
27	0.00	0.00	7.12	0.07	0.64	0.02	2.09	0.03
46	0.00	0.00	6.73	0.11	0.60	0.02	1.65	0.26
50	0.00	0.00	6.09	0.22	0.59	0.04	1.48	0.29
54	0.00	0.00	5.71	0.31	0.56	0.04	1.38	0.26
58	0.00	0.00	5.14	0.15	0.51	0.04	1.27	0.25
72	0.00	0.00	3.95	0.30	0.46	0.02	1.39	0.14

AVE and STD indicate arithmetic mean and standard deviation values of three independent results, respectively.

Glucose consumption behavior was almost the same for both strains. The only slight difference was observed at the 12^{th} h of cultivation. Glucose was almost exhausted at the 15^{th} h of cultivation in both cultures (Figure 3.19).

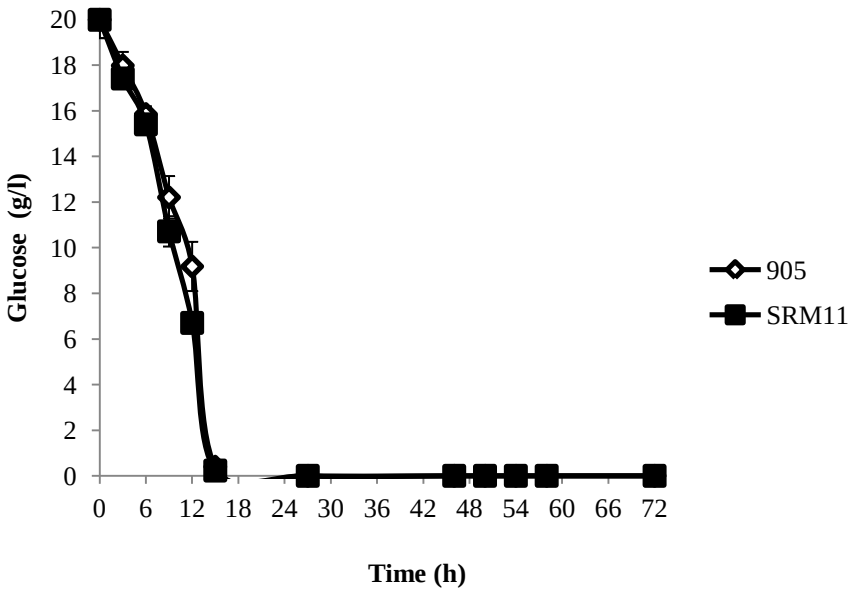

Figure 3.19 : Glucose consumption behavior of 905 and SRM11 grown in 2% YMM.

In 2% YMM, 905 produced more ethanol than SRM11 at the end of the exponential phase (12^{th} h) (Figure 3.20). The maximum amount of ethanol produced was 8.28 g/l for 905, and 7.12 g/l for SRM11, respectively. After the 15^{th} h of incubation, ethanol concentration in the cultures almost did not change until the 46^{th} h of incubation. After the 46^{th} h of incubation, ethanol concentration started to decrease, probably due to the utilization of ethanol by oxidative metabolism. According to the obtained results, it can be concluded that the mutant SRM11 has a more active respiratory metabolism than the reference strain in the respirofermentative state (exponential phase). This regulation could be due to maximizing ATP production rather than converting glucose to ethanol.

As shown in Figure 3.21, the mutant SRM11 produced less glycerol than 905 in the exponential phase. Glycerol concentrations of both cultures reached its maximum at the 27^{th} h of incubation. After the 46^{th} h of incubation, glycerol was utilized by both 905 and SRM11, therefore, a decrease in glycerol concentration was observed in both cultures. After the 48^{th} h of incubation, there was no significant difference between the glycerol concentrations of SRM11 and the reference strain.

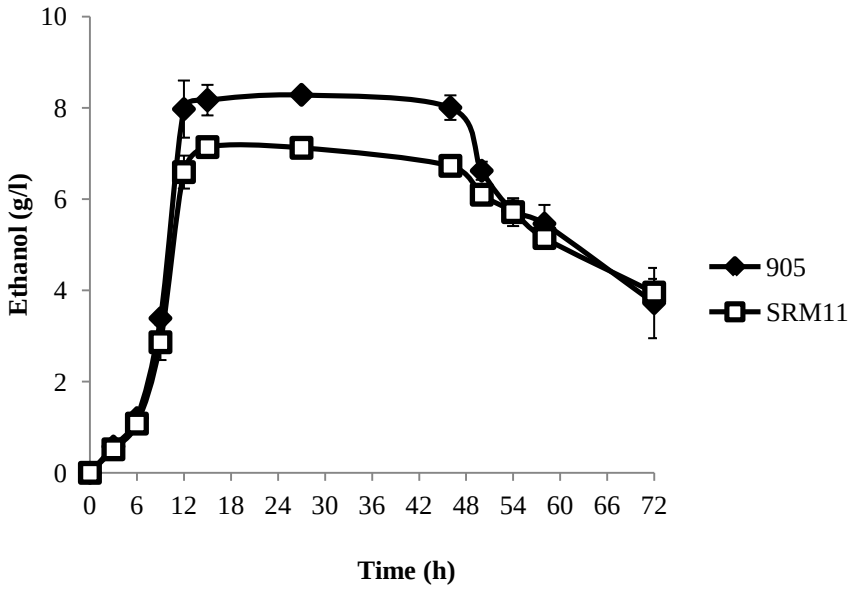

Figure 3.20 : Ethanol profiles of 905 and SRM11 grown in 2% YMM.

Acetate concentration in the cultures increased until the 12th hour for both 905 and the mutant SRM11. Acetate production of SRM11 was lower than that of 905. The maximum acetate concentration was 2.60 g/l for 905, whereas it was 2.09 g/l for SRM11. After 27th h of incubation, acetate concentration gradually decreased in both SRM11 and 905, most likely because of its utilization by the cells (Figure 3.22).

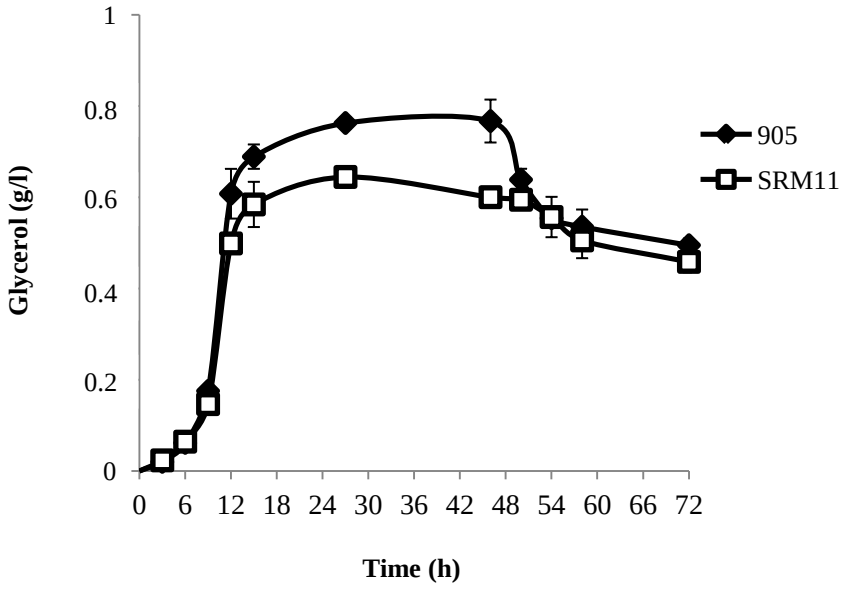

Figure 3.21 : Glycerol profiles of 905 and SRM11 grown in 2% glucose medium (YMM).

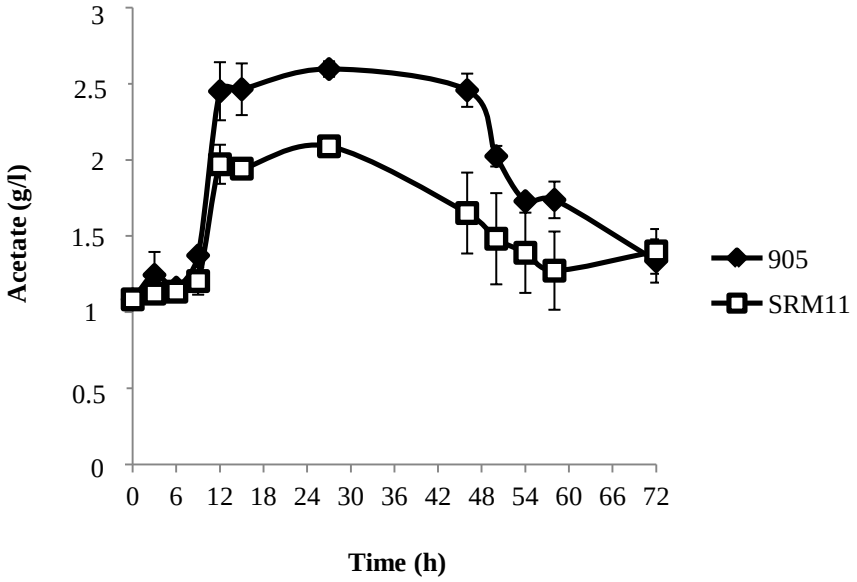

Figure 3.22 : Acetate profiles of 905 and SRM11 grown in 2% YMM.

HPLC analysis was also carried out in calorie-restricted medium (0.5% YMM) to gain insight into the metabolism of the mutant SRM11 under glucose limitation. The calculated metabolite concentrations are shown in Tables 3.13 and 3.14, and plotted in Figures 3.23-3.25.

Table 3.13 : Glucose, ethanol and glycerol concentrations of 905 grown in 0.5% YMM during 72 h of cultivation.

	Glucose (g/l)		Ethanol (g/l)		Glycerol (g/l)	
Time (h)	**AVE.**	**STD.**	**AVE.**	**STD.**	**AVE.**	**STD.**
0	5.01	0.17	0.00	0.00	0.0000	0.0000
3	1.81	0.10	0.67	0.02	0.0155	0.0003
6	0.24	0.08	1.35	0.06	0.0322	0.0039
9	0.00	0.00	1.24	0.11	0.0259	0.0029
12	0.00	0.00	1.25	0.05	0.0174	0.0015
18	0.00	0.00	0.85	0.02	0.0000	0.0000
21	0.00	0.00	0.64	0.03	0.0000	0.0000
24	0.00	0.00	0.51	0.00	0.0000	0.0000
27	0.00	0.00	0.50	0.01	0.0000	0.0000
30	0.00	0.00	0.50	0.01	0.0000	0.0000
50	0.00	0.00	0.34	0.09	0.0000	0.0000
58	0.00	0.00	0.00	0.00	0.0000	0.0000
72	0.00	0.00	0.00	0.00	0.0000	0.0000

AVE and STD indicate arithmetic mean and standard deviation values of three independent results, respectively.

Table 3.14 : Glucose, ethanol and glycerol concentrations of SRM11 grown in 0.5% YMM during 72 h of cultivation.

	Glucose (g/l)		Ethanol (g/l)		Glycerol (g/l)	
Time (h)	**AVE.**	**STD.**	**AVE.**	**STD.**	**AVE.**	**STD.**
0	5.01	0.17	0.00	0.00	0.0000	0.0000
3	1.65	0.05	0.64	0.00	0.0148	0.0001
6	0.22	0.08	1.22	0.14	0.0284	0.0020
9	0.00	0.00	1.21	0.08	0.0254	0.0013
12	0.00	0.00	1.27	0.01	0.0189	0.0012
18	0.00	0.00	0.82	0.04	0.0000	0.0000
21	0.00	0.00	0.70	0.07	0.0000	0.0000
24	0.00	0.00	0.50	0.01	0.0000	0.0000
27	0.00	0.00	0.00	0.00	0.0000	0.0000
30	0.00	0.00	0.00	0.00	0.0000	0.0000
50	0.00	0.00	0.00	0.00	0.0000	0.0000
58	0.00	0.00	0.00	0.00	0.0000	0.0000
72	0.00	0.00	0.00	0.00	0.0000	0.0000

AVE and STD indicate arithmetic mean and standard deviation values of three independent results, respectively.

In 0.5% YMM, the glucose concentration decreased from about 5 g/l to 0 g/l during the first nine hours of incubation. According to results, it can be concluded that there is no significant difference between the glucose metabolism of 905 and SRM11 in calorie-restricted medium (0.5% YMM) (Figure 3.23).

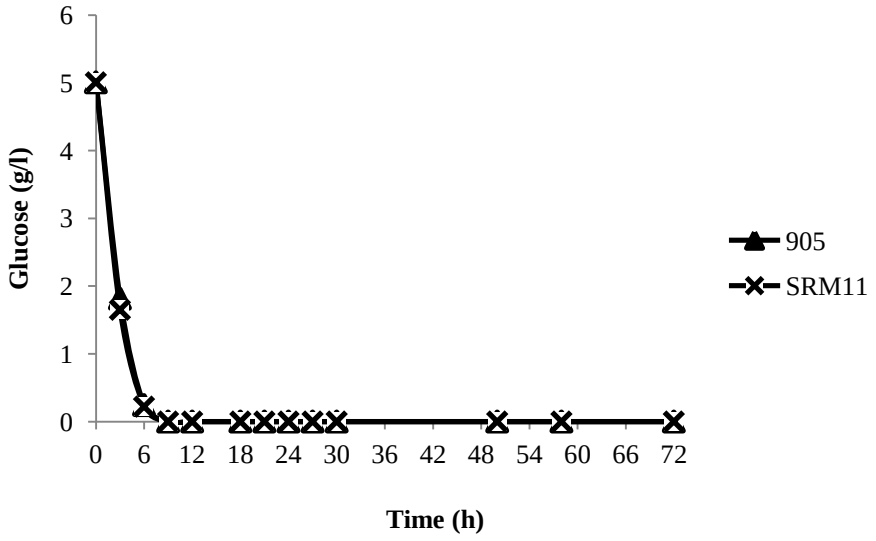

Figure 3.23 : Glucose consumption of 905 and SRM11 in calorie-restricted medium (0.5% YMM).

In 0.5% YMM, there was no significant difference between the ethanol production profiles of SRM11 and 905, either (Figure 3.24). The maximum ethanol concentration of the mutant SRM11 and the reference strain were about 1.31 g/l and

1.35 g/l, respectively. However, there was a significant difference in ethanol consumption of the strains. The mutant SRM11 consumed ethanol faster than 905. SRM11 consumed all ethanol in the medium until the 27th h of cultivation, while 905 needed 58 h for the total consumption of ethanol (Figure 3.24).

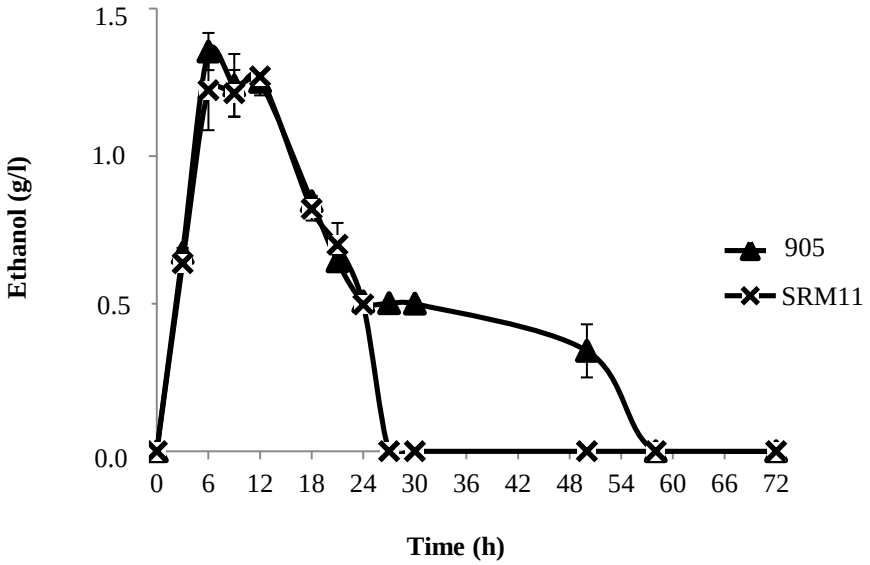

Figure 3.24 : Ethanol production and consumption of 905 and SRM11 grown in 0.5% YMM.

There was no difference in the glycerol metabolism between the mutant SRM11 and the reference strain in 0.5% YMM (Figure 3.25). Low levels of glycerol production was observed in both cultures. The glycerol produced was exhausted by both cultures by the 18th h of incubation (Figure 3.25).

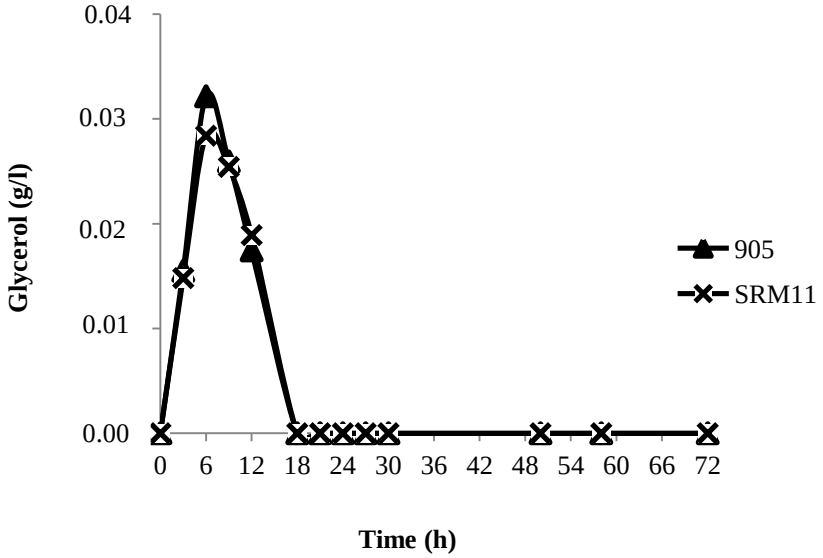

Figure 3.25 : Glycerol profiles of 905 and SRM11 grown in 0.5% YMM.

It is important to note that acetate production was not observed in both cultures in 0.5% YMM.

3.2.3.1 Stress resistance estimation

Since longevity is highly associated with stress resistance (Barsyte et al., 2001; Longo, 2003; Martin et al., 1996; Murakami and Johnson, 1998; Service et al., 1985), stress resistance of the mutant strain SRM11 was investigated by semi-quantitative spot assay method. SRM11 and 905 were exposed to various stress types. Results showed that RM11 highly resisted to copper stress (Figure 3.26).

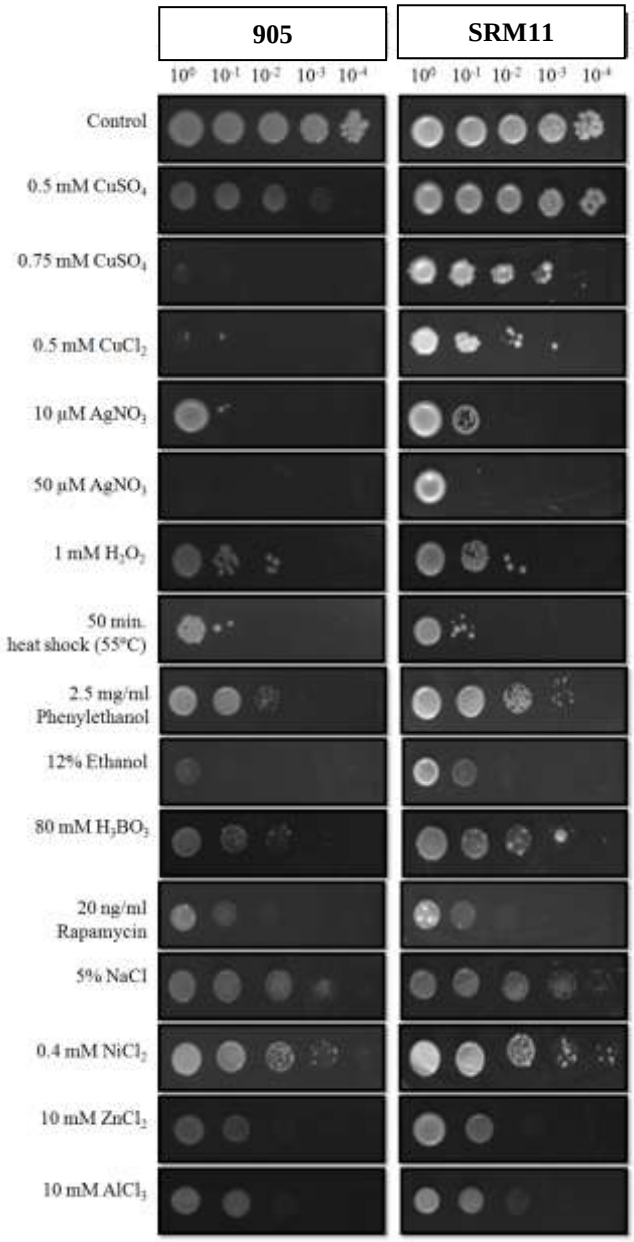

Figure 3.26 : Stress resistance analysis results of the mutant SRM11 and the reference strain 905 by spot assay.

SRM11 had resistance to silver, boric acid, and also slight resistance to nickel stress. SRM11 showed resistance to alcohol stresses, ethanol and phenylethanol. However, there was no sensitivity or resistance for heat shock and oxidative stress (H_2O_2), aluminum, zinc and salt stresses. In SRM11, rapamycin resistance was also tested to check the potential involvement of TOR pathway in its extended lifespan. However, no significant resistance or sensitivity to rapamycin was observed in SRM11 (Figure 3.26).

3.2.4 Whole genome transcriptomic analysis

Whole genome transcriptomic analysis was carried out in the mutant SRM11, to gain insight into the molecular mechanisms of chronological longevity. Using DNA microarray technology (Agilent, USA), expression profile of nearly 6000 genes in SRM11 was investigated in comparison to the reference strain. To do that, overnight precultures were transferred into fresh medium (2% YMM) and incubated at optimal condition until mid-exponential phase of growth. OD_{600} values of the cultures are shown in Table 3.15. At that time, 1 ml samples (1 OD_{600} unit of cells) were withdrawn from the cultures and RNA isolation was carried out using RNeasy Mini Kit (Qiagen, Germany). At the end of the RNA isolation protocol, purified total RNA concentration was determined spectrophotometrically (Nanodrop 2000). RNA concentrations of the samples are shown in Table 3.16. To those samples with RNA concentrations higher than 150 ng/µl, RNA integrity number (RIN) determination step was applied. To determine the RIN value, Agilent 2100 BioAnalyzer was used. RIN values of the samples are shown in Table 3.17. RNA samples with RIN values higher than 9 were used for microarray analysis.

Table 3.15 : OD_{600} values of the cultures just before the RNA isolation.

Culture	**OD_{600} of the cultures just before the RNA isolation**				
	Replicate 1	Replicate 2	Replicate 3	Replicate 4	Replicate 5
905	1.16	1.08	1.09	1.12	1.13
SRM11	1.10	1.02	1.19	1.13	1.11

Table 3.16 : RNA concentrations of the samples.

Sample	**Total RNA (ng/µl)**				
	Replicate 1	Replicate 2	Replicate 3	Replicate 4	Replicate 5
905	625	455	595	455	302
SRM11	373	263	263	338	190

Table 3.17 : RIN values for the parallel sets of cultures.

Sample	RIN of the samples				
	Replicate 1	Replicate 2	Replicate 3	Replicate 4	Replicate 5
905	9.9	10.0	9.7	9.6	9.4
SRM11	8.8	9.6	9.4	9.4	9.2

Microarray signals were analyzed by GeneSpring software. Genes whose expression changed more than 2-fold in SRM11 compared to the reference strain were accepted as meaningful in the data analysis. In the mutant SRM11, 769 ORF (open reading frame) were upregulated, 838 ORF were downregulated as two-fold and higher in the long-lived mutant SRM11, compared to the reference strain. Five-fold and higher up- and downregulated genes are shown in Tables 3.18 and 3.19, respectively.

Table 3.18 : Upregulated genes in the mutant SRM11 compared to 905. The genes which were upregulated less than 5-fold are not represented.

Fold change	Systematic/Gene name
151-100	*HXK1, YMR206W*
100-50	*GPH1, HSP26, TMA10, HXT7, HXT6*
50-20	*CYC7,ISF1,RGI1, YNL194C, GPM2,YNR034W-A, DDR2, TSL1, MAL12, HSP12, BDH2, SPG4, MRK1, PGM2, YBR285W, SUE1, MAL32, SSA4, MAL11, ALD4, SOL4*
20-10	*GSY1, EMI2, GLC3,FMP16, RTN2, SPI1, RGI2, YLR149C,BTN2, GAC1, YLR252-W, GPG1, YER121W, YGP1, YFL012W-A, STF1, UIP4, ALD3, HSP82, JEN1, YJL144W, CYB2, DCS2, YKR075C, RTS3, LEE1, YJL220W, OM14, FMP45, RSB1, IGD1, YLR030W, RTC3, MSC1, HXT2, YJR115W, SYM1, YDR379C-A, RNY1, HSP78, PHM7, GRE3*
10-5	*GCY1, INO1, GRX1, GSY2, CUP1-1, SDS24, YER079W, YPT53, YJL163C, MTH1, COX5B, RIM4, GAD1, MAM1, YKL091C, TFS1, XBP1, AMS1, CUP1-2, OYE3, OPI10, GLK1, CTT1, YLR162W, UGP1, YFL015C, TIP1, PDC6, AIM17, YPS5, CUR1, OPT2, Q0017, GUT2, CAR1, TMA17, IKS1, SLZ1, YLR312C, EMP46, YGL258W-A, YNL200C, ATG8, YCR013C, HSP33, ATO2, SRX1, HSP32, DSF1, GAL7, PUT1, TDA10, PBI2, YHR097C, FMP33, YCT1, CAR2, YOR289W, HBN1, APJ1, ATG15, NQM1, YOR186W, UGX2, YER188W, HSP42, APE1, TSA2, YMR196W, SAP4, GTO1, XKS1, HXT5, YNR014W, YBR099C, STF2, RRT8, BXI1, SNO4, YGR130C, YKL151C, YAL004W, CPR6, YBR178W, YMR090W, OSW2, YLR345W, YBR053C, SSA1, YML034C-A, GND2, STB2, HSP30, MGA1, YNL195C, YLR271W, YIL059C, RRT6, MMS2, CRC1, URA10, DDR48, UBI4, YJL199C, GPT2, VID30, SED1, ECM8, GIP2, SDP1, ETR1, HOR7, TPS2, ATG17, YMR326C, YCR097W-A, ZTA1, YFL054C, FMP46, PIN3, YMR173W-A, PNS1*

Table 3.19 : Downregulated genes in the mutant SRM11 compared to 905. The genes which were downregulated less than 5-fold are not represented.

Fold change	Systematic/Gene name
151-100	*PHO84*
100-50	*BI2*
50-20	*YAR075W,AI1, SDA1, ERG20, ARO3, NSR1, ZRT1, DBP2, PCS60, VAR1, AI5_BETA, RSA4, RLP24, AAH1, DHR2, YGR190C, RCL1, BFR2, PRP24*
20-10	*ADH4, MTC3, TOD6, TRM13, YBR255C-A, PNO1, AI3, KRE33, DBP9, GFD2, RPC53, GRC3, HMT1, RRS1, RPG1, ECM1, NOG2, UTP23, MAK16, EFM2, TRM1, ALB1, PHM6, IMD4, YBR266C, RNA14, NOG1, KRE29, YGR160W, DRS1, YTM1, YJR124, CCIC1, REI1, RAS1, DBP7, SAD1, EFG1, YIL096C, MRT4, NOP2, YAR073W, CBF5, RGS2, DAD2, RIX7, RRP8, ARX1, PUF6, FAL1*
10-5	*NIP7, LCP5, AQR1, NOP1, RRB1, EBP2, FAF1, URA7, ESF2, RFU1, IPI3, GCD10, RPA43, EFM1, YHL050C, RPF2 RRP36, MPP10, HCA4, KAP123, SEE1, IMP4, FIN1, SNU13, RPA12, BUD23, SYO1,TIR2, NOP9, NOP7, SPB4, NOP10, YGR054W, UTP25, DBP8, VPS62, RKI1, FPR4, SCD6, ATC1, SSF1, UTP13, YDR344C, HAS1, FAR3, RPC37, RPB5, HGH1, YMR193C-A, PWP1, SOF1, UTP21, RRT14, BMT2, RRN11, TMA46, YVH1, RPC17, YKL165C-A, SGD1, NRP1, NSA2, FCF2, NUG1, URA1, PRS3, FUI1, MRD1, SPO19, NOP53, BRX1, IPI1, BMS1, NOP8, FCY2, MAK21, BCP1, LTV1, NCS2,REX4, TSR1, RRP5, YCR087C-A, RMT2, YGR079W, NAF1, SEO1, ENP1, UTP14, YHM2, RMD9, ENP2, SET6, YPL044C, WSS1, UTP18, NOP14, FYV7, YOR309C, DDC1, VTS1, BUD22, RLP7, YBL028C, RIX1, YCR016W, UTP8, NMD3, NOC4, MTR4, RRT5, NOP58, SPB1, SAM3, SUI1, NOP4, PWP2, RPL41, BRRP12, ERB1, YGR283C, TMA16, YHL029C, PPT1, CDC3, DIP2, IMP3, YML082W, NOP12, RPL21A, KCH1, DBP3, RIO2, SUA5, AIR1, MSS116, NOB1, UBP12, YNL024C, GEP3, RPA135, NCL1, ROK1, YEF3, HEM12, BDF2, TRM8, UTP5, ELP2, YDL129W, RPA49, YBL081W, TSR2, CGR1, GAR1, UTP9, BUD27, RTT10, YLR363W-A, UTP11, DUS1, NOP13, SLX9, UTP10, YHL029C, HOS2, RLI1, TRM82, CSI2, VHT1, SSP1, RSC58, YNL174W*

The upregulated and downregulated genes were classified based on 'Biological process', 'Molecular function' and 'Cellular components', using Slim Mapper in Yeast Genome Database (SGD, www.yeastgenome.org). The upregulated and downregulated genes were also classified based on 'Functional category', using 'MIPS Functional Catalogue (*FunCat*)' database (http://mips.helmholtz-muenchen.de/funcatDB/).

Biological process analysis of the upregulated genes showed that 'oligosaccharide metabolic processes, 'response to oxidative stress,' 'carbohydrate transport and metabolic process' were significantly induced in the long-lived mutant SRM11 (Figure 3.27A). Furthermore, biological analysis of the downregulated genes revealed that 'ribosome subunit biogenesis and assembly', and 'RNA processing' were significantly repressed in the mutant SRM11 (Figure 3.27B).

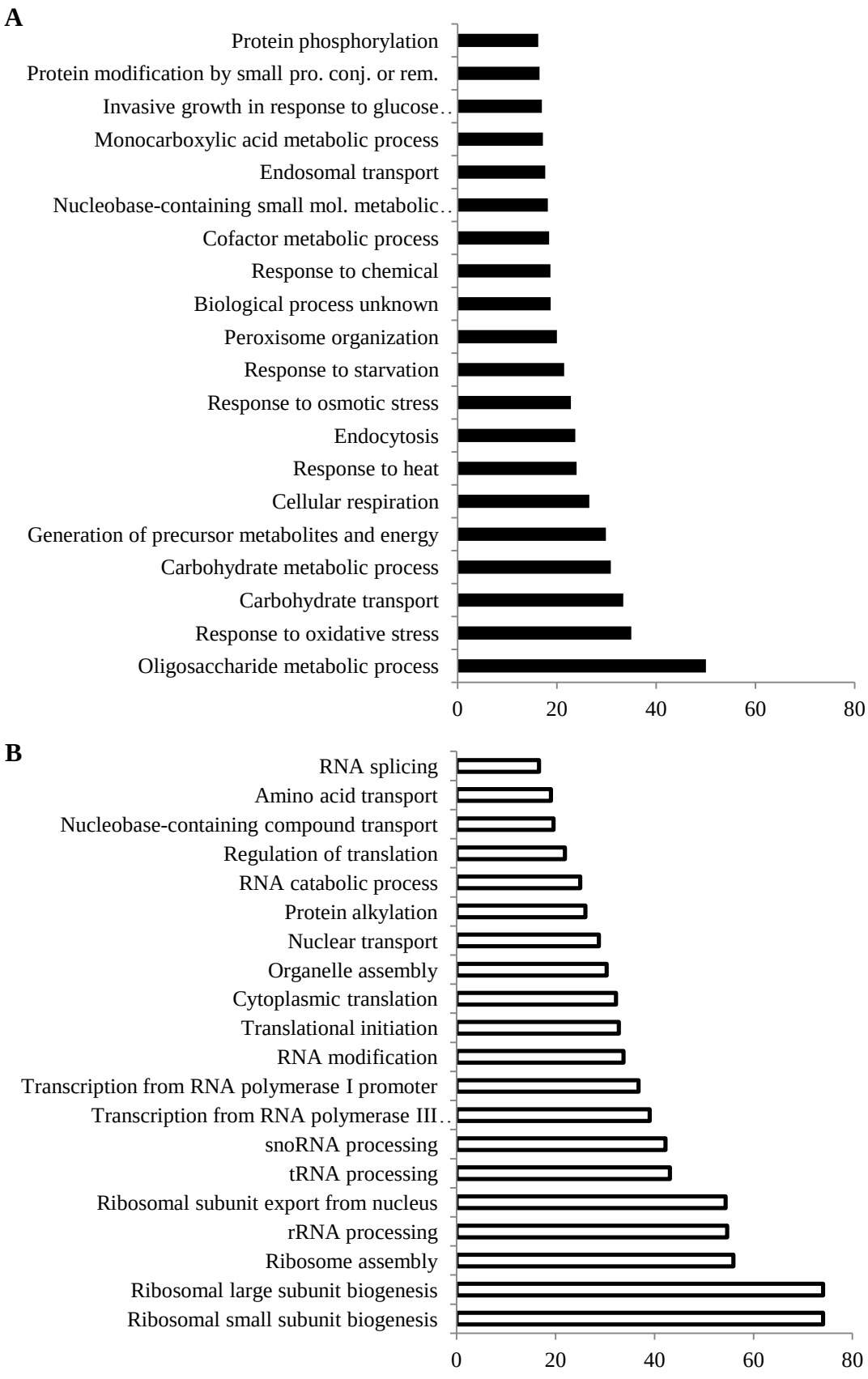

Figure 3.27 : Percentage of two-fold and higher A) induced and B) repressed genes of SRM11 in each biological process. The highest twenty different biological processes are shown.

‘Molecular function’ analysis of upregulated and downregulated genes in the mutant SRM11 showed that ‘hydrolase activity acting on glycosyl bonds’, ‘oxidoreductase activity’ and ‘ubiquitin-like protein binding’ were the highest induced molecular functions, whereas ‘methyltransferase activity’, ‘translation factor activity-RNA binding’ and ‘helicase activity’ were the most repressed molecular functions in the mutant SRM11 (Figure 3.28).

‘Cellular component’ analysis of upregulated and downregulated genes in SRM11 revealed that ‘peroxisome’, ‘extracellular region’ and ‘vacuole’ -related genes were the most induced ones in the long-lived mutant SRM11, whereas nucleolus, ribosome and nucleus regions were the most reduced cellular components. Among these, nucleolus had the highest downregulation level (56%) (Figure 3.29).

To classify the upregulated and downregulated genes in the mutant SRM11, *FunCat* database was also used. Using *FunCat* database, upregulated and downregulated genes (two-fold and higher) were analyzed according to their functional categories (Yasokawa et al., 2008). According to the results (Figure 3.30), ‘Energy’ was the highest upregulated functional category in the long-lived mutant SRM11 compared to the reference strain. Nearly 23% of genes in this category were significantly upregulated. In the subcategories of ‘Energy’, ‘metabolism of energy reserves (e.g. glycogen, trehalose)’ was the highest induced category (about 42%) among the subcategories. Furthermore, nearly 20% of the genes related with cell rescue and defense were induced in SRM11. In the subcategories of this category, ‘detoxification’ and ‘stress response’ were induced by about 20%. On the other hand, about 34% of the genes related with protein synthesis were downregulated. ‘Ribosome biogenesis’ functional category was the nearly 42% repressed subcategory of the highest downregulated ‘Protein synthesis’ category. ‘RNA modification’ was the highest repressed subcategory of ‘Transcription’. Nearly 60% of genes in this subcategory were downregulated.

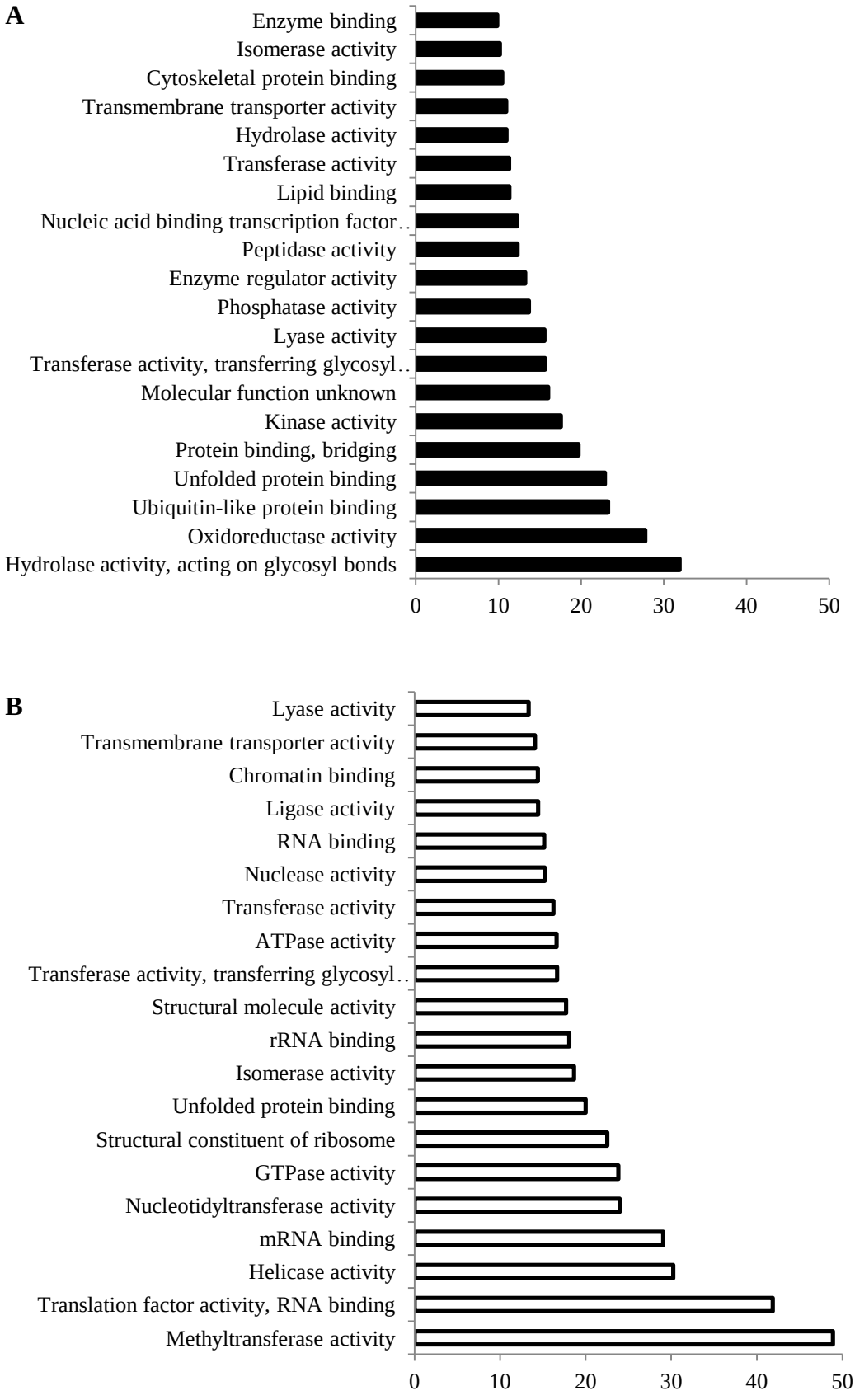

Figure 3.28 : Percentage of A) induced and B) repressed genes (two-fold and higher) in the mutant SRM11 for each molecular function. The highest twenty different molecular functions are shown.

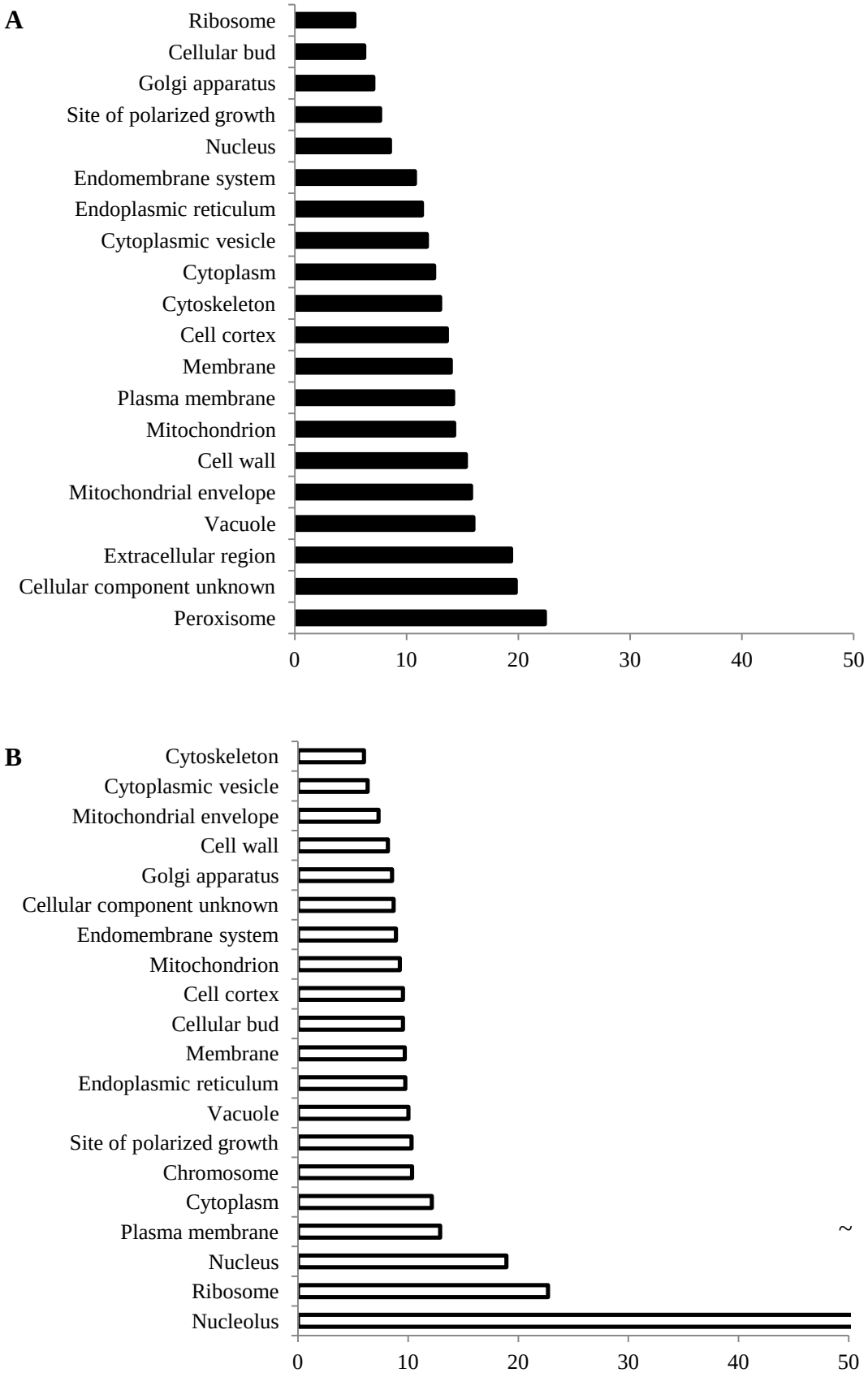

Figure 3.29 : Percentage of A) induced and B) repressed genes (two-fold and higher) in the mutant SRM11 for each biological component. The highest twenty different cellular components are shown.

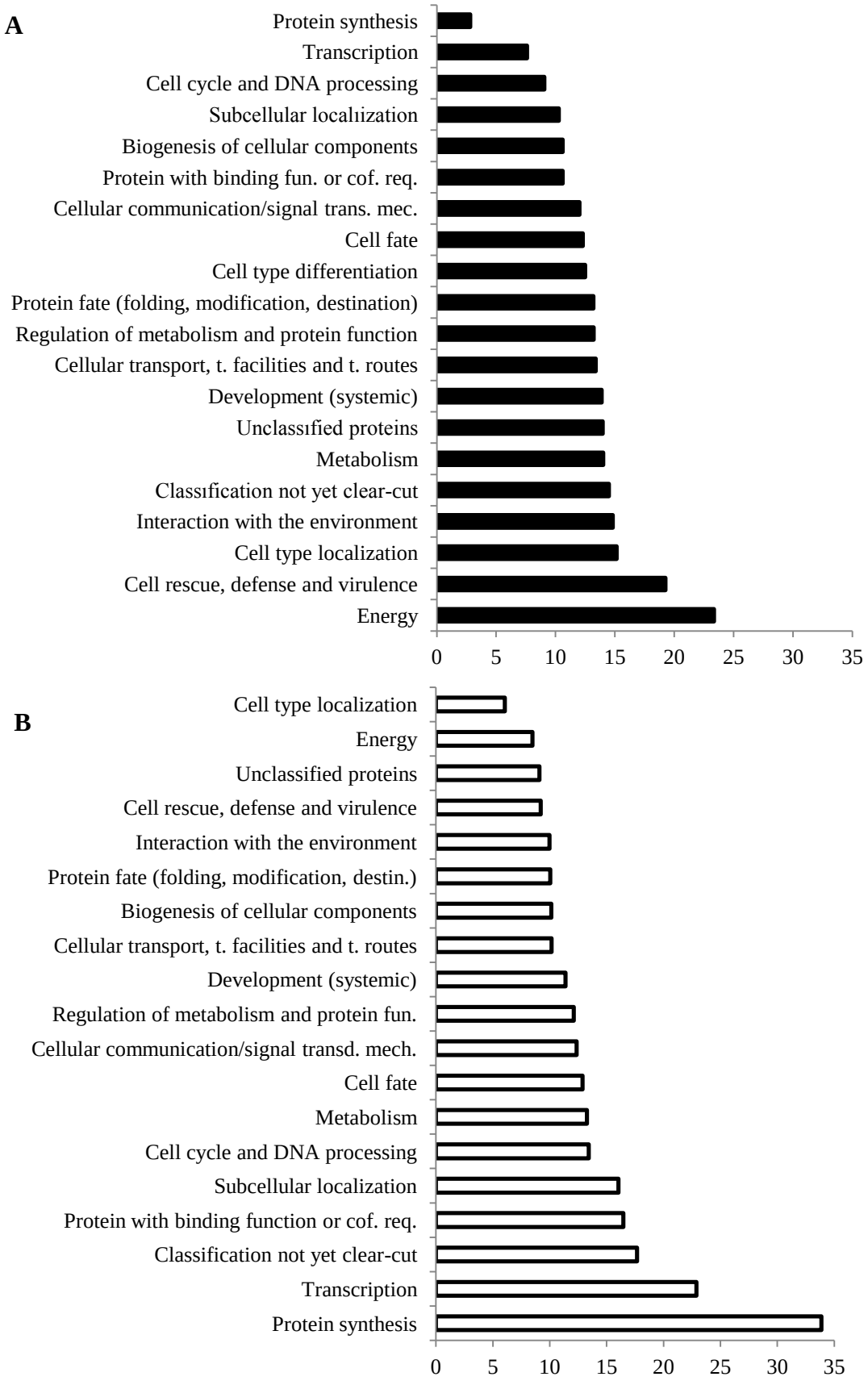

Figure 3.30 : Percentage of A) induced and B) repressed genes (two-fold and higher of SRM11) in each functional category. The data were obtained by *FunCat* database analysis.

According to *FunCat* analysis, the prominent functional categories of the upregulated genes in the long-lived mutant SRM11 are shown in Table 3.20. Also, prominent functional categories of the downregulated genes in the mutant SRM11 are shown in Table 3.21.

Table 3.20 : Selected major functional categories (*FunCat*) of the upregulated genes in the mutant SRM11.

Funcat Category	Systematic name	Gene name	Fold change	Systematic name	Gene name	Fold change
TCA cycle	YPL017C	*IRC15*	4.75	YMR118C	*SHH3*	3.20
	YNR001C	*CIT1*	3.67	YOR136W	*IDH2*	3.09
	YKL148C	*SDH1*	3.54	YDL215C	*GDH2*	2.95
	YAL062W	*GDH3*	3.51	YDR178W	*SDH4*	2.16
	YLR174W	*IDP2*	3.39	YNL037C	*IDH1*	2.15
	YOL126C	*MDH2*	3.35			
Glyoxylate cycle	YNR001C	*CIT1*	3.67	YPR006C	*ICL2*	2.52
	YOL126C	*MDH2*	3.35			
Respiration	YLR327C	*TMA10*	73.79	YMR118C	*SHH3*	3.20
	YEL039C	*CYC7*	46.84	YLR201C	*COQ9*	3.09
	YMR081C	*ISF1*	43.61	YGL191W	*COX13*	3.05
	YOR374W	*ALD4*	20.51	YKL093W	*MBR1*	2.96
	YDL130W-A	*STF1*	14.29	YML129C	*COX14*	2.89
	YML054C	*CYB2*	12.95	YHR067W	*HTD2*	2.86
	YIL111W	*COX5B*	8.79	YDL149W	*ATG9*	2.82
	YGR087C	*PDC6*	7.91	YBR024W	*SCO2*	2.59
	YIL155C	*GUT2*	7.55	YDL085W	*NDE2*	2.41
	YGR008C	*STF2*	6.05	YGR174C	*CBP4*	2.36
	YBR026C	*ETR1*	5.23	YHR001W-A	*QCR10*	2.33
	YNL237W	*YTP1*	4.96	YMR030W	*RSF1*	2.29
	YKL150W	*MCR1*	4.44	YMR056C	*AAC1*	2.27
	YDR216W	*ADR1*	4.34	YDR178W	*SDH4*	2.16
	YPL061W	*ALD6*	4.08	YDL004W	*ATP16*	2.11
	YCR061W	-	4.04	YJR034W	*PET191*	2.09
	YMR256C	*COX7*	3.70	YDR231C	*COX20*	2.07
	YKL148C	*SDH1*	3.54	YEL024W	*RIP1*	2.06
	YML120C	*NDI1*	3.50	YNL055C	*POR1*	2.03
Oxygen and radical detoxification	YCL035C	*GRX1*	9.33	YIR038C	*GTT1*	2.46
	YGR088W	*CTT1*	8.07	YLR109W	*AHP1*	2.44
	YKL086W	*SRX1*	7.06	YER042W	*MXR1*	2.43
	YDR453C	*TSA2*	6.30	YKR066C	*CCP1*	2.30
	YBL064C	*PRX1*	4.80	YJL068C	-	2.27
	YDR513W	*GRX2*	4.63	YHR008C	*SOD2*	2.15
	YGR209C	*TRX2*	3.91	YML028W	*TSA1*	2.14
	YKL026C	*GPX1*	2.88	YJR104C	*SOD1*	2.07
	YLR205C	*HMX1*	2.49			

Table 3.20 (continued) : Selected major functional categories (*FunCat*) of the upregulated genes in the mutant SRM11.

Funcat Category	Systematic name	Gene name	Fold change	Systematic name	Gene name	Fold change
Metabolism of energy reserves (e.g. glycogen, trehalose)	YPR160W	*GPH1*	96.14	YBR126C	*TPS1*	3.80
	YML100W	*TSL1*	35.64	YIL045W	*PIG2*	3.55
	YGR292W	*MAL12*	33.74	YKR058W	*GLG1*	3.34
	YMR105C	*PGM2*	27.20	YDR001C	*NTH1*	3.33
	YBR299W	*MAL32*	22.89	YIL172C	*IMA3*	2.88
	YFR015C	*GSY1*	19.64	YJL221C	*IMA4*	2.80
	YEL011W	*GLC3*	17.62	YMR085W	-	2.66
	YOR178C	*GAC1*	15.18	YMR084W	-	2.66
	YPL240C	*HSP82*	13.15	YGR032W	*GSC2*	2.64
	YLR258W	*GSY2*	9.23	YPR184W	*GDB1*	2.59
	YKL035W	*UGP1*	8.05	YFR003C	*YPI1*	2.28
	YER054C	*GIP2*	5.27	YHR060W	*VMA22*	2.25
	YDR074W	*TPS2*	5.21	YKL157W	*APE2*	2.13
	YGR287C	*IMA1*	4.23	YHR039C-A	*VMA10*	2.07
	YMR261C	*TPS3*	4.01	YMR164C	*MSS11*	2.03
	YPR026W	*ATH1*	3.87			
Heavy metal binding	YEL039C	*CYC7*	46.84	YHR113W	*APE4*	2.71
	YAL061W	*BDH2*	31.20	YBR024W	*SCO2*	2.59
	YHR053C	*CUP1-1*	9.20	YNL097C	*PHO23*	2.50
	YHR055C	*CUP1-2*	8.37	YOR113W	*AZF1*	2.46
	YBR018C	*GAL7*	6.80	YML004C	*GLO1*	2.33
	YBR026C	*ETR1*	5.23	YMR009W	*ADI1*	2.27
	YNL036W	*NCE103*	4.45	YPR176C	*BET2*	2.21
	YKL150W	*MCR1*	4.44	YNL045W	*LAP2*	2.20
	YDR096W	*GIS1*	4.34	YHL010C	*ETP1*	2.17
	YPL230W	*USV1*	4.07	YHR008C	*SOD2*	2.15
	YLR070C	*XYL2*	4.00	YPR107C	*YTH1*	2.13
	YAL060W	*BDH1*	3.96	YKL157W	*APE2*	2.13
	YDL008W	*APC11*	3.31	YDR151C	*CTH1*	2.08
	YBL049W	*MOH1*	3.22	YJR104C	*SOD1*	2.07
	YML131W	-	3.15	YNL155W	-	2.03
Assimilation of ammonia, metabolism of the glutamate group	YMR250W	*GAD1*	8.78	YOR136W	*IDH2*	3.09
	YPL111W	*CAR1*	7.54	YER119C	*AVT6*	2.97
	YLR142W	*PUT1*	6.79	YDL215C	*GDH2*	2.95
	YLR438W	*CAR2*	6.65	YMR085W	-	2.66
	YNR001C	*CIT1*	3.67	YMR084W	-	2.66
	YAL062W	*GDH3*	3.51	YNL037C	*IDH1*	2.15
	YLR174W	*IDP2*	3.39	YJL060W	*BNA3*	2.08

Table 3.20 (continued) : Selected major functional categories (*FunCat*) of the upregulated genes in the mutant SRM11.

Funcat Category	Systematic name	Gene name	Fold change	Systematic name	Gene name	Fold change
Classification not yet clear-cut	YLR251W	*SYM1*	10.77	YOL060C	*MAM3*	3.22
	YCL035C	*GRX1*	9.33	YJR008W	*MHO1*	3.16
	YLR178C	*TFS1*	8.65	YLR201C	*COQ9*	3.09
	YBL078C	*ATG8*	7.18	YPL170W	*DAP1*	3.08
	YNR002C	*ATO2*	7.08	YDR032C	*PST2*	2.94
	YOR289W	-	6.61	YPL247C	-	2.65
	YCR068W	*ATG15*	6.56	YBR052C	*RFS1*	2.57
	YGR043C	*NQM1*	6.55	YNL321W	*VNX1*	2.51
	YMR196W	-	6.28	YMR068W	*AVO2*	2.50
	YBR046C	*ZTA1*	5.15	YNL097C	*PHO23*	2.50
	YCR091W	*KIN82*	4.78	YMR020W	*FMS1*	2.45
	YOR292C	-	4.52	YLR109W	*AHP1*	2.44
	YJR096W	-	4.45	YPR002W	*PDH1*	2.32
	YPL003W	*ULA1*	4.32	YKL013C	*ARC19*	2.28
	YIL097W	*FYV10*	4.07	YLR128W	*DCN1*	2.27
	YGR209C	*TRX2*	3.91	YPL006W	*NCR1*	2.23
	YPR026W	*ATH1*	3.87	YPR066W	*UBA3*	2.23
	YMR304W	*UBP15*	3.47	YPR127W	-	2.19
	YPL191C	-	3.41	YPR107C	*YTH1*	2.13
	YJL034W	*KAR2*	3.40	YIL063C	*YRB2*	2.08

Table 3.21 : Selected major functional categories (*FunCat*) of the downregulated genes in the mutant SRM11.

Funcat Category	Systematic name	Gene name	Fold change	Systematic name	Gene name	Fold change
Ribosome biogenesis*	YGR245C	*SDA1*	40.23	YAL025C	*MAK16*	13.69
	YGR159C	*NSR1*	35.62	YPL093W	*NOG1*	12.50
	YCR072C	*RSA4*	28.13	YLL008W	*DRS1*	12.29
	YLR009W	*RLP24*	26.66	YOR272W	*YTM1*	11.75
	YKL078W	*DHR2*	24.87	YKR024C	*DBP7*	11.21
	YDR299W	*BFR2*	20.14	YKL009W	*MRT4*	10.91
	YLR276C	*DBP9*	16.45	YNL061W	*NOP2*	10.86
	YOR294W	*RRS1*	14.85	YLL034C	*RIX7*	10.47
	YAL059W	*ECM1*	14.36	YDR101C	*ARX1*	10.32
	YNR053C	*NOG2*	14.29			

*****Funcat categories with at least 10-fold upregulated genes.

Table 3.21 (continued): Selected major functional categories (*FunCat*) of the downregulated genes in the mutant SRM11.

Funcat Category	Systematic name	Gene name	Fold change	Systematic name	Gene name	Fold change
RNA synthesis*	YNL112W	*DBP2*	33.16	YDR120C	*TRM1*	13.07
	YKL078W	*DHR2*	24.87	YMR061W	*RNA14*	12.56
	YOL010W	*RCL1*	23.10	YLL008W	*DRS1*	12.29
	YDR299W	*BFR2*	20.14	YOR272W	*YTM1*	11.75
	YBL054W	*TOD6*	19.28	YKR024C	*DBP7*	11.21
	YLR276C	*DBP9*	16.45	YNL061W	*NOP2*	10.86
	YDL150W	*RPC53*	15.84	YDR101C	*ARX1*	10.32
	YOR294W	*RRS1*	14.85	YDR496C	*PUF6*	10.27
TCA cycle	YDR234W	*LYS4*	2.90	YJL200C	*ACO2*	2.06
Glyoxylate cycle	YBR084W	*MIS1*	2.03			
Transcription activation	YNR054C	*ESF2*	9.14	YDR492W	*IZH1*	2.97
	YNL175C	*NOP13*	5.15	YAL019W	*FUN30*	2.87
	YLR014C	*PPR1*	4.33	YPR052C	*NHP6A*	2.53
	YOR140W	*SFL1*	4.07	YOR315W	*SFG1*	2.52
	YOR337W	*TEA1*	3.73	YBL052C	*SAS3*	2.42
	YEL009C	*GCN4*	3.73	YGL112C	*TAF6*	2.02
	YER130C	-	3.43			
Translational control	YGR159C	*NSR1*	35.62	YJL125C	*GCD14*	3.41
	YKL078W	*DHR2*	24.87	YPL237W	*SUI3*	3.24
	YDR101C	*ARX1*	10.32	YBR189W	*RPS9B*	3.16
	YGR054W	-	8.05	YML014W	*TRM9*	3.03
	YJL050W	*MTR4*	5.96	YCL037C	*SRO9*	3.00
	YNL244C	*SUI1*	5.86	YOR276W	*CAF20*	2.88
	YPL043W	*NOP4*	5.85	YML016C	*PPZ1*	2.75
	YGR123C	*PPT1*	5.65	YDR025W	*RPS11A*	2.73
	YPR041W	*TIF5*	4.37	YJR007W	*SUI2*	2.39
	YNR038W	*DBP6*	3.86	YDR429C	*TIF35*	2.37
	YGL236C	*MTO1*	3.57	YBR048W	*RPS11B*	2.29
	YER153C	*PET122*	3.46	YER176W	*ECM32*	2.00
Cellular signaling	YNL132W	*KRE33*	16.73	YJL098W	*SAP185*	3.35
	YPL093W	*NOG1*	12.50	YCL024W	*KCC4*	3.27
	YOR101W	*RAS1*	11.26	YBR028C	*YPK3*	3.17
	YOR107W	*RGS2*	10.55	YDR126W	*SWF1*	2.93
	YLL034C	*RIX7*	10.47	YAR018C	*KIN3*	2.92
	YLR449W	*FPR4*	7.92	YML097C	*VPS9*	2.84
	YLR222C	*UTP13*	7.78	YER031C	*YPT31*	2.81
	YIR026C	*YVH1*	7.42	YJR057W	*CDC8*	2.79
	YMR229C	*RRP5*	6.57	YOL128C	*YGK3*	2.75

*****Funcat categories with at least 10-fold upregulated genes.

Table 3.21 (continued): Selected major functional categories (*FunCat*) of the downregulated genes in the mutant SRM11.

Funcat Category	Systematic name	Gene name	Fold change	Systematic name	Gene name	Fold change
Cellular signaling	YCR057C	*PWP2*	5.75	YML016C	*PPZ1*	2.75
	YGR123C	*PPT1*	5.65	YLR389C	*STE23*	2.68
	YNL207W	*RIO2*	5.54	YPR048W	*TAH18*	2.66
	YGR200C	*ELP2*	5.27	YNL154C	*YCK2*	2.58
	YOR119C	*RIO1*	4.94	YDR364C	*CDC40*	2.39
	YLR397C	*AFG2*	4.92	YGR040W	*KSS1*	2.36
	YDR075W	*PPH3*	4.82	YMR138W	*CIN4*	2.34
	YDL031W	*DBP10*	4.75	YOR127W	*RGA1*	2.34
	YOR233W	*KIN4*	4.46	YOL045W	*PSK2*	2.24
	YDR523C	*SPS1*	4.30	YJR072C	*NPA3*	2.24
	YOR140W	*SFL1*	4.07	YBR175W	*SWD3*	2.24
	YGR173W	*RBG2*	4.03	YCR027C	*RHB1*	2.19
	YIL159W	*BNR1*	3.91	YLR243W	*GPN3*	2.17
	YBR276C	*PPS1*	3.57	YOR171C	*LCB4*	2.17
	YNL238W	*KEX2*	3.50	YOL105C	*WSC3*	2.06
	YDR524C	*AGE1*	3.36	YGR152C	*RSR1*	2.06
Classification not yet clear-cut	YDR299W	*BFR2*	20.14	YIL103W	*DPH1*	4.25
	YPL093W	*NOG1*	12.50	YGR169C	*PUS6*	4.24
	YNL061W	*NOP2*	10.86	YCL059C	*KRR1*	4.04
	YLR175W	*CBF5*	10.67	YKL191W	*DPH2*	3.69
	YIL064W	*SEE1*	8.46	YHR070W	*TRM5*	3.58
	YIL091C	*UTP25*	8.04	YGL236C	*MTO1*	3.57
	YHR066W	*SSF1*	7.83	YER095W	*RAD51*	3.55
	YLR222C	*UTP13*	7.78	YOR243C	*PUS7*	3.54
	YLR196W	*PWP1*	7.57	YNL110C	*NOP15*	3.51
	YLR409C	*UTP21*	7.55	YIL003W	*CFD1*	3.35
	YNL124W	*NAF1*	6.46	YHR187W	*IKI1*	3.13
	YBR247C	*ENP1*	6.37	YDR312W	*SSF2*	3.10
	YCL054W	*SPB1*	5.90	YML014W	*TRM9*	3.03
	YPL012W	*RRP12*	5.73	YGL246C	*RAI1*	3.00
	YMR049C	*ERB1*	5.72	YER156C	-	2.99
	YLR129W	*DIP2*	5.64	YOR001W	*RRP6*	2.93
	YNL207W	*RIO2*	5.54	YAR018C	*KIN3*	2.92
	YGL169W	*SUA5*	5.52	YNR020C	*ATP23*	2.79
	YBL024W	*NCL1*	5.43	YKR051W	-	2.77
	YDL201W	*TRM8*	5.32	YNR029C	-	2.76
	YKL099C	*UTP11*	5.16	YEL040W	*UTR2*	2.69
	YOR119C	*RIO1*	4.94	YFR048W	*RMD8*	2.51
	YBR061C	*TRM7*	4.56	YJR072C	*NPA3*	2.24
	YKR079C	*TRZ1*	4.29	YBR175W	*SWD3*	2.24
	YML018C	-	4.28	YOR006C	*TSR3*	2.08

To determine which transcription factors regulate the upregulated genes in the long-lived mutant SRM11, Yeastract database was used (Abdulrehman et al., 2011). The ten most important transcription factors which regulate most of the upregulated genes are shown in Table 3.22.

Table 3.22 : Transcription factors and their contribution percentage to the upregulated genes in SRM11. The first ten transcription factors with the highest contribution to the upregulated genes are indicated.

Transcription Factor	Percentage of Contribution of Upregulated Genes
Ace2p	81.69%
Sfp1p	79.61%
Msn2p	72.47%
Tec1p	67.53%
Ste12p	67.27%
Bas1p	62.08%
Msn4p	61.04%
Sok2p	59.35%
Gcn4p	55.84%
Ash1p	54.94%

According to Yeastract analysis results (Table 3.22), the main transcription factor that is responsible for the majority of the upregulated genes in the long-lived SRM11 is Ace2p, which contributes to 81.69% of the upregulated genes. Ace2p is mainly responsible for the transcription of *CUP1* genes and is required for septum destruction after cytokinesis (Butler and Thiele, 1991; Mazanka and Weiss, 2010). The second transcription factor, Sfp1p, covers 79.61% of the upregulated genes in the mutant SRM11. It is one of the downstream effectors of the Target of Rapamycin (TOR) kinase. Sfp1 negatively regulates TORC1 phosphorylation of Sch9. The Target of Rapamycin (TOR) kinase is part of a highly conserved signaling pathway to regulate ribosomal protein and ribosome biogenesis-related gene transcription. Sfp1 interacts directly with TOR complex 1 (TORC1) in a rapamycin-regulated manner, and the phosphorylation of Sfp1 by this kinase complex regulates its function (Lempiainen et al., 2009). The third transcription factor which is responsible for 72% of the upregulated genes in SRM11 is Msn2p. Msn2p and Msn4p transcription factors control response to various stress types, and are known as environmental stress response regulators (Estruch and Carlson, 1993; Martinez-Pastor et al., 1996). However, it should be noted that the generally low levels of

expression changes in transcription factors may be well below the detection limits or sensitivity of the microarray systems (e.g. lower than 2-fold changes). Thus, there may be other transcription factors the expression changes of which remained undetected.

3.3 CLS analysis of various stress-resistant *S. cerevisiae* mutants

3.3.1 Semi-quantitative CLS analysis of various stress-resistant *S. cerevisiae* mutants

Aging studies have shown that stress resistance is associated with longevity in a range of model organisms (Barsyte et al., 2001; Longo, 2003; Martin et al., 1996; Murakami and Johnson, 1998; Service et al., 1985). Therefore, another aim of the present study was to investigate which particular stress type(s) is/are associated with chronological longevity. For this purpose, various stress resistant yeast mutants which had been previously obtained by evolutionary engineering approach (Table 2.1) were used. Traditional quantitative CLS method can be labor-intensive to analyze CLS in a high number of yeast strains. Thus, CLS of the yeast mutants was preliminarily determined using the semi-quantitative CLS method (improved in the present study, Section 2.2.1.4). Culture densities of the reference and mutant yeast strains were determined at the stationary phase of growth (72^{nd} h of incubation) by spectrophotometer and are shown in Table 3.23.

Table 3.23 : OD_{600} values of 905 and various stress-resistant yeast cultures on the third day of incubation in 2% YMM.

Strains	OD_{600}	OD_{600}	OD_{600}	AVE.	STD.
905	6.12	6.09	6.12	6.11	0.01
B8	6.00	6.02	5.98	6.00	0.02
T8	7.80	7.60	7.72	7.71	0.10
M8FE	6.60	6.40	6.52	6.51	0.10
H7	8.40	8.30	8.38	8.36	0.05
F3	7.20	6.60	6.95	6.92	0.30
M9	6.21	6.07	6.12	6.13	0.07
F1	8.70	8.75	8.78	8.74	0.04
2E	6.39	6.42	6.38	6.40	0.02
FD11	6.90	6.85	6.89	6.88	0.03
C9	7.93	7.95	7.92	7.93	0.02

AVE and STD indicate arithmetic mean and standard deviation values of three independent results, respectively.

Culture densities at the stationary phase of growth were significantly different (Table 3.23). This difference in culture densities was considered as a critical factor for the improvement of the semi-quantitative CLS assay for a more comparable CLS analysis of the cultures at significantly different culture densities. Since OD_{600} values of all cultures were higher than 6, they were adjusted to 6. By doing so, an equal number of cells could be spotted onto YPD plates at the beginning and during the CLS experiment (from Day 0 to Day 12-14). At the end of the experiment, photographs belonging to different days of the CLS experiments were joined to compare CLS of various yeast mutants (Figure 3.31).

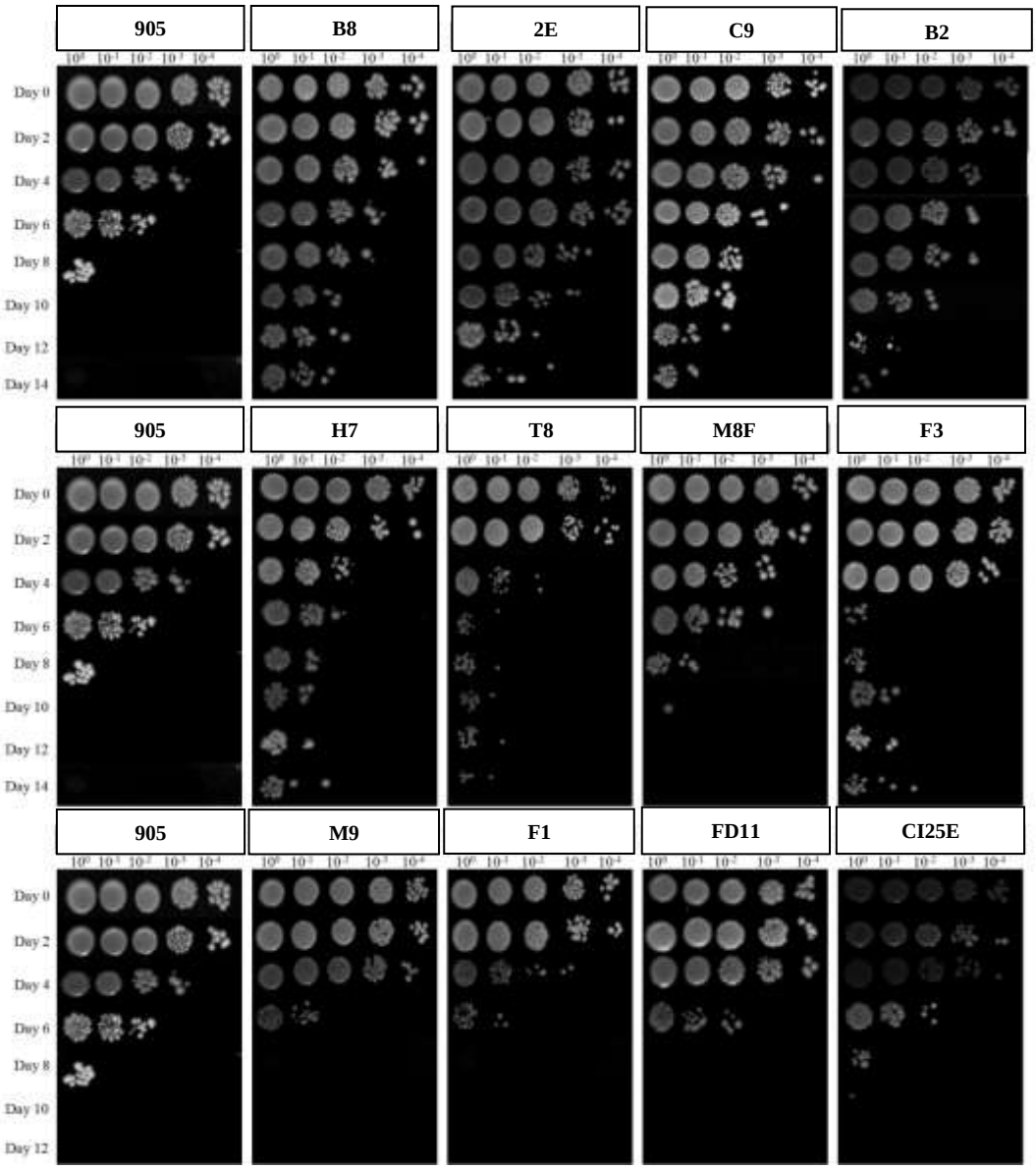

Figure 3.31 : Semi-quantitative CLS results of the stress-resistant *S. cerevisiae* mutants in 2% glucose (YMM) (Modified from Arslan et al., (in press)).

An equal number of spots was obtained at the beginning of the CLS experiment for the mutant cultures tested, which shows that an equal number of cells was spotted onto the YPD plates (Figure 3.31). On Day 2 of the CLS experiment, there was no viability difference in the cultures, however, differences were observed on Day 4 of the CLS experiment. On day 8 of the CLS experiment, B2, B8, 2E, C9 and H7 had significantly higher viability compared to 905 (100, 100, 100 and 10-fold, respectively), suggesting that these stress resistant mutants are long-lived. There were no significant differences in viability between 905 and H7 on the 8^{th} day of chronological aging, however, the viability of H7 was higher than that of 905 at the 10^{th}, 12^{th} and 14^{th} days of chronological aging. The viability of F3 increased at the 10^{th} day of chronological aging. The reason could be the adaptive regrowth caused by the nutrients released from death cells (Fabrizio et al., 2004; Fabrizio and Longo, 2003).

3.3.2 Quantitative CLS analysis of the stress-resistant and long-lived *S. cerevisiae* mutants

Semi-quantitative CLS analysis results showed the prominent long-lived stress-resistant mutants. To quantitatively determine CLS of the mutants and verify semi-quantitative results, conventional quantitative CLS analysis was carried out in the selected stress-resistant and long-lived yeast mutants in expired medium. Since the cultures reach the stationary phase on day 3 of incubation in 2% YMM, that day was considered as 'Day 0' of the CLS experiment. Cell viability of the cultures was determined by viable cell counting method and assumed as 100%. Every second day, the viability of the cultures was determined and % viability of the culture was calculated. Survival curves of the yeast mutants are shown in Figure 3.32.

On day 2 of the CLS experiment, no apparent differences in viabilities were observed between the reference and the tested stress-resistant yeast mutants (Figure 3.32). On day 4 of the CLS experiment, the viability of H7 was significantly lower than those of the other yeast strains. However, viability of H7 was higher than the reference strain on day 8 of the CLS experiment. Significant differences in viabilities were observed on days 8 and 10 of the CLS experiment. Viabilities of the mutant strains 2E, B8 and C9 were higher than those of the reference strain and the mutants, H7 and B2. It should be noted that the viability variations between the mutants C9, 2E and

B8 became significant on day 12 of the CLS experiment, therefore, the experiment was ended and CLS of B8, 2E and C9 in 2% YMM were determined as approximately day 12. The mutant B8, 2E and C9 were chosen for further analysis, due to their high viability.

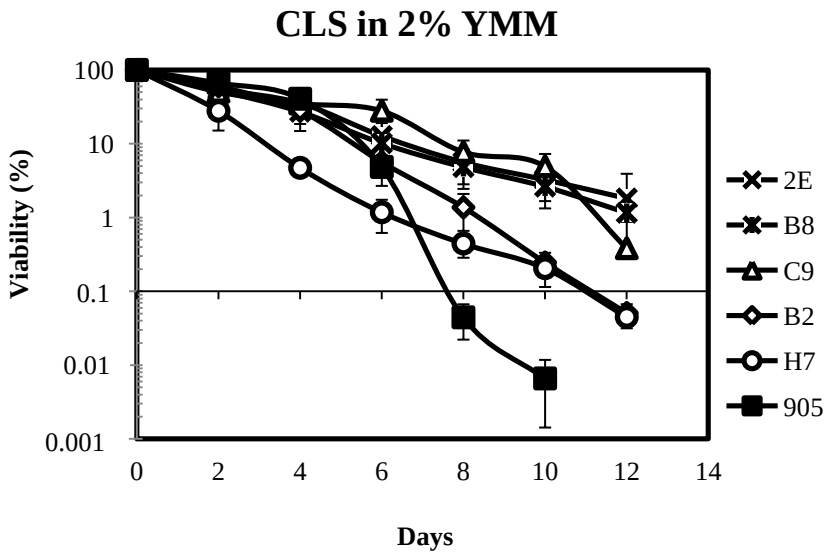

Figure 3.32 : Quantitative CLS analysis of 905 and stress-resistant mutants B2, B8, C9, 2E and H7 in 2% YMM.

It has been recommended that CLS of the long-lived yeast mutants should be tested in water or calorie-restricted medium (Longo et al., 2012). Therefore, CLS of the long-lived mutants was also investigated in calorie-restricted medium (0.5% YMM) in the present study. Survival curves of the mutant B8, 2E and C9 in calorie-restricted medium are shown in Figure 3.33.

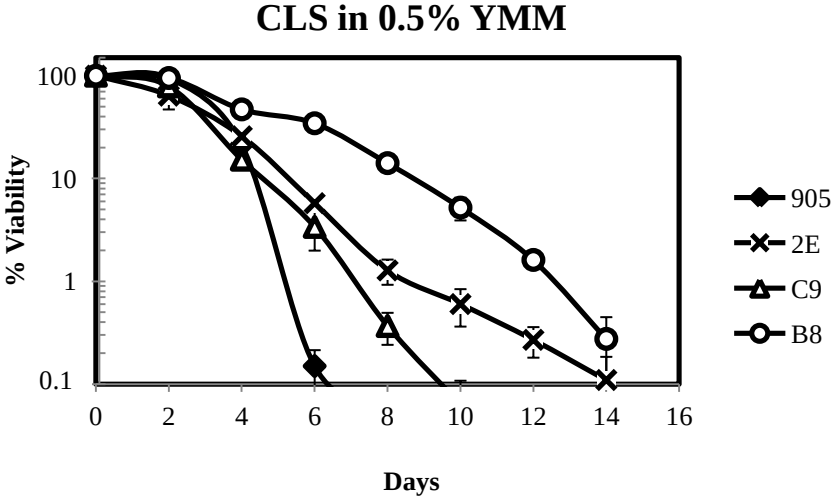

Figure 3.33 : CLS of 2E, C9, B2, B8 and 905 in calorie-restricted medium (0.5% glucose YMM).

The mutants 2E, B8 and C9 had longer lifespan than the reference strain also in the calorie-restricted medium (0.5% YMM) (Figure 3.33). Thus, these mutants were chosen for further analyses.

CLS of the long-lived mutants was also investigated in water. To optimize the procedure, C9 and the reference strain were tested first. Stationary phase cultures were washed with sterile distilled water and incubated in water in shake flasks. Every second day, culture viabilities were determined by counting CFU and cells were washed every four days. Survival curves of the tested strains are shown in Figure 3.34.

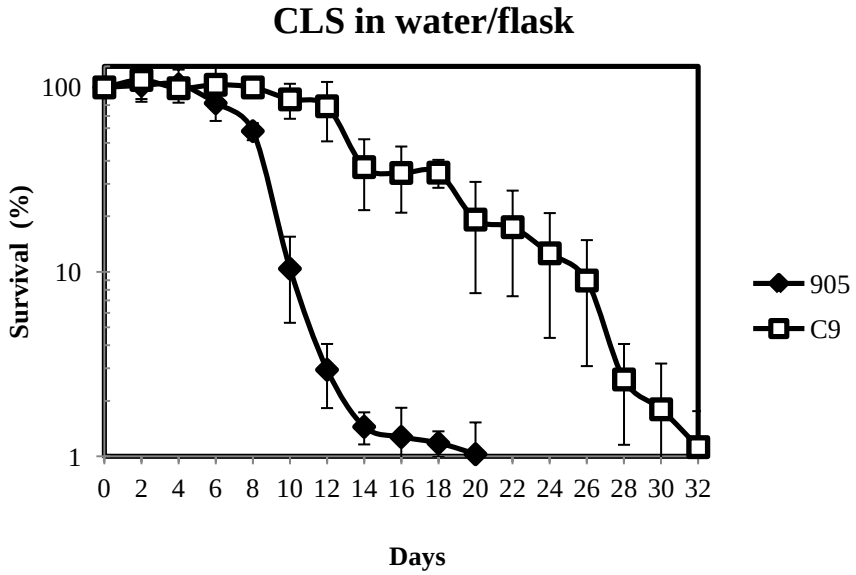

Figure 3.34 : CLS of 905 and C9, cultivated in flasks with water only.

CLS of the mutant strain C9 was almost 2-fold higher than that of the reference strain (Figure 3.34). The results also showed a prolonged lifespan of C9. During the experimental procedure, some difficulties occurred. To wash the cells cultured in flasks, the culture had to be transferred from flasks into centrifuge/culture tubes. After centrifugation and washing steps, cultures were transferred back to flasks. This procedure was labor-intensive and also increased the contamination risk of the aging cultures. To overcome this difficulty, 50 ml-culture/centrifuge tubes were used for CLS cultivation for easier washing of the cells. Using culture tubes, survival curves of the mutant B8 and the reference strain were obtained (Figure 3.35). According to the results of the CLS experiment, an interesting observation was made. Viabilities of the cells tested in culture tubes were higher than those cultivated in flasks. Even though the viability of 905 in flasks decreased to 1% on day 16 of the CLS

experiment, its viability in culture tubes did not decrease under 10% on day 32 of the CLS experiment. Comparative survival curves of 905 in flasks and culture tubes are shown in Figure 3.36. Apparently, the type of the culture tube/flask strongly affects CLS, which could be due to differences in the aeration of the culture.

Since CLS in calorie-restricted medium (0.5% and lower glucose) is acceptable for the verification of chronological longevity (Longo et al., 2012), detailed analysis in water was not performed. According to the quantitative CLS results in 2% and 0.5% YMM, the long-lived mutants 2E, B8 and C9 were chosen for further analysis.

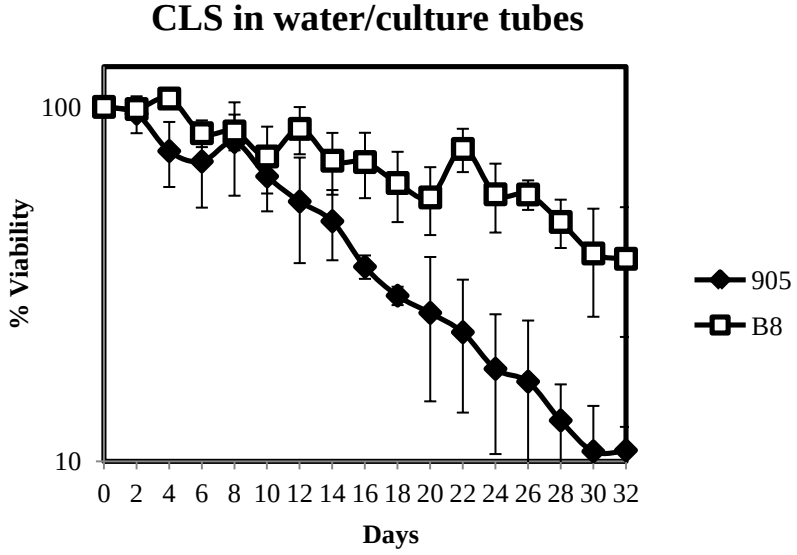

Figure 3.35 : CLS of 905 and the mutant strain B8 cultivated in culture tubes in water.

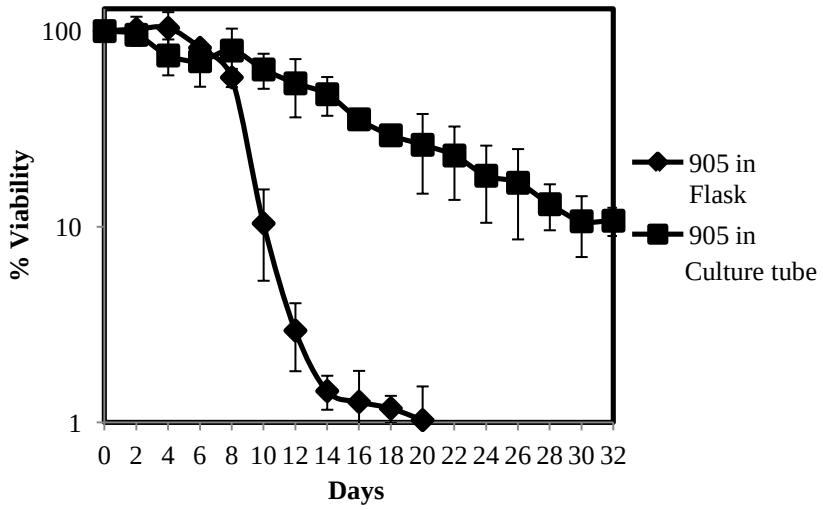

Figure 3.36 : Comparative CLS of 905 cultivated in flasks and culture tubes, using water.

3.3.3 Comparative transcriptomic analysis of stress-resistant and long-lived *S. cerevisiae* mutants

Transcriptomic data of the stress-resistant and long-lived mutants were compared to the reference strain and each other to gain insight into the molecular basis of chronological longevity.

Genes the expression of which has changed by 2-fold and higher in the mutants C9, B8, 2E and SRM11 compared to the reference strain were determined using GeneSpring software. As a result of the comparative transcriptomic analysis, 17 downregulated genes were found as common in the mutants C9, B8, 2E and SRM11, and similarly, 48 upregulated genes were found as common in the mutants C9, B8, 2E and SRM11. The list of the overlapping up- and downregulated genes in all four mutants are given in Tables 3.24 and Tables 3.25, respectively.

Table 3.24 : The list of the 48 commonly upregulated genes in long-lived and stress-resistant mutants C9, B8, 2E and SRM11, compared to the reference strain.

Gene Symbol	Systematic name	Fold Change [C9] vs [905]	Fold Change [B8] vs [905]	Fold Change [2E] vs [905]	Fold Change [SRM11] vs [905]
HXK1	YFR053C	174.20	7.58	125.99	150.41
GPH1	YPR160W	184.49	6.27	59.87	96.13
MAL12	YGR292W	168.93	8.93	52.97	33.73
MAL32	YBR299W	164.16	9.51	42.10	22.89
	YNL194C	39.91	4.85	107.42	40.75
PGM2	YMR105C	93.34	10.42	27.21	27.19
MAL11	YGR289C	100.15	6.21	20.56	20.68
RTN2	YDL204W	76.64	5.85	20.97	16.88
TSL1	YML100W	54.88	7.59	28.20	35.63
ISF1	YMR081C	21.08	2.51	63.98	43.60
HSP26	YBR072W	64.54	5.03	10.01	94.89
GAC1	YOR178C	34.74	3.73	20.56	15.18
GLC3	YEL011W	24.80	3.57	24.93	17.62
GSY1	YFR015C	18.28	3.09	28.37	19.63
SOL4	YGR248W	22.76	4.19	15.92	4.45
GPM2	YDL021W	12.37	3.89	19.56	39.24
DCS2	YOR173W	17.49	3.72	9.19	12.73
YPT53	YNL093W	4.71	3.21	21.81	8.99
GAD1	YMR250W	16.12	5.04	5.79	8.78
GSY2	YLR258W	16.66	2.77	5.31	9.22
RTS3	YGR161C	5.72	4.80	13.40	12.43
UIP4	YPL186C	11.32	2.95	8.77	13.54
	YJL144W	3.51	5.54	10.25	13.05

Table 3.24 (continued) : The list of the 48 commonly upregulated genes in long-lived and stress-resistant mutants C9, B8, 2E and SRM11, compared to the reference strain.

Gene Symbol	Systematic name	Fold Change [C9] vs [905]	Fold Change [B8] vs [905]	Fold Change [2E] vs [905]	Fold Change [SRM11] vs [905]
GCY1	YOR120W	10.17	2.64	6.31	9.98
GRE3	YHR104W	12.09	2.79	3.57	10.03
AGP2	YBR132C	5.30	2.75	10.28	4.39
	YJL163C	6.86	3.52	7.69	8.90
HSP82	YPL240C	6.66	5.04	4.54	13.14
RNY1	YPL123C	6.92	2.11	6.57	10.57
YPK2	YMR104C	5.09	3.00	7.45	3.80
FMP33	YJL161W	6.49	3.16	4.90	6.66
COX5B	YIL111W	5.90	2.19	6.31	8.79
XKS1	YGR194C	5.10	2.33	6.94	6.14
	YKL151C	7.81	2.40	4.06	5.91
SDP1	YIL113W	7.04	2.70	3.60	5.23
STB2	YMR053C	6.50	2.90	3.56	5.65
TPK1	YJL164C	5.01	3.38	3.79	4.86
ATG29	YPL166W	2.45	3.01	5.92	2.43
	YBR085C-A	3.80	2.25	4.84	4.41
CIT1	YNR001C	3.85	2.42	4.30	3.67
MAL13	YGR288W	2.84	2.51	5.12	3.02
OPI10	YOL032W	2.92	2.72	4.26	8.26
PIN3	YPR154W	2.02	2.11	5.61	5.12
ATG7	YHR171W	2.55	2.06	4.11	3.37
RRI2	YOL117W	2.38	2.01	3.98	3.54
SAF1	YBR280C	3.11	2.07	2.86	2.79
CUR1	YPR158W	2.42	3.07	2.07	7.66
CPR6	YLR216C	2.45	2.16	2.63	5.89

Table 3.25 : The list of the 17 commonly downregulated genes in long-lived and stress-resistant mutants C9, B8, 2E and SRM11, compared to the reference strain.

Gene Symbol	Systematic name	Fold Change [C9] vs [905]	Fold Change [B8] vs [905]	Fold Change [2E] vs [905]	Fold Change [SRM11] vs [905]
AAH1	YNL141W	11.54	2.27	8.16	24.93
DBP2	YNL112W	8.99	2.54	9.91	33.15
	YGR079W	4.29	2.72	11.99	6.46
	YNL024C	3.52	2.68	12.74	5.46
GFD2	YCL036W	6.47	2.00	10.25	16.27
RAS1	YOR101W	11.25	2.54	4.30	11.25
AQR1	YNL065W	3.58	2.10	10.38	9.73
RGS2	YOR107W	3.27	2.04	9.53	10.55
	YGR160W	2.55	2.21	8.62	12.29
IPI3	YNL182C	4.88	2.12	5.61	9.07
ALB1	YJL122W	2.95	2.25	7.38	13.05

Table 3.25 (continued) : The list of the 17 commonly downregulated genes in long-lived and stress resistant mutants C9, B8, 2E and SRM11, compared to the reference strain.

Gene Symbol	Systematic name	Fold Change [C9] vs [905]	Fold Change [B8] vs [905]	Fold Change [2E] vs [905]	Fold Change [SRM11] vs [905]
UTP23	YOR004W	3.47	2.29	6.82	13.74
MCH5	YOR306C	2.51	2.23	6.95	3.37
FAL1	YDR021W	4.69	2.02	4.31	10.19
DBP7	YKR024C	2.55	2.96	5.17	11.20
RRP36	YOR287C	3.08	2.15	5.03	8.75
GAP1	YKR039W	2.27	2.27	2.67	2.05

The overlapping genes in the long-lived and stress-resistant mutants C9, B8, 2E and SRM11 were also classified based on Gene Ontology (GO) analysis of biological processes, using GO Slim Mapper database (www.yeastgenome.org). GO analysis results of commonly upregulated and downregulated genes are shown in Table 3.26 and 3.27, respectively. The twenty highest induced or repressed biological processes are shown.

Table 3.26 : GO analysis results of the commonly upregulated genes in C9, B8, 2E and SRM11 according to their biological process.

Biological Process	% of induced genes in the category	Gene symbol/ Systematic name	Number of genes upregulated in C9, B8, 2E and SRM11 in the category	Total number of genes in the category
Oligosaccharide metabolic process	16.13	*MAL32, MAL11, MAL12, TSL1, PGM2*	5	31
Generation of precursor metabolites and energy	6.54	*GLC3, GSY1, HXK1, COX5B, GSY2, ISF, PGM2, CIT1, GAC1, GPH1*	10	153
Carbohydrate metabolic process	6.25	*MAL32, GLC3, GSY1, HXK1, XKS1, MAL13, MAL11, MAL12, GRE3, GSY2, TSL, PGM2, OPI10, GCY1, GAC1, GPH1*	16	256
Carbohydrate transport	6.06	*HXK1, MAL11*	2	33
Response to heat	4.23	*HSP26, GAC1 ,CUR1*	3	71
Protein folding	4.21	*HSP26, CPR6, HSP82, CUR1*	4	95
Cellular respiration	3.61	*COX5B, ISF1, CIT1*	3	83
Cell morphogenesis	3.45	*RNY1*	1	29
Response to oxidative stress	2.91	*GRE3, GAD1, GCY1*	3	103
Cofactor metabolic process	2.25	*HXK1, SOL4, YKL151C, CIT1*	4	178
Protein lipidation	2.22	*ATG7*	1	45
Response to osmotic stress	2.17	*GRE3, HSP82*	2	92
Protein maturation	2.04	*HSP82*	1	49
Nucleobase-containing small molecule metabolic process	2.02	*HXK1, SOL4, COX5B, YKL151C*	4	198
Response to starvation	1.79	*DCS2*	1	56
Organelle inheritance	1.67	*RTN2*	1	60
RNA catabolic process	1.52	*DCS2, RNY1*	2	132
Protein phosphorylation	1.51	*SDP1, TPK1, YPK2*	3	199
Peroxisome organization	1.37	*RTN2*	1	73
Telomere organization	1.28	*HSP82*	1	78
Signaling	1.25	*SDP1, TPK1, RRI2*	3	240

Table 3.27 : GO analysis results of the commonly downregulated genes in C9, B8, 2E and SRM11 according to their biological process.

Biological process	% of induced genes in the category	Gene symbol/ Systematic name	Number of genes downregulated in C9, B8, 2E and SRM11 in the category	Total number of genes in the category
Amino acid transport	5.00	*GAP1, AQR1*	2	40
Ribosomal large subunit biogenesis	2.88	*ALB1, DBP7, IPI3*	3	104
Ribosomal small subunit biogenesis	2.22	*FAL1, UTP23, RRP36*	3	135
rRNA processing	1.93	*FAL1, DBP7, DBP2, IPI3, UTP23, RRP36*	6	311
Ribosome assembly	1.69	*IPI3*	1	59
Nucleobase-containing small molecule metabolic process	1.01	*AAH1, RAS1*	2	198
Regulation of DNA metabolic process	0.97	*IPI3*	1	103
Signaling	0.83	*RAS1, RGS2*	2	240
Organelle assembly	0.76	*IPI3*	1	131
RNA catabolic process	0.76	*DBP2*	1	132
DNA replication	0.72	*IPI3*	1	139
Ion transport	0.62	*AQR1*	1	162
Transmembrane transport	0.43	*AQR1*	1	230
Biological process unknown	0.29	*GFD2, YGR079W, EFM6*	3	1047
Response to chemical	0.22	*AQR1*	1	442

4. DISCUSSION

In this study, an inverse metabolic engineering approach was used to obtain chronologically long-lived yeast *S. cerevisiae.* Also, chronological longevity of various stress-resistant *S. cerevisiae* mutants was investigated to understand the relationship between stress resistance and longevity in *S. cerevisiae*. Molecular and physiological analyses were carried out with the long-lived mutant strains to shed light on the molecular mechanisms of chronological longevity in the yeast *S. cerevisiae.*

S. cerevisiae has had a pivotal role to understand cellular aging process. An important discovery on the cellular aging mechanisms using yeast was published in Science in 2001(Fabrizio et al., 2001). In that study, transposon-based mutagenesis was used to detect stress-resistant and long-lived yeast mutants. Mutation analysis in the long-lived mutants showed that transposon was placed in the Sch9 gene and Cyr, which indicated that TOR/S6K/Sch9 pathway and Ras/AC/PKA pathway have an important role in the cellular aging mechanism. Furthermore, aging studies using single-knockout yeast deletion collection highlighted the mitochondrial function, *de novo* purine biosynthesis, vacuole function, autophagy process, ergosterol-biosynthesis and chromatin-modification in cellular aging (Fabrizio et al., 2010; Garay et al., 2014; Matecic et al., 2010; Powers et al., 2006).

Transposon-based or yeast knockout collection strategies as described above show similarities to the inverse metabolic engineering approach used in the present study. In the inverse metabolic engineering approach, firstly the desired phenotype is obtained, and then, the molecular mechanisms underlying the phenotype are determined (Bailey et al., 1996; Çakar et al., 2012). The approach is particularly useful for obtaining genetically complex, desired microbial phenotypes. As cellular aging is a complex process (Fontana et al., 2010; Goldberg et al., 2009), inverse metabolic engineering approach based on random mutation and selection of the desired phenotype could be a useful strategy to obtain long-lived mutant strain(s). However, the method has not been used so far to obtain chronologically long-lived

mutant *S. cerevisiae*. This study is the first report on physiological and transcriptomic profiling of a chronologically long-lived *S. cerevisiae* mutant strain that has been obtained by inverse metabolic engineering approach.

In the present study, caloric restriction was chosen as the selection strategy since it is a well-known non-pharmacological and non-genetical intervention of aging in yeast (Fabrizio et al., 2005; Smith et al., 2007a). To determine which glucose concentration should be used in the selection process, both the chemically mutated culture (906) and the reference strain (905) were cultivated in calorie-restricted media at varying glucose concentrations. According to the results (Figure 3.1), 0.5% glucose (w/v) was chosen as the initial glucose concentration of the selection procedure, since this caloric restriction condition leads to a mild reduction of the growth rate and is generally used for lifespan studies (Lin et al., 2000; Lin et al., 2002; Longo et al., 2012). Glucose concentration of the calorie-restricted medium was dropped by 0.02% at each successive passage to prevent a sharp decrease in the growth rate of the mutant culture during the first few populations. The selection strategy was stopped at the 53rd population, since the growth ratio decreased to about 10% (Figure 3.2). Glucose concentration of the last passage was 0.02%, which was lower than the extreme caloric restriction value (0.05% glucose) in yeast aging studies (Kaeberlein, 2010).

CLS assay measures the survival time of stationary phase yeast cells and the experiment begins at the beginning of the stationary phase of growth (Fabrizio and Longo, 2003). Therefore, growth analysis in different glucose media was performed to determine when yeast cells reach the stationary phase in these media (Figure 3.4). In standard medium, the reference strain CEN.PK 113.7D showed different growth behavior depending on the time of incubation. Cell growth almost stopped at the 24th h of incubation, however, it continued then slowly until the 72nd h of incubation. This difference could be due to carbon utilization. Yeast cells use respiro-fermentative metabolism in their logarithmic phase of growth, and as a result of their fermentative metabolism, metabolites such as ethanol and glycerol are produced during their logarithmic growth phase (Werner-Washburne et al., 1996). When glucose is exhausted in culture, yeast cells use ethanol that was produced during the logarithmic phase, therefore, they show a second growth called as ‘diauxic shift’ (Werner-Washburne et al., 1996). In the standard glucose medium, diauxic shift was clearly

observed from the 24th h to the 72nd h of cultivation. In the calorie-restricted media (0.5% YMM and 0.25% YMM), post-diauxic shift was not observed. In a previous study, it has been reported that 0.5% and lower glucose concentrations in the medium promote aerobic cell growth in *S. cerevisiae.* (Kaeberlein, 2010). Due to the respirative usage of glucose during exponential phase of growth in the calorie-restricted media, fermentative metabolites could not be produced. This oxidative usage of glucose in the medium could be the reason for the unobserved diauxic shift. Fabrizio and Longo (2003) selected the third day of incubation as the initial time for the CLS experiment, as the culture densities of the wild-type strains they used did not increase after the day 3 of incubation. Therefore, in the present study, day 3 of incubation in standard glucose medium was chosen as the initial time for the CLS experiment, while in calorie-restricted medium, day 1 was chosen.

CLS of the twelve mutant individuals obtained from the last population was determined by the semi-quantitative CLS method. The results showed that a mutant individual called SRM11 had the highest viability compared to the reference strain and the other individual mutants (Figure 3.5). Thus, for SRM11, quantitative CLS analysis was also performed in calorie-restricted media (Figure 3.8 and Figure 3.9) and standard glucose medium (Figure 3.10). In the standard glucose medium, the mutant SRM11 had about 50% longer lifespan than the reference strain. Thus, in SRM11, physiological and molecular analyses were carried out to gain insight into the chronological longevity in *S. cerevisiae*.

The last population was obtained at 0.02% glucose-YMM. This glucose concentration was 100-fold lower than that of the standard medium (2% YMM). During the selection process, C:N ratio of the medium also changed from 3-fold to 0.03-fold. A previous study showed that ammonium concentration affects CLS negatively in yeast (Santos et al., 2012). Since ammonium is toxic for the chronologically aging yeast cells and the C:N ratio significantly decreased during the selection procedure in the study, CLS of the mutant SRM11 was investigated in ammonium sulfate solution. Results showed that the mutant significantly had a better lifespan in ammonium sulfate, compared to the reference strain (Figure 3.11). Transcriptomic results also showed that most of the genes related with ammonium assimilation and glutamate metabolism were upregulated in SRM11 (Table 3.20). In the mutant SRM11, *GAD1* was the highest upregulated gene in ammonium

assimilation and glutamate metabolism. *GAD1* synthesizes the gamma-aminobutyrate (GABA) from glutamate, and is also required for normal oxidative stress tolerance (Coleman et al., 2001) A previous study showed that Gad1-null yeast cells showed decreased replicative lifespan (RLS) in yeast (Schleit et al., 2013). However, no studies have been reported about the role of the *GAD1* gene in CLS of *S. cerevisiae*. The present study suggests that *GAD1* gene might be related with CLS extension in the presence of ammonium and the standard medium.

In the yeast, NADP(+)-dependent glutamate dehydrogenases, *GDH3* and *GDH1*, are the key enzymes for glutamate synthesis and ammonium metabolism, which synthesize glutamate from α-ketoglutarate and ammonia (DeLuna et al., 2001). It has been shown that *GDH3*-null yeast cells show accelerated chronological aging and sensitivity to thermal and oxidative stress during stationary phase (Lee et al., 2012). In the mutant SRM11, *GDH3* gene was upregulated (Table 3.20). Extended chronological survival of the mutant SRM11 in ammonium solution could be related to the upregulation of *GDH3*. The synthesis of glutamate, which is the nontoxic form of ammonium, from ammonia by *GDH3* could neutralize the toxic effect of ammonia (DeLuna et al., 2001).

Growth physiological analysis showed that the growth behavior of the mutant SRM11 and the reference strain was not different in 0.5% and 2% YMM. In the calorie-restricted medium, two different exponential phases were clearly observed (Figure 3.15). This finding indicates that the mutant SRM11 and 905 use a highly respirative metabolism than in the standard glucose medium. Thus, when glucose is exhausted in the medium, cells directly used the metabolites produced and continued growing on them. In a previous study, it has been reported that 0.5% and lower glucose concentrations in the medium promote aerobic cell growth in *S. cerevisiae* (Kaeberlein, 2010). However, in the present study, in 0.5% glucose medium, a limited ethanol and glycerol production was observed, which indicates limited fermentation. Besides, the metabolites produced, ethanol and glycerol, were depleted until the 48^{th} h of incubation in the medium (Figure 3.24 and Figure 3.25). Additionally, no acetate production was observed in 0.5% glucose medium.

Growth physiological analysis also indicated that the growth rate of the strains was the same in both standard 2% glucose and calorie-restricted 0.5% glucose, during glucose utilization. When glucose was utilized, μ_{max} of the reference strain and

SRM11 were the same in 2% YMM and 0.5% YMM. 75% reduction of the glucose concentration in the medium did not significantly change the growth rate. Tahara et al. (2013) also showed that caloric restriction did not quantitatively affect cellular growth. This finding supports the results of the present study and suggests a simple strategy to increase biomass production from fermentable carbon sources.

Metabolite analysis showed that SRM11 produced less ethanol in standard glucose medium at the end of the exponential phase of growth (12 h) (Figure 3.20). This result indicates respirative shift in the mutant SRM11. Fast consumption of ethanol in 0.5% glucose medium may be another evidence for the metabolic changes of the mutant SRM11 (Figure 3.24). The yeast *S. cerevisiae* exhibits a different metabolism at elevated glucose concentrations. High glucose induces catabolite repression response, which results in low levels of transcription of the genes involved in respiration and the tricarboxylic acid (TCA) cycle. This regulation leads to both respiration and fermentation-based metabolism (respiro-fermentative) under even fully aerobic conditions (Cortassa and Aon, 1998; Gancedo, 1998; Postma et al., 1989). The mutant SRM11 regulated its metabolism based on more respiration for a more efficient glucose utilization. Transcriptomic data also supported this finding. Nearly all TCA cycle genes were upregulated (Table 3.20). The characteristic changes in the metabolism of the mutant SRM11 could be maximizing glucose utilization using oxidative-respiration rather than fermentation to ethanol.

The present finding that respirative shift occurs in caloric restriction is consistent with a previous study (Ferea et al., 1999). In that study, fitter yeast cells were obtained under glucose-limited selection process (0.08% glucose (w/v)), and DNA microarray analysis of the selected evolved strains showed that the expression levels of the genes involved in the TCA cycle, ATP generation, and oxidative phosphorylation increased, however, the genes encoding glycolytic enzymes were found to be downregulated. Wu et al. (2004) also found that yeast cells switched on the ORFs encoding TCA cycle enzymes under glucose limitation. Lin et al. (2002) reported that the extension of lifespan in yeast cells by caloric restriction is due to the switching of carbon metabolism toward the mitochondrial TCA cycle. A recent study showed that the deletion of *TOR1* gene extends CLS primarily by increasing mitochondrial respiration (Bonawitz et al., 2007). This finding supports the extended lifespan of the mutant SRM11 by a higher respiration. However, the findings of the

present study were not consistent with the study of Wei et al. (2009). In that study, downregulation of the genes encoding mitochondrial proteins, including proteins functioning in the TCA cycle and oxidative phosphorylation, was shown in the long-lived mutants (*sch9*Δ*, tor1*Δ *and ras2*Δ). This different result could be due to the different physiological states of the cultures used in the microarray experiments. In that study, a 2.5 days old culture (stationary phase of growth) was used in the microarray experiment, however, in the present study, a mid-exponential phase culture was used in which both respirative and fermentative metabolism occurs.

The question is how respirative shift affects chronological longevity in yeast. Previous studies showed that ethanol and acetic acid, the main products of fermentative metabolism, have a detrimental effect on cell viability and decrease lifespan (Burtner et al., 2009; Fabrizio et al., 2005). The metabolic regulation (respirative shift) in the mutant SRM11 could be to get rid of the detrimental effects of fermentative byproducts.

Microarray analysis results also indicated that glyoxylate cycle is highly activated in the mutant SRM11 (Table 3.20). *ICL2*, a fundamental gene for the glyoxylate cycle, was upregulated in the mutant SRM11. The gene product, isocitrate lyase, catalyses glyoxylate and succinate synthesis in yeast cells. Although a direct effect of the *ICL* gene has not been described as a response to starvation; a range of studies in various starved animals, plants and single cell microorganisms indicated that the lyase enzyme was upregulated (Chen et al., 2000; Popov et al., 1996; Xu et al., 2016).

Longevity is highly associated with stress resistance in yeast and the other model organisms (Barsyte et al., 2001; Longo, 2003; Martin et al., 1996; Murakami and Johnson, 1998; Service et al., 1985). Thus, stress resistance test were applied to the mutant SRM11. Stress resistance analysis results showed that the mutant SRM11 highly resisted to copper stress (Figure 3.26). Resistance to copper in the long-lived worm *C. elegans* has been previously reported (Barsyte et al., 2001). However, resistance to copper stress in the long-lived yeast models has not been reported, yet. The present study suggests that copper resistance is also related to chronological survival in the yeast *S. cerevisiae*.

Metallothioneins (MTs) are small cysteine-rich metal-binding proteins and prevent copper toxicity by binding free copper ions in the cell. MTs may play a more subtle

role in metal homeostasis in the cell (Butt and Ecker, 1987; Kagi and Schaffer, 1988). Yasokawa et al. (2008) have shown that when yeast cells were exposed to high concentrations of copper, *CUP1-1* and *CUP1-2* genes were significantly upregulated. Furthermore, it was recently reviewed that yeast cells tolerate copper, by inducing metallothionein (MT) *CUP1* genes (*CUP1-1 and CUP1-2*), metallothionein-like protein *CRS5* and cytosolic Cu/Zn superoxide dismutase *SOD1* (Nevitt et al., 2012). In the present study, DNA microarray analysis showed the upregulation of MTs (*CUP1-1* and *CUP1-2*) and *SOD2* in SRM11, even in the absence of copper stress (Table 3.20). This finding might explain the copper resistance mechanism in the mutant strain SRM11.

May caloric restriction induce metallothionein response in yeast cells and thereby extend their CLS? In a previous study, Tamai et al. (1994) reported that the transcription of *CUP1* was activated during glucose starvation in the yeast *S. cerevisiae*. Furthermore, upregulation of MTs in the tissues of fasted and CR-fed mice has also been shown (Dhahbi et al., 2004; Swindell, 2008a, 2008b, 2009). Microarray analysis showed an increased expression of MTs in the mutant SRM11, which may suggest that caloric restriction extends life span in yeast by inducing MTs.

Resistance to oxidative and heat shock stresses is associated with chronological longevity in *S. cerevisiae* (Fabrizio et al., 2001). However, resistance to oxidative stress and heat shock stress was not higher than the reference strain in the long-lived mutant SRM11(Figure 3.26). The microarray results, however, revealed that the oxidative and heat stress responses were induced in the mutant SRM11(Figure 3.27). The reason could be an increased oxidative metabolism in the mutant SRM11. The use of oxidative metabolism may result in increased ROS production and the mutant SRM11 can respond to this by inducing oxidative stress response genes.

The mutant SRM11 had resistance to silver (Figure 3.26). Silver resistance may be related to the induced copper resistance mechanisms in the mutant SRM11. A previous study showed that silver acts as a toxic copper-mimetic that can be imported by copper carriers (Vest et al., 2013). Also, the study of Niazi et al. (2011) showed a strong upregulation of copper resistance genes (*CUP1-1* and *CUP1-2*) when yeast cells were exposed to silver stress. The *CUP1-1* and *CUP1-2* were upregulated in the mutant SRM11. That might explain the silver resistance of the mutant SRM11. A

similar molecular mechanism might also be valid for the silver-resistant mutant 2E, which is cross-resistant to copper stress (Terzioğlu, unpublished).

The mutant SRM11 also resisted to ethanol and phenylethanol stresses (Figure 3.26). Fabrizio et al. (2005) showed that ethanol accelerates chronological aging in yeast. In the present study, it was demonstrated that ethanol resistance is also associated with chronological longevity in yeast cells. Furthermore, in the present study, it was shown that phenylethanol stress is another stress type that may be related with chronological longevity in the yeast *S.cerevisiae,* as the phenylethanol-resistant mutant C9 is a long-lived mutant and the long-lived mutant SRM11 is resistant to phenylethanol stress.

Phenylethanol carries basic characteristics of alcohols with its amphipathic structure. Phenylethanol and other alcohols increase fluidization of cell membrane (Silver and Wendt, 1967), and alter the helix-helix interactions of proteins in membrane structure (Anbazhagan et al., 2010). The alcohols also cause respiratory deficiency due to increased mitochondrial permeability in yeast (Wilkie and Maroudas, 1969). In the yeast *S. cerevisiae* alcohol tolerance is mainly structurally provided by altered cell wall structure and thereby increased osmotic stress resistance (Lam et al., 2014). The mutant SRM11 did not show particular resistance to osmotic stress (Figure 3.26), suggesting that cell wall structure may not have been changed.

Ethanol tolerance in yeast has also been associated with heat shock and reduced reactive oxygen species (Du and Takagi, 2007; Plesset et al., 1982). However, the mutant SRM11 had no improved resistance to hydrogen peroxide and heat shock stresses (Figure 3.26), indicating another ethanol tolerance mechanism in SRM11.

A previous study showed that *ALD* genes were upregulated in the phenylethanol-resistant *S. cerevisiae* mutant C9 (Holyavkin, 2013). The mutant C9 also had tolerance to ethanol stress. In the mutant SRM11, showing the same phenotype, aldehyde dehydogenases (*ALD3*, *ALD4*, *ALD6*) were also upregulated. Aldehyde dehydrogenases convert acetaldehyde to acetyl-CoA. In yeast, Ald3p and Ald6p are cytosolic enzymes and Ald3p are induced in response to ethanol stress. Ald4p is a mitochondrial aldehyde dehydrogenase and ald4 null yeast mutants have no ability to grow on ethanol (Tessier et al., 1998; Wang et al., 1998) It has been reported that aldehyde dehydrogenase activity is higher when yeast cells grow on ethanol, to

overcome the excess amount of aldehyde byproducts of alcohol catabolism (Aranda and del Olmo Ml, 2003). These findings suggest that alcohol tolerance mechanism can be achieved by its catabolism.

In the mutant SRM11, hexokinase *(HXK1*) and hexose transporters *(HXT6, HXT7)* were the highly upregulated genes, compared to the reference strain (Table 3.18). *HXK1* encodes glucose phosphorylase enzyme, converting glucose into glucose-6-phosphate which is a key enzyme for the carbohydrate metabolism (Lobo and Maitra, 1977). *HXT* is high-affinity glucose transporter and mediates glucose uptake in *S. cerevisiae* (Reifenberger et al., 1995). Upregulation of hexokinase and glucose transporters in SRM11 may imply that glucose in the environment is transported into the cell at high rates and is included in the metabolism, which may be related to the extension of CLS. Wei et al. (2009) showed that *HXK1* is an overlapping upregulated gene in the chronologically long-lived sch9, tor1 and ras2 mutant strains. Matecic et al. (2010) showed that deletion of *HXT5* in yeast decreased CLS. These findings suggest that the uptake of glucose into the cell and its catabolism might be associated with chronological longevity in the yeast *S.cerevisiae.*

Biological process analysis of the upregulated genes in the long-lived mutant SRM11 and long-lived stress-resistant mutants showed induction of oligosaccharide and carbohydrate metabolic process and carbohydrate transport, response to oxidative stress and cellular respiration (Figure 3.27), implying that these biological processes are associated with longevity in yeast.

In the mutant SRM11, nearly all genes related to glycogen and trehalose pathway were upregulated (Table 3.20). In the mutant SRM11, *GPH1* gene was the highest upregulated gene (96-fold) in the metabolism of energy reserves. *GPH1* encodes glycogen phosphorylase required for the mobilization of glycogen in yeast (Hwang et al., 1989). Favre et al. (2008) showed that gph1 lacking yeast mutants had a shortened CLS. This finding supports the role of *GPH1* in the CLS of the yeast *S. cerevisiae.*

Induction of reserve carbohydrate metabolism in the mutant SRM11 suggests that increased reserve carbohydrate (trehalose and glycogen) storage might provide survival advantage in stationary phase. Previous studies showed that yeast energy metabolism is mainly carried out through catabolizing glycogen during long-term

starvation (Lillie and Pringle, 1980; Samokhvalov et al., 2004). Powers et al. (2006) showed an increased glycogen accumulation in the long-lived yeast mutants (gln3Δ, agp1Δ, mep2Δ, mep3Δ, and lys12Δ). Similarly, Hu et al. (2014) reported a high level of trehalose in tor1Δ and sch9Δ mutants. Ocampo et al. (2012) reported a positive correlation between chronological survival and carbohydrate storage in the yeast *S. cerevisiae*. These evidences might explain the upregulation of the genes related to the metabolism of energy reserves in the long-lived mutant SRM11.

In the mutant SRM11, *PHO84* gene was the most downregulated gene compared to the reference strain (Table 3.19). *PHO84* is a high-affinity inorganic phosphate (P_i) transporter in *S. cerevisiae* (Bun-Ya et al., 1991). Jensen et al. (2003) showed that *PHO84*-lacking yeast mutants resisted to high concentrations of zinc, cobalt and copper, by preventing metal accumulation in the cell. Ofiteru et al. (2012) reported that overexpression of *PHO84* gene induces heavy metal uptake (Mn^{2+},Cu^{2+},Co^{2+}, and Zn^{2+}), increasing metal accumulation in yeast cells. These findings suggest that copper resistance mechanism of the mutant SRM11 might be associated with downregulation of *PHO84* gene.

Biological process analysis of the downregulated genes in the long-lived mutant SRM11 and stress-resistant mutants (C9, B8 and 2E) showed that ribosome subunit biogenesis, ribosome assembly and RNA processing were the significantly repressed biological processes (Figure 3.27 and Table 3.21). This suggests that repression of protein synthesis is associated with chronological survival in yeast.

Previous studies showed that reduced protein translation is related with longevity. Martin and Hall (2005) reported that lifespan extension of rapamycin is related to inhibition of rRNA genes, tRNA genes and processing of 35S rRNA and ribosomal protein genes. Also, it was shown that deletion of ribosomal large subunit genes significantly increases RLS in yeast (Kaeberlein et al., 2005). Furthermore, in *C.elegans,* RNAi knockdown of several ribosomal proteins was associated with increased adult lifespan (Hansen et al., 2007; Pan et al., 2007). These evidences support the finding of the present study that repression of protein synthesis may be associated with life span extension.

Caloric restriction is a well-established non-genetic intervention to slow aging of model organisms, ranging from yeast to primates (Anderson and Weindruch, 2010;

Masoro, 2005; Omodei and Fontana, 2011; Smith et al., 2007a; Smith et al., 2007b; Wei et al., 2008). However, in the present study, caloric restriction did not seem to extend the CLS of the reference strain. The reason could be the strain background: in this study, strain background (the reference strain) was CEN.PK 113-7D (Alkım et al., 2013; Çakar et al., 2009; Küçükgöze et al., 2013; van Dijken et al., 2000). Vanhalewyn et al. (1999) showed that a non-synonymous mutation resulted in an amino acid substitution (Lys1876Met) in *CYR1* gene in CEN.PK strain family. *CYR1* gene encodes adenylate cyclase, which is a key enzyme for cAMP production and cAMP-dependent protein kinase signaling. This mutation was accompanied by the absence of a cAMP peak upon exposure to high glucose concentration. Also, a recent study, using next generation sequencing method, confirmed the occurrence of this mutation in *CYR1* gene in CEN.PK113-7D strain, and also revealed several other mutations found in genes coding for the components of the cAMP signaling pathway, including *PLC1, GPA2, GPB2, IRA2* (Nijkamp et al., 2012). These findings suggested that extended life span of the mutant SRM11 may be independent of the cAMP signaling pathway.

In the present study, it was observed that CLS results in culture tubes and shake flasks were significantly different (Figure 3.36). Longo et al. (2012) stated that different types of caps and media/flask volume ratios used in CLS method can lead to differences in culture aeration and redox status, and so, quantitative differences can be obtained in CLS studies. Culture tubes have plastic caps and less void volume/geometry, whereas flasks have aluminum foil-cotton caps and provide more volume at their bottom for aeration/shaking, which most probably resulted in culture aeration differences and CLS differences, as stated by Longo et al. (2012)**.** This observation also indicates the importance of redox status and reactive oxygen species in lifespan. Reactive oxygen species (ROS) include superoxide anions, hydroxyl radicals and hydrogen peroxide which cause oxidative damage to DNA, proteins, and lipids (Fontana et al., 2010). Thus, they are accepted as the major contributors to aging and degenerative diseases of aging (Ames et al., 1993; Harman, 1956). Stationary phase survival of yeast cells has been shown to have a strong relationship with the anti-oxidant system (Fabrizio et al., 2003; Longo et al., 1996). The impact of ROS on CLS has been well-established in yeast. Null mutations in either or both genes encoding superoxide dismutase (*SOD1* and *SOD2*) shorten CLS (Longo et al.,

1996), and overexpression of both *SOD1* and *SOD2* extends CLS in *S. cerevisiae* (Fabrizio et al., 2003).

The conventional quantitative CLS method can be labor-intensive and has some disadvantages when a wide range of strains or conditions are tested, where a high number of plates and flasks are needed. Therefore, the semi-quantitative spot assay method can be a feasible alternative to rapidly determine CLS of various strains or conditions.

Spot assay is a useful, cost-effective and common method in yeast research for testing viability, growth, stress- or drug resistance and genotoxicity (Abegg et al., 2010; Çakar et al., 2009; Lahiri et al., 2013; Mukhopadhyay et al., 2002; Steinacher et al., 2013). In a previous study, the semi-quantitative spot assay-based CLS method was used to determine CLS in yeast (Smith et al., 2007a). In that study, the spot assay method was performed by directly spotting culture dilutions onto YPD plates without any adjustment of cell number/density. However, in this study, stationary phase culture densities of the tested yeast strains and cultures grown in different growth media were significantly different. Because of the differences in culture density at the stationary phase, the method was improved for a more reliable determination of CLS of different strains or culture conditions. In the present study, thus, a culture density (OD_{600}) adjustment step was introduced to the previously described method (Smith et al., 2007a) (Figure 2.1).

In the study of Smith et al. (2007a), at the beginning of the CLS experiment, differences were observed in the number of spots when testing CLS of different strains or different cultivation conditions. However, in the present study, an equal number of spots was obtained at the beginning of the CLS experiment in various yeast strains and growth conditions. That became possible because of the initial adjustment of culture densities. By doing so, all cultures to be tested were spotted at equal cell amounts at the beginning and during the CLS experiments. This allowed a more reliable comparative CLS analysis of the cultures or strains at different cell densities or growth rates. It is thus suggested that the improved semi-quantitative method might be a practical and reliable screening method for studies with a high number of samples, before applying the labor-intensive, quantitative CLS method used in yeast aging studies.

CLS analysis of the stress-resistant yeast mutants showed that ethanol, phenylethanol, silver and oxidative stress-resistant mutants had prolonged lifespan in their stationary growth phase. The results suggest that these stress types may be associated with chronological longevity. Oxidative stress resistance is known to be related with the extension of CLS (Fabrizio et al., 2001). However, ethanol, phenylethanol and silver resistance have not been associated with longevity, yet. Furthermore, the long-lived mutant SRM11 had resistance to ethanol, phenylethanol and silver stresses, as well (Figure 3.26). The present study suggests that ethanol, phenylethanol and silver stress resistance are also associated with chronological longevity in the yeast *S. cerevisiae*. Further detailed analysis of the long-lived mutant SRM11 at genomic and proteomic levels would help better understand the complex molecular mechanisms of longevity and the association between resistance to various stress types and longevity in *S. cerevisiae*.

5. CONCLUSIONS

In this thesis work, inverse metabolic engineering approach was used to obtain chronologically long-lived *S. cerevisiae*. Physiological and transcriptomic investigation was carried out in the obtained long-lived *S. cerevisiae* mutant strains. Physiological analysis results indicate that increased respirative metabolism, resistance to copper, silver, ethanol and phenylethanol stress are associated with longevity in *S. cerevisiae*. Gene expression data by DNA microarray suggest that repression of protein synthesis and induction of oligosaccharide and carbohydrate metabolic processes are related to chronological longevity in the yeast *S. cerevisiae.* For a better understanding of the complex molecular mechanisms of the longevity in *S. cerevisiae,* genomic and proteomic analyses would be recommended as future studies.

REFERENCES

Abdulrehman, D., Monteiro, P. T., Teixeira, M. C., Mira, N. P., Lourenco, A. B., dos Santos, S. C., Cabrito, T. R., Francisco, A. P., Madeira, S. C., Aires, R. S., et al. (2011). YEASTRACT: providing a programmatic access to curated transcriptional regulatory associations in *Saccharomyces cerevisiae* through a web services interface. *Nucleic Acids Res, 39*, D136-140.

Abegg, M. A., Alabarse, P. V., Casanova, A., Hoscheid, J., Salomon, T. B., Hackenhaar, F. S., Medeiros, T. M. and Benfato, M. S. (2010). Response to oxidative stress in eight pathogenic yeast species of the genus *Candida*. *Mycopathologia, 170*, 11-20.

Alberts, B., Johnson, A., Lewis, J., Raff, M., Roberts, K. and Walter, P. (2002). *Molecular biology of the cell*. 4th Edition. USA, New York: Garland Science.

Alberts, B., Johnson, A., Lewis, J., Raff, M., Roberts, K. and Walter, P. (2008). *Molecular biology of the cell*. 5th Edition. USA, New York: Garland Science, Taylor & Francis Group.

Alkım, C., Benbadis, L., Yılmaz, Ü., Çakar, Z. P. and Francois, J. M. (2013). Mechanisms other than activation of the iron regulon account for the hyper-resistance to cobalt of a *Saccharomyces cerevisiae* strain obtained by evolutionary engineering. *Metallomics, 5*, 1043-1060.

Ames, B. N., Shigenaga, M. K. and Hagen, T. M. (1993). Oxidants, antioxidants, and the degenerative diseases of aging. *P Natl Acad Sci USA, 90*, 7915-7922.

Anbazhagan, V., Munz, C., Tome, L. and Schneider, D. (2010). Fluidizing the membrane by a local anesthetic: phenylethanol affects membrane protein oligomerization. *J Mol Biol, 404*, 773-777.

Anderson, R. M. and Weindruch, R. (2010). Metabolic reprogramming, caloric restriction and aging. *Trends Endocrinol Metab, 21*, 134-141.

Aranda, A. and del Olmo Ml, M. (2003). Response to acetaldehyde stress in the yeast *Saccharomyces cerevisiae* involves a strain-dependent regulation of several *ALD* genes and is mediated by the general stress response pathway. *Yeast, 20*, 747-759.

Arslan, M., Turanlı-Yıldız, B., Yılmaz, B., Kocaefe, N. and Çakar, Z. P. (in press). An improved semi-quantitative spot assay to analyse chronological lifespan in yeast. *Rom Biotech Lett*, DOI: 10.26327/RBL2017.29.

Babu, R. S., Prasad, S. B. C., Chakrapani, R., Padmavathi, M., Rao, C. S. V. R. and Narasu, M. L. (2011). Studies on bioethanol production from spoiled starch rich and cellulose rich vegetables by two stage batch fermentation. *J Pure Appl Microbio, 5*, 853-857.

Bailey, J. E. (1991). Toward a science of metabolic engineering. *Science, 252*, 1668-1675.

Bailey, J. E., Sburlati, A., Hatzimanikatis, V., Lee, K., Renner, W. A. and Tsai, P. S. (1996). Inverse metabolic engineering: a strategy for directed genetic engineering of useful phenotypes. *Biotechnol Bioeng, 52*, 109-121.

Balaban, B. G. (2016). *Molecular and physiological characterization of iron-resistant Saccharomyces cerevisiae*. (Ph.D. thesis). Istanbul Tecnical University, Graduate School of Science, Engineering and Technology, Istanbul, Turkey.

Barsyte, D., Lovejoy, D. A. and Lithgow, G. J. (2001). Longevity and heavy metal resistance in daf-2 and age-1 long-lived mutants of *Caenorhabditis elegans*. *The FASEB Journal, 15*, 627-634.

Bishop, N. A. and Guarente, L. (2007). Genetic links between diet and lifespan: shared mechanisms from yeast to humans. *Nature Reviews Genetics, 8*, 835-844.

Bonawitz, N. D., Chatenay-Lapointe, M., Pan, Y. and Shadel, G. S. (2007). Reduced TOR signaling extends chronological life span via increased respiration and upregulation of mitochondrial gene expression. *Cell Metab, 5*, 265-277.

Botstein, D., Chervitz, S. A. and Cherry, J. M. (1997). Genetics - yeast as a model organism. *Science, 277*, 1259-1260.

Bun-Ya, M., Nishimura, M., Harashima, S. and Oshima, Y. (1991). The *PHO84* gene of *Saccharomyces cerevisiae* encodes an inorganic phosphate transporter. *Mol Cell Biol, 11*, 3229-3238.

Burtner, C. R., Murakami, C. J., Kennedy, B. K. and Kaeberlein, M. (2009). A molecular mechanism of chronological aging in yeast. *Cell Cycle, 8*, 1256-1270.

Busti, S., Coccetti, P., Alberghina, L. and Vanoni, M. (2010). Glucose signaling-mediated coordination of cell growth and cell cycle in *Saccharomyces cerevisiae*. *Sensors (Basel), 10*, 6195-6240.

Butler, G. and Thiele, D. J. (1991). *ACE2*, an activator of yeast metallothionein expression which is homologous to *SWI5*. *Mol Cell Biol, 11*, 476-485.

Butt, T. R. and Ecker, D. J. (1987). Yeast metallothionein and applications in biotechnology. *Microbiol Rev, 51*, 351-364.

Chen, Z. H., Walker, R. P., Acheson, R. M., Tecsi, L. I., Wingler, A., Lea, P. J. and Leegood, R. C. (2000). Are isocitrate lyase and phosphoenolpyruvate carboxykinase involved in gluconeogenesis during senescence of barley leaves and cucumber cotyledons? *Plant Cell Physiol, 41*, 960-967.

Cherry, J. M., Adler, C., Ball, C., Chervitz, S. A., Dwight, S. S., Hester, E. T., Jia, Y., Juvik, G., Roe, T., Schroeder, M., et al. (1998). SGD: Saccharomyces Genome Database. *Nucleic Acids Res, 26*, 73-79.

Coleman, S. T., Fang, T. K., Rovinsky, S. A., Turano, F. J. and Moye-Rowley, W. S. (2001). Expression of a glutamate decarboxylase homologue is

required for normal oxidative stress tolerance in *Saccharomyces cerevisiae*. *J Biol Chem, 276*, 244-250.

Cortassa, S. and Aon, M. A. (1998). The onset of fermentative metabolism in continuous cultures depends on the catabolite repression properties of *Saccharomyces cerevisiae*. *Enzyme Microb Technol, 22*, 705-712.

Cypser, J. R. and Johnson, T. E. (1999). The spe-10 mutant has longer life and increased stress resistance. *Neurobiol Aging, 20*, 503-512.

Çakar, Z. P. (2009). Metabolic and evolutionary engineering research in Turkey and beyond. *Biotechnol J, 4*, 992-1002.

Çakar, Z. P., Alkım, C., Turanlı, B., Tokman, N., Akman, S., Sarıkaya, M., Tamerler, C., Benbadis, L. and Francois, J. M. (2009). Isolation of cobalt hyper-resistant mutants of *Saccharomyces cerevisiae* by *in vivo* evolutionary engineering approach. *J Biotechnol, 143*, 130-138.

Çakar, Z. P., Şeker, U. O., Tamerler, C., Sonderegger, M. and Sauer, U. (2005). Evolutionary engineering of multiple-stress resistant *Saccharomyces cerevisiae*. *FEMS Yeast Res, 5*, 569-578.

Çakar, Z. P., Turanlı-Yıldız, B., Alkım, C. and Yılmaz, Ü. (2012). Evolutionary engineering of *Saccharomyces cerevisiae* for improved industrially important properties. *FEMS Yeast Res, 12*, 171-182.

DeLuna, A., Avendano, A., Riego, L. and Gonzalez, A. (2001). NADP-glutamate dehydrogenase isoenzymes of *Saccharomyces cerevisiae*. Purification, kinetic properties, and physiological roles. *J Biol Chem, 276*, 43775-43783.

Demir, F. (2016). *Inverse metabolic engineering of propolis-resistant Saccharomyces cerevisiae*. (M.Sc. thesis). Istanbul Technical University, Graduate School of Science, Engineering and Technology, Istanbul, Turkey.

Dhahbi, J. M., Kim, H. J., Mote, P. L., Beaver, R. J. and Spindler, S. R. (2004). Temporal linkage between the phenotypic and genomic responses to caloric restriction. *Proc Natl Acad Sci U S A, 101*, 5524-5529.

Du, X. and Takagi, H. (2007). N-Acetyltransferase Mpr1 confers ethanol tolerance on *Saccharomyces cerevisiae* by reducing reactive oxygen species. *Appl Microbiol Biot, 75*, 1343-1351.

El-Fiky, Z. A., Hassan, G. M. and Emam, A. M. (2012). Quality parameters and RAPD-PCR differentiation of commercial baker's yeast and hybrid strains. *J Food Sci, 77*, M312-317.

Emini, E. A., Ellis, R. W., Miller, W. J., Mcaleer, W. J., Scolnick, E. M. and Gerety, R. J. (1986). Production and immunological analysis of recombinant Hepatitis-B vaccine. *J Infect, 13*, 3-9.

Estruch, F. and Carlson, M. (1993). Two homologous zinc finger genes identified by multicopy suppression in a *SNF1* protein kinase mutant of *Saccharomyces cerevisiae*. *Mol Cell Biol, 13*, 3872-3881.

Fabrizio, P., Battistella, L., Vardavas, R., Gattazzo, C., Liou, L. L., Diaspro, A., Dossen, J. W., Gralla, E. B. and Longo, V. D. (2004). Superoxide is a

mediator of an altruistic aging program in *Saccharomyces cerevisiae*. *J Cell Biol, 166*, 1055-1067.

Fabrizio, P., Gattazzo, C., Battistella, L., Wei, M., Cheng, C., McGrew, K. and Longo, V. D. (2005). Sir2 blocks extreme life-span extension. *Cell, 123*, 655-667.

Fabrizio, P., Hoon, S., Shamalnasab, M., Galbani, A., Wei, M., Giaever, G., Nislow, C. and Longo, V. D. (2010). Genome-wide screen in *Saccharomyces cerevisiae* identifies vacuolar protein sorting, autophagy, biosynthetic, and tRNA methylation genes involved in life span regulation. *PLOS Genetics, 6*, (7): e1001024.

Fabrizio, P., Liou, L. L., Moy, V. N., Diaspro, A., SelverstoneValentine, J., Gralla, E. B. and Longo, V. D. (2003). *SOD2* functions downstream of Sch9 to extend longevity in yeast. *Genetics, 163*, 35-46.

Fabrizio, P. and Longo, V. D. (2003). The chronological life span of Saccharomyces cerevisiae. *Aging Cell, 2*, 73-81.

Fabrizio, P. and Longo, V. D. (2007). The chronological life span of *Saccharomyces cerevisiae*. *Methods Mol Biol, 371*, 89-95.

Fabrizio, P., Pozza, F., Pletcher, S. D., Gendron, C. M. and Longo, V. D. (2001). Regulation of longevity and stress resistance by Sch9 in yeast. *Science, 292*, 288-290.

Favre, C., Aguilar, P. S. and Carrillo, M. C. (2008). Oxidative stress and chronological aging in glycogen-phosphorylase-deleted yeast. *Free Radic Biol Med, 45*, 1446-1456.

Ferea, T. L., Botstein, D., Brown, P. O. and Rosenzweig, R. F. (1999). Systematic changes in gene expression patterns following adaptive evolution in yeast. *Proc Natl Acad Sci USA, 96*, 9721-9726.

Fontana, L., Partridge, L. and Longo, V. D. (2010). Extending healthy life span-from yeast to humans. *Science, 328*, 321-326.

Gancedo, J. M. (1998). Yeast carbon catabolite repression. *Microbiol Mol Biol Rev, 62*, 334-361.

Garay, E., Campos, S. E., de la Cruz, J. G., Gaspar, A. P., Jinich, A. and DeLuna, A. (2014). High-resolution profiling of stationary-phase survival reveals yeast longevity factors and their genetic interactions. *Plos Genetics, 10*, (2): e1004168.

Goffeau, A. (2000). Four years of post-genomic life with 6,000 yeast genes. *FEBS Lett, 480*, 37-41.

Goffeau, A., Barrell, B. G., Bussey, H., Davis, R. W., Dujon, B., Feldmann, H., Galibert, F., Hoheisel, J. D., Jacq, C., Johnston, M., et al. (1996). Life with 6000 genes. *Science, 274*, 546, 563-547.

Goldberg, A. A., Bourque, S. D., Kyryakov, P., Gregg, C., Boukh-Viner, T., Beach, A., Burstein, M. T., Machkalyan, G., Richard, V., Rampersad, S., et al. (2009). Effect of calorie restriction on the metabolic history of chronologically aging yeast. *Exp Gerontol, 44*, 555-571.

Guarente, L., Partridge, L. and Wallace, D. (2008). *Molecular biology of aging*. USA, New York: Cold Spring Harbor Laboratory Press.

Hahn-Hagerdal, B., Karhumaa, K., Larsson, C. U., Gorwa-Grauslund, M., Gorgens, J. and van Zyl, W. H. (2005). Role of cultivation media in the development of yeast strains for large scale industrial use. *Microb Cell Fact, 4*, 31.

Hansen, M., Taubert, S., Crawford, D., Libina, N., Lee, S. J. and Kenyon, C. (2007). Lifespan extension by conditions that inhibit translation in *Caenorhabditis elegans*. *Aging Cell, 6*, 95-110.

Harford, J. (2009). Population ageing and dental care. *Community Dent Oral Epidemiol, 37*, 97-103.

Harman, D. (1956). Aging: a theory based on free radical and radiation chemistry. *J Gerontol, 11*, 298-300.

Harris, N., Costa, V., MacLean, M., Mollapour, M., Moradas-Ferreira, P. and Piper, P. W. (2003). MnSOD overexpression extends the yeast chronological (G(0)) life span but acts independently of Sir2p histone deacetylase to shorten the replicative life span of dividing cells. *Free Radic Biol Med, 34*, 1599-1606.

Harrison, D. E., Strong, R., Sharp, Z. D., Nelson, J. F., Astle, C. M., Flurkey, K., Nadon, N. L., Wilkinson, J. E., Frenkel, K., Carter, C. S., et al. (2009). Rapamycin fed late in life extends lifespan in genetically heterogeneous mice. *Nature, 460*, 392-395.

Hartwell, L. H. (2002). Yeast and cancer. *Bioscience Rep, 22*, 373-394.

Herskowitz, I. (1988). Life cycle of the budding yeast *Saccharomyces cerevisiae*. *Microbiol Rev, 52*, 536-553.

Hinnen, A., Hicks, J. B. and Fink, G. R. (1978). Transformation of yeast. *Proc Natl Acad Sci USA, 75*, 1929-1933.

Holyavkin, C. (2013). *Evolutionary egineering of phenylethanol-resistant Saccharomyces cerevisiae*. (M. Sc. thesis). Istanbul Technical University, Graduate School of Science, Engineering and Technology, Istanbul, Turkey.

Honjoh, S. and Nishida, E. (2011). Two sides of lifespan regulating genes: pro-longevity or anti-longevity? *J Biochem, 149*, 381-388.

Hu, J., Wei, M., Mirzaei, H., Madia, F., Mario, M., Amparo, C., Chagoury, S., Kennedy, B. and Longo, V. D. (2014). Tor-Sch9 deficiency activates catabolism of the ketone body-like acetic acid to promote trehalose accumulation and longevity. *Aging Cell, 13*, 457-467.

Huxley, C., Green, E. D. and Dunham, I. (1990). Rapid assessment of *S. cerevisiae* mating type by PCR. *Trends Genet, 6*, 236.

Hwang, P. K., Tugendreich, S. and Fletterick, R. J. (1989). Molecular analysis of *GPH1*, the gene encoding glycogen phosphorylase in *Saccharomyces cerevisiae*. *Mol Cell Biol, 9*, 1659-1666.

Jensen, L. T., Ajua-Alemanji, M. and Culotta, V. C. (2003). The *Saccharomyces cerevisiae* high affinity phosphate transporter encoded by *PHO84* also functions in manganese homeostasis. *J Biol Chem, 278*, 42036-42040.

Kaeberlein, M. (2010). Lessons on longevity from budding yeast. *Nature, 464*, 513-519.

Kaeberlein, M., McVey, M. and Guarente, L. (1999). The *SIR2/3/4* complex and *SIR2* alone promote longevity in *Saccharomyces cerevisiae* by two different mechanisms. *Genes Dev, 13*, 2570-2580.

Kaeberlein, M., Powers, R. W., Steffen, K. K., Westman, E. A., Hu, D., Dang, N., Kerr, E. O., Kirkland, K. T., Fields, S. and Kennedy, B. K. (2005). Regulation of yeast replicative life span by TOR and Sch9 in response to nutrients. *Science, 310*, 1193-1196.

Kagi, J. H. and Schaffer, A. (1988). Biochemistry of metallothionein. *Biochemistry, 27*, 8509-8515.

Karathia, H., Vilaprinyo, E., Sorribas, A. and Alves, R. (2011). *Saccharomyces cerevisiae* as a model organism: a comparative study. *PLoS One, 6*, (2): e16015.

Klis, F. M., Boorsma, A. and De Groot, P. W. (2006). Cell wall construction in *Saccharomyces cerevisiae*. *Yeast, 23*, 185-202.

Kollar, R., Reinhold, B. B., Petrakova, E., Yeh, H. J., Ashwell, G., Drgonova, J., Kapteyn, J. C., Klis, F. M. and Cabib, E. (1997). Architecture of the yeast cell wall. Beta(1-->6)-glucan interconnects mannoprotein, beta(1-->)3-glucan, and chitin. *J Biol Chem, **272***, 17762-17775.

Korkmaz, K. (2011). *Evolutionary engineering of sulphur dioxide-resistant Saccharomyces cerevisiae*. (M.Sc. thesis). Istanbul Technical University, Graduate School of Science, Engineering and Technology, Istanbul, Turkey.

Küçükgöze, G., Alkım, C., Yılmaz, U., Kısakesen, H. I., Gündüz, S., Akman, S. and Çakar, Z. P. (2013). Evolutionary engineering and transcriptomic analysis of nickel-resistant *Saccharomyces cerevisiae*. *FEMS Yeast Research, 13*, 731-746.

Lahiri, S., Mehta, G. D. and Ghosh, S. K. (2013). Iml3p, a component of the Ctf19 complex of the budding yeast kinetochore is required to maintain kinetochore integrity under conditions of spindle stress. *FEMS Yeast Res, 13*, 375-385.

Lam, F. H., Ghaderi, A., Fink, G. R. and Stephanopoulos, G. (2014). Biofuels. Engineering alcohol tolerance in yeast. *Science, 346*, 71-75.

Lawrence, C. W. (1991). Classical mutagenesis techniques. *Methods Enzymol, 194*, 273-281.

Lee, Y. J., Kim, K. J., Kang, H. Y., Kim, H. R. and Maeng, P. J. (2012). Involvement of GDH3-encoded NADP+-dependent glutamate dehydrogenase in yeast cell resistance to stress-induced apoptosis in stationary phase cells. *J Biol Chem, 287*, 44221-44233.

Lempiainen, H., Uotila, A., Urban, J., Dohnal, I., Ammerer, G., Loewith, R. and Shore, D. (2009). Sfp1 interaction with TORC1 and Mrs6 reveals feedback regulation on TOR signaling. *Mol Cell, 33*, 704-716.

Lillie, S. H. and Pringle, J. R. (1980). Reserve carbohydrate metabolism in *Saccharomyces cerevisiae*: responses to nutrient limitation. *J Bacteriol, 143*, 1384-1394.

Lin, S. J., Defossez, P. A. and Guarente, L. (2000). Requirement of NAD and *SIR2* for life-span extension by calorie restriction in *Saccharomyces cerevisiae*. *Science, 289*, 2126-2128.

Lin, S. J., Kaeberlein, M., Andalis, A. A., Sturtz, L. A., Defossez, P. A., Culotta, V. C., Fink, G. R. and Guarente, L. (2002). Calorie restriction extends *Saccharomyces cerevisiae* lifespan by increasing respiration. *Nature, 418*, 344-348.

Lin, Y. H., Chen, Y. C., Kao, T. Y., Lin, Y. C., Hsu, T. E., Wu, Y. C., Ja, W. W., Brummel, T. J., Kapahi, P., Yuh, C. H., et al. (2014). Diacylglycerol lipase regulates lifespan and oxidative stress response by inversely modulating TOR signaling in *Drosophila* and *C. elegans*. *Aging cell, 13*, 755-764.

Lindquist, S. L., Alberti, S., Halfmann, R. and Jackson, W. (2009). Prion proteins: one surprise after another. *FASEB J, 23*, 324.

Lobo, Z. and Maitra, P. K. (1977). Physiological role of glucose-phosphorylating enzymes in *Saccharomyces cerevisiae*. *Arch Biochem Biophys, 182*, 639-645.

Lodish, H., Berk, A., Zipursky, S., Matsudaira, P., Baltimore, B. and Darnell, J. (1995). *Molecular cell biology*. 3rd Edition. USA: Scientific American Books.

Longo, V. D. (1999). Mutations in signal transduction proteins increase stress resistance and longevity in yeast, nematodes, fruit flies, and mammalian neuronal cells. *Neurobiol Aging, 20*, 479-486.

Longo, V. D. (2003). The Ras and Sch9 pathways regulate stress resistance and longevity. *Exp Gerontol, 38*, 807-811.

Longo, V. D., Gralla, E. B. and Valentine, J. S. (1996). Superoxide dismutase activity is essential for stationary phase survival in *Saccharomyces cerevisiae* - Mitochondrial production of toxic oxygen species *in vivo*. *J Biol Chem, 271*, 12275-12280.

Longo, V. D., Shadel, G. S., Kaeberlein, M. and Kennedy, B. (2012). Replicative and chronological aging in *Saccharomyces cerevisiae*. *Cell Metab, 16*, 18-31.

MacLean, M., Harris, N. and Piper, P. W. (2001). Chronological lifespan of stationary phase yeast cells; a model for investigating the factors that might influence the ageing of postmitotic tissues in higher organisms. *Yeast, 18*, 499-509.

Maclean, M. J., Aamodt, R., Harris, N., Alseth, I., Seeberg, E., Bjoras, M. and Piper, P. W. (2003). Base excision repair activities required for yeast to attain a full chronological life span. *Aging Cell, 2*, 93-104.

Madigan, M. T. and Martinko, J. M. (2006). *Brock biology of microorganisms*. 11th Edition. USA: Pearson Prentice Hall.

Martin, D. E. and Hall, M. N. (2005). The expanding TOR signaling network. *Curr Opin Cell Biol, 17*, 158-166.

Martin, G. M., Austad, S. N. and Johnson, T. E. (1996). Genetic analysis of ageing: role of oxidative damage and environmental stresses. *Nat Genet, 13*, 25-34.

Martinez-Pastor, M. T., Marchler, G., Schuller, C., Marchler-Bauer, A., Ruis, H. and Estruch, F. (1996). The *Saccharomyces cerevisiae* zinc finger proteins Msn2p and Msn4p are required for transcriptional induction through the stress response element (STRE). *EMBO J, 15*, 2227-2235.

Masoro, E. J. (2005). Overview of caloric restriction and ageing. *Mech Ageing Dev, 126*, 913-922.

Matecic, M., Smith, D. L., Pan, X., Maqani, N., Bekiranov, S., Boeke, J. D. and Smith, J. S. (2010). A microarray-based genetic screen for yeast chronological aging factors. *PLOS Genetics, **6***, (4): e1000921.

Mazanka, E. and Weiss, E. L. (2010). Sequential counteracting kinases restrict an asymmetric gene expression program to early G1. *Mol Biol Cell, 21*, 2809-2820.

Moller, T. S., Hay, J., Saxton, M. J., Bunting, K., Petersen, E. I., Kjaerulff, S. and Finnis, C. J. (2017). Human beta-defensin-2 production from *S. cerevisiae* using the repressible *MET17* promoter. *Microb Cell Fact, 16*, 11.

Mortimer, R. K. and Johnston, J. R. (1959). Life span of individual yeast cells. *Nature, 183*, 1751-1752.

Mukhopadhyay, K., Kohli, A. and Prasad, R. (2002). Drug susceptibilities of yeast cells are affected by membrane lipid composition. *Antimicrob Agents Ch, 46*, 3695-3705.

Murakami, S. and Johnson, T. E. (1998). Life extension and stress resistance in *Caenorhabditis elegans* modulated by the tkr-1 gene. *Curr Biol, 8*, 1091-1094.

Nakano, A. (2004). Yeast Golgi apparatus - dynamics and sorting. *Cell Mol Life Sci, 61*, 186-191.

Nevitt, T., Ohrvik, H. and Thiele, D. J. (2012). Charting the travels of copper in eukaryotes from yeast to mammals. *Biochim Biophys Acta, 1823*, 1580-1593.

Niazi, J. H., Sang, B. I., Kim, Y. S. and Gu, M. B. (2011). Global gene response in *Saccharomyces cerevisiae* exposed to silver nanoparticles. *Appl Biochem Biotechnol, 164*, 1278-1291.

Niccoli, T. and Partridge, L. (2012). Ageing as a risk factor for disease. *Curr Biol, 22*, R741-R752.

Nicholls, D. G. (2002). Mitochondrial function and dysfunction in the cell: its relevance to aging and aging-related disease. *Int J Biochem Cell Biol, 34*, 1372-1381.

Nigam, P. S. and Singh, A. (2011). Production of liquid biofuels from renewable resources. *Progress in Energy and Combustion Science, 37*, 52-68.

Nigam, Y., Knight, J., Bhattacharya, S. and Bayer, A. (2012). Physiological changes associated with aging and immobility. *J Aging Res, 2012*, 468469.

Nijkamp, J. F., van den Broek, M., Datema, E., de Kok, S., Bosman, L., Luttik, M. A., Daran-Lapujade, P., Vongsangnak, W., Nielsen, J., Heijne, W. H., et al. (2012). De novo sequencing, assembly and analysis of the genome of the laboratory strain *Saccharomyces cerevisiae* CEN.PK113-7D, a model for modern industrial biotechnology. *Microb Cell Fact, 11*, 36.

Ocampo, A., Liu, J. J., Schroeder, E. A., Shadel, G. S. and Barrientos, A. (2012). Mitochondrial respiratory thresholds regulate yeast chronological life span and its extension by caloric restriction. *Cell Metab, 16*, 55-67.

Ofiteru, A. M., Ruta, L. L., Rotaru, C., Dumitru, I., Ene, C. D., Neagoe, A. and Farcasanu, I. C. (2012). Overexpression of the *PHO84* gene causes heavy metal accumulation and induces Ire1p-dependent unfolded protein response in *Saccharomyces cerevisiae* cells. *Appl Microbiol Biotechnol, 94*, 425-435.

Oliver, S. G., van der Aart, Q. J., Agostoni-Carbone, M. L., Aigle, M., Alberghina, L., Alexandraki, D., Antoine, G., Anwar, R., Ballesta, J. P., Benit, P., et al. (1992). The complete DNA sequence of yeast chromosome III. *Nature, 357*, 38-46.

Omodei, D. and Fontana, L. (2011). Calorie restriction and prevention of age-associated chronic disease. *FEBS Lett, 585*, 1537-1542.

Pan, K. Z., Palter, J. E., Rogers, A. N., Olsen, A., Chen, D., Lithgow, G. J. and Kapahi, P. (2007). Inhibition of mRNA translation extends lifespan in *Caenorhabditis elegans*. *Aging Cell, 6*, 111-119.

Piskur, J., Rozpedowska, E., Polakova, S., Merico, A. and Compagno, C. (2006). How did *Saccharomyces* evolve to become a good brewer? *Trends Genet, 22*, 183-186.

Plesset, J., Palm, C. and McLaughlin, C. S. (1982). Induction of heat shock proteins and thermotolerance by ethanol in *Saccharomyces cerevisiae*. *Biochem Bioph Res Co, 108*, 1340-1345.

Popov, V. N., Igamberdiev, A. U., Schnarrenberger, C. and Volvenkin, S. V. (1996). Induction of glyoxylate cycle enzymes in rat liver upon food starvation. *FEBS Lett, 390*, 258-260.

Postma, E., Verduyn, C., Scheffers, W. A. and Van Dijken, J. P. (1989). Enzymic analysis of the Crabtree effect in glucose-limited chemostat cultures of *Saccharomyces cerevisiae*. *Appl Environ Microbiol, 55*, 468-477.

Powers, R. W., Kaeberlein, M., Caldwell, S. D., Kennedy, B. K. and Fields, S. (2006). Extension of chronological life span in yeast by decreased TOR pathway signaling. *Genes Dev, 20*, 174-184.

Ratledge, C. K. B. (2001). *Basic biotechnology*. 2nd edition. UK: Cambridge University Press.

Reifenberger, E., Freidel, K. and Ciriacy, M. (1995). Identification of novel *HXT* genes in *Saccharomyces cerevisiae* reveals the impact of individual hexose transporters on glycolytic flux. *Mol Microbiol, 16*, 157-167.

Samokhvalov, V. A., Mel'nikov, G. V. and Ignatov, V. V. (2004). [Role of trehalose and glycogen in the survival of aging *Saccharomyces cerevisiae* cells]. *Mikrobiologiia, 73*, 449-454.

Sanderson, W. C. and Scherbov, S. (2007). A new perspective on population aging. *Demographic Research, 16*, 27-57.

Santos, J., Sousa, M. J. and Leao, C. (2012). Ammonium is toxic for aging yeast cells, inducing death and shortening of the chronological lifespan. *PLoS One, 7*, (5): e37090.

Schleit, J., Johnson, S. C., Bennett, C. F., Simko, M., Trongtham, N., Castanza, A., Hsieh, E. J., Moller, R. M., Wasko, B. M., Delaney, J. R., et al. (2013). Molecular mechanisms underlying genotype-dependent responses to dietary restriction. *Aging Cell, 12*, 1050-1061.

Schmelzle, T. and Hall, M. N. (2000). TOR, a central controller of cell growth. *Cell, 103*, 253-262.

Sen, M., Yilmaz, U., Baysal, A., Akman, S. and Cakar, Z. P. (2011). *In vivo* evolutionary engineering of a boron-resistant bacterium: *Bacillus boroniphilus*. *Antonie Van Leeuwenhoek, 99*, 825-835.

Service, P. M., Hutchinson, E. W., Mackinley, M. D. and Rose, M. R. (1985). Resistance to environmental-stress in *Drosophila*-melanogaster selected for postponed senescence. *Physiol Zool, 58*, 380-389.

Sezgin, T. (2010). *Evolutionary engineering of Saccharomyces cerevisiae for improved industrial properties*. (Ph.D. thesis). Istanbul Technical University, Graduate School of Science, Engineering and Technology, Istanbul, Turkey.

Sherman, F. (1991). Getting started with yeast. *Method Enzymol, 194*, 3-21.

Sherman, F. (2002). Getting started with yeast. *Methods Enzymol, 350*, 3-41.

Shima, J. and Takagi, H. (2009). Stress-tolerance of baker's-yeast (*Saccharomyces cerevisiae*) cells: stress-protective molecules and genes involved in stress tolerance. *Biotechnol Appl Biochem, 53*, 155-164.

Silver, S. and Wendt, L. (1967). Mechanism of action of phenethyl alcohol: breakdown of the cellular permeability barrier. *J Bacteriol, 93*, 560-566.

Sinclair, D. A. and Guarente, L. (1997). Extrachromosomal rDNA circles--a cause of aging in yeast. *Cell, 91*, 1033-1042.

Siqueira, P. F., Karp, S. G., Carvalho, J. C., Sturm, W., Rodriguez-Leon, J. A., Tholozan, J. L., Singhania, R. R., Pandey, A. and Soccol, C. R. (2008). Production of bio-ethanol from soybean molasses by *Saccharomyces cerevisiae* at laboratory, pilot and industrial scales. *Bioresource Technology, 99*, 8156-8163.

Smith, D. L., Jr., McClure, J. M., Matecic, M. and Smith, J. S. (2007a). Calorie restriction extends the chronological lifespan of *Saccharomyces cerevisiae* independently of the Sirtuins. *Aging Cell, 6*, 649-662.

Smith, E. D., Kennedy, B. K. and Kaeberlein, M. (2007b). Genome-wide identification of conserved longevity genes in yeast and worms. *Mech Ageing Dev, 128,* 106-111.

Solomon, E. P., Berg, L. R. and Martin, D. W. (1999). *Biology*. 5th Edition. USA: Saunders College Publishing.

Steffen, K. K., Kennedy, B. K. and Kaeberlein, M. (2009). Measuring replicative life span in the budding yeast. *J Vis Exp, 28,* 1209.

Steinacher, R., Osman, F., Lorenz, A., Bryer, C. and Whitby, M. C. (2013). Slx8 removes Pli1-dependent protein-SUMO conjugates including SUMOylated topoisomerase I to promote genome stability. *PLoS One, 8,* (8): e71960.

Sun, Y. and Cheng, J. (2002). Hydrolysis of lignocellulosic materials for ethanol production: a review. *Bioresour Technol, 83,* 1-11.

Swindell, W. R. (2008a). Comparative analysis of microarray data identifies common responses to caloric restriction among mouse tissues. *Mech Ageing Dev, 129,* 138-153.

Swindell, W. R. (2008b). Genes regulated by caloric restriction have unique roles within transcriptional networks. *Mech Ageing Dev, 129,* 580-592.

Swindell, W. R. (2009). Genes and gene expression modules associated with caloric restriction and aging in the laboratory mouse. *BMC Genomics, 10,* 585.

Tahara, E. B., Cunha, F. M., Basso, T. O., Della Bianca, B. E., Gombert, A. K. and Kowaltowski, A. J. (2013). Calorie restriction hysteretically primes aging *Saccharomyces cerevisiae* toward more effective oxidative metabolism. *PLoS One, 8,* (2): e56388.

Tamai, K. T., Liu, X. D., Silar, P., Sosinowski, T. and Thiele, D. J. (1994). Heat-shock transcription factor activates yeast metallothionein gene-expression in response to heat and glucose starvation via distinct signaling pathways. *Mol Cell Biol, 14,* 8155-8165.

Tessier, W. D., Meaden, P. G., Dickinson, F. M. and Midgley, M. (1998). Identification and disruption of the gene encoding the K(+)-activated acetaldehyde dehydrogenase of *Saccharomyces cerevisiae*. *FEMS Microbiol Lett, 164,* 29-34.

Turanli-Yildiz, B., Benbadis, L., Alkim, C., Sezgin, T., Aksit, A., Gokce, A., Ozturk, Y., Baykal, A. T., Cakar, Z. P. and Francois, J. M. (2017). *In vivo* evolutionary engineering for ethanol-tolerance of *Saccharomyces cerevisiae* haploid cells triggers diploidization. *J Biosci Bioeng, 124,* 309-318.

Url-1 United Nations, Word Population Aging (2015): Department of Economic and Social Affairs: Population Division <http://www.un.org/en/development/desa/population/theme/ageing/WPA2015.shtml>, Date retrieved 30.10.2017.

Url-2 Elderly statistics (2013). Turkey Statistical Institute. <http://www.tuik.gov.tr/Kitap.do?metod=KitapDetay&KT_ID=11&KITAP_ID=265>, Date retrieved 30.10.2017.

van Dijken, J. P., Bauer, J., Brambilla, L., Duboc, P., Francois, J. M., Gancedo, C., Giuseppin, M. L. F., Heijnen, J. J., Hoare, M., Lange, H. C., et al. (2000). An interlaboratory comparison of physiological and genetic properties of four *Saccharomyces cerevisiae* strains. *Enzyme Microb Technol, 26*, 706-714.

Vanhalewyn, M., Dumortier, F., Debast, G., Colombo, S., Ma, P., Winderickx, J., Van Dijck, P. and Thevelein, J. M. (1999). A mutation in *Saccharomyces cerevisiae* adenylate cyclase, Cyr1K1876M, specifically affects glucose- and acidification-induced cAMP signalling and not the basal cAMP level. *Mol Microbiol, 33*, 363-376.

Vest, K. E., Leary, S. C., Winge, D. R. and Cobine, P. A. (2013). Copper import into the mitochondrial matrix in *Saccharomyces cerevisiae* is mediated by Pic2, a mitochondrial carrier family protein. *J Biol Chem, 288*, 23884-23892.

Walker, G. M. and Stewart, G. G. (2016). *Saccharomyces cerevisiae* in the production of fermented beverages. *Beverages, 2*, (30): doi:10.3390.

Wang, X., Mann, C. J., Bai, Y., Ni, L. and Weiner, H. (1998). Molecular cloning, characterization, and potential roles of cytosolic and mitochondrial aldehyde dehydrogenases in ethanol metabolism in *Saccharomyces cerevisiae*. *J Bacteriol, 180*, 822-830.

Wei, M., Fabrizio, P., Hu, J., Ge, H. Y., Cheng, C., Li, L. and Longo, V. D. (2008). Life span extension by calorie restriction depends on Rim15 and transcription factors downstream of Ras/PKA, Tor, and Sch9. *PLOS Genetics, 4*, (1): e13.

Wei, M., Fabrizio, P., Madia, F., Hu, J., Ge, H. Y., Li, L. M. and Longo, V. D. (2009). Tor1/Sch9-regulated carbon source substitution is as effective as calorie restriction in life span extension. *Plos Genetics, 5*, (5): e1000467.

Werner-Washburne, M., Braun, E. L., Crawford, M. E. and Peck, V. M. (1996). Stationary phase in *Saccharomyces cerevisiae*. *Mol Microbiol, 19*, 1159-1166.

Wilkie, D. and Maroudas, N. G. (1969). Induction of cytoplasmic respiratory deficiency in yeast by phenethyl alcohol. *Genet Res, 13*, 107-111.

Wu, J., Zhang, N. S., Hayes, A., Panoutsopoulou, K. and Oliver, S. G. (2004). Global analysis of nutrient control of gene expression in *Saccharomyces cerevisiae* during growth and starvation. *Proc Natl Acad Sci USA, 101*, 3148-3153.

Xu, Z., Zhi, Y., Dong, J., Lin, B., Ye, D. and Liu, X. (2016). Requirement of the isocitrate lyase gene ICL1 for VPS41-mediated starvation response in Cryptococcus neoformans. *J Microbiol, 54*, 487-491.

Yasokawa, D., Murata, S., Kitagawa, E., Iwahashi, Y., Nakagawa, R., Hashido, T. and Iwahashi, H. (2008). Mechanisms of copper toxicity in *Saccharomyces cerevisiae* determined by microarray analysis. *Environ Toxicol, 23*, 599-606.

Yılmaz, B. (2009). *Investigation of oxidative stress response in yeast and rat*. (M.Sc. thesis). Istanbul Technical University, Graduate School of Science, Engineering and Technology, Istanbul, Turkey.

Yılmaz Ü (2013). *Evolutionary engineering and molecular characterization of freeze-thaw resistant Saccharomyces cerevisiae*. (Ph. D. thesis). Istanbul Technical University, Graduate School of Science, Engineering and Technology, Istanbul, Turkey.

Zhao, X. Q. and Bai, F. W. (2009). Mechanisms of yeast stress tolerance and its manipulation for efficient fuel ethanol production. *J Biotechnol*, *144*, 23-30.

Zweifel, P., Felder, S. and Meiers, M. (1999). Ageing of population and health care expenditure: a red herring? *Health Econ*, *8*, 485-496.

CURRICULUM VITAE

Name Surname **:** Mevlüt ARSLAN

Place and Date of Birth **:** Yerköy/YOZGAT, 1985

Present Address **:** Istanbul Technical University Dr. Orhan Öcalgiray Molecular Biology-Biotechnology and Genetics Research Center Ayazağa Campus, 34469 Maslak-Istanbul

E-Mail **:** arslanmevlut@itu.edu.tr
: arslanmevlut85@gmail.com

EDUCATION

- **B.Sc. and M.Sc** **:** Yüzüncü Yıl University, Faculty of Veterinary Medicine (2009).

PUBLICATIONS AND PRESENTATIONS ON THE THESIS:

- **Arslan, M.,** Turanlı-Yıldız, B., Yılmaz, B., Kocaefe, N. and Çakar Z.P**.** (in press). An improved semi-quantitative spot assay to analyse chronological lifespan in yeast. Romanian Biotechnological Letters, DOI: 10.26327/RBL2017.29
- **Arslan, M.,** Holyavkin, C., Kısakesen, H.İ., Topaloğlu, A., Sürmeli, Y. and Çakar, Z.P. (in revision) Physiological and transcriptomic analysis of a chronologically long-lived *Saccharomyces cerevisiae* strain obtained by evolutionary engineering. Molecular Biotechnology.
- **Arslan, M.,** Sürmeli, Y., Topaloğlu, A. and Çakar, P. 2017: Chronological life span of stress resistant yeast mutants obtained by inverse metabolic engineering. International ITU student congress. October 6-8, Maslak, Istanbul, Turkey. (Poster presentation, received the third best poster award).
- **Arslan, M.,** Sürmeli, Y., Topaloğlu, A. and Çakar, P. 2016: Longevity of stress resistant yeast mutants obtained by evolutionary engineering. International Congress, Cell Symposium: Metabolism and Aging. July 10-12, Melia Sitges, Spain. (Poster presentation).

OTHER PUBLICATIONS AND PRESENTATIONS:

- Sürmeli, Y., **Arslan, M.,** Topaloğlu, A. and Çakar, Z.P**.** 2016: Evolutionary engineering of caffeine-resistant *Saccharomyces cerevisiae*. PYFF6-6th Conference on Physiology of Yeast and Filamentous Fungi. July 11-14, 2016, Lisbon, Portugal. (Poster presentation).

- Terzioğlu, E., Alkım, C., **Arslan, M.,** Kısakesen, H.İ., Yılmaz, Ü., Balaban, B.G., Selçuki, C. and Çakar, Z.P. 2015: Physiological and transcriptomic analysis of a silver-resistant *Saccharomyces cerevisiae* strain obtained by evolutionary engineering. International conference, Microbial Stress: From Molecules to System. November 12-15, Sitges, Spain. (Oral presentation).